THE UNIVERSITY
of EDINBURGH

Defining the functional role of laminin isoforms in the regulation of the adult hepatic progenitor cell

Michael John Williams

PhD Thesis

The University of Edinburgh

2015

Declaration

I declare that:

(a) the thesis has been composed by myself,

(b) the work is my own, or where a contribution has been made by other members of the research group, such contribution is clearly indicated, and

(c) that the work has not been submitted for any other degree or professional qualification.

Signed,

Michael Williams

Contents

Table of Figures

Acknowledgements

I would like to thank all of my supervisors, Prof Stuart Forbes, Prof Charles ffrench-Constant and Prof John Iredale, for their encouragement and enthusiasm throughout the last 3 years. I would also like to thank all of the members of the Forbes lab, and especially Davina Wojtacha for her tireless patience and good humour. Most importantly, I would like to thank my wife and children for keeping me (mostly) sane throughout it all.

Abstract

During chronic and severe acute liver injury, regeneration is thought to occur through hepatic progenitor cells (HPCs). Understanding the regulation of HPCs may offer therapeutic opportunities to enhance liver regeneration. HPCs are associated with an increase in laminins in the extracellular matrix. Laminins are heterotrimeric proteins, composed of an alpha, beta and gamma chain. There are 5 alpha chains with different distributions and functions, but the relative contributions of these in HPC-mediated liver regeneration are not known. My aims were to describe the laminin alpha chains associated with the HPC response and to define the functional effects of specific laminin chains on HPCs.

I examined the laminin alpha chains in two mouse models of HPC activation: a transgenic model using conditional deletion of Mdm2 in hepatocytes, and a dietary model using 3,5-diethoxycarbonyl-1,4-dihydrocollidine (DDC). The laminin alpha 5 (Lama5) chain is significantly upregulated in both models and forms a basement membrane which surrounds the progenitor cells. I have also demonstrated Lama5 expression in the ductular reaction seen in human liver disease. Using primary mouse cell cultures, I have shown that Lama5 is produced predominantly by the HPCs themselves, rather than by stellate cells. The HPCs express the cell surface receptor alpha-6 beta-1 integrin, a binding partner of Lama5.

I then studied the functional effects of matrix on cell behaviour in vitro using recombinant laminins and a line of spontaneously immortalised mouse HPCs. Compared to other laminin chains, Lama5 selectively promotes HPC adhesion and spreading. These effects are partially blocked by antibodies against beta-1 integrin. Lama5 also significantly enhances HPC migration, resulting in an increase in cell migration. Furthermore, only Lama5 enhances HPC survival in serum-free medium, with an increase in cell viability. Culturing HPCs on HPCs maintained in culture on plastic synthesise Lama5 chain. Knock-down of endogenous Lama5 production using siRNA results in reduced proliferation and increased hepatocytic differentiation, with increased albumin production.

I then studied the effects in vivo using transgenic Cre-lox mouse strains that allow conditional knock-out of either laminin alpha 5 or beta-1 integrin in HPCs. The effects of gene deletion were examined in healthy mice and two dietary models of HPC activation: the DDC diet and a choline-deficient, ethionine-supplemented (CDE) diet. Although these experiments were limited by a low number of experimental animals and low recombination rates, there was a suggestion of impaired HPC expansion associated with loss of laminin alpha 5. There was also a significant increase in hepatocellular injury and fibrosis in response to the DDC diet seen with loss of laminin alpha 5 expression.

Laminin alpha 5-containing matrix is deposited around HPCs during liver regeneration and supports progenitor cell attachment, migration and maintenance of an undifferentiated phenotype. This work identifies a novel target for enhancing liver regeneration.

Abbreviations

2-AAF	2-acetylaminofluorene
7-AAD	7-Aminoactinomycin D
Ah	Aryl hydrocarbon
ALT	Alanine transaminase
ANOVA	Analysis of variance
BCAM	Basal cell adhesion molecule
BEC	Biliary epithelial cell
BrdU	Bromodeoxyuridine
BSA	Bovine serum albumin
CDE	Choline-deficient, ethionine-supplemented
Cre	Cyclic recombinase
CTGF	Connective tissue growth factor
DAB	3,3'-Diaminobenzidine
DAPI	4',6-diamidino-2-phenylindole
DDC	3,5-diethoxycarbonyl-1,4-dihydrocollidine
DMSO	Dimethyl sulfoxide
DR	Ductular reaction
ECM	Extracellular matrix
EDTA	Ethylenediaminetetraacetic acid

EdU	Ethynyldeoxyuridine
EGF	Epidermal growth factor
EGFP	Enhanced green fluorescent protein
EHS	Engelbreth-Holm-Swarm
ELISA	Enzyme-linked immunosorbent assay
EpCAM	Epithelial cell adhesion molecule
ES	Embryonic stem
EYFP	Enhanced yellow fluorescent protein
FACS	Fluorescence-activated cell sorting
FAK	Focal adhesion kinase
FCS	Fetal calf serum
Flp	Flippase
FSC	Forward scatter
GFP	Green fluorescent protein
GFAP	Glial fibrillary acidic protein
HCC	Hepatocellular carcinoma
HGF	Hepatocyte growth factor
HNF	Hepatocyte nuclear factor
HPC	Hepatic progenitor cell
ILK	Integrin-linked kinase

K19	Keratin-19
MMP	Matrix metalloproteinase
MTT	3-(4,5-dimethylthiazol-2-yl)-2,5-diphenyltetrazolium bromide
OCT	Optimal cutting temperature
panCK	Pancytokeratin
PBS	Phosphate buffered saline
PI3K	Phosphoinositide 3-kinase
PPIA	Peptidylprolyl isomerase A
qPCR	Quantitative polymerase chain reaction
siRNA	Small interfering ribonucleic acid
SSC	Side scatter
TIMP	Tissue inhibitor of metalloproteinase
TWEAK	Tumour necrosis factor-like weak inducer of apoptosis

Chapter 1: Introduction

The liver has key roles in nutrient metabolism, detoxification, serum protein synthesis and bile secretion. It has a dual blood supply, receiving arterial inflow from the hepatic artery and blood from the intestine and spleen via the portal vein. The latter is a source of not only nutrients but also toxins and drugs. The liver is therefore the primary barrier to many forms of injury. Perhaps for this reason, the liver has a remarkable regenerative capacity.

Despite the liver's ability to regenerate, however, liver disease is the 5th most common cause of death in the United Kingdom and deaths from cirrhosis are rapidly rising, even amongst 15-44 year olds (Leon and McCambridge, 2006). A recent population-based study estimated that the incidence of cirrhosis increased by around 50% over the 12 year period from 1998 to 2009 (Ratib et al., 2014). Cirrhosis can arise in response to a wide range of chronic insults, including alcohol, viral hepatitis, fatty liver, autoimmune diseases and inherited metabolic conditions. Orthotopic liver transplantation is currently the only effective treatment for end-stage cirrhosis or severe acute liver failure. Transplantation is severely limited by donor organ availability and is associated with significant complications related to operative risk, long-term immunosuppression and rejection. There is therefore an urgent need for alternative treatments for chronic liver disease. Understanding the mechanisms that control liver regeneration may allow novel strategies to enhance endogenous liver regeneration.

1.1 Liver regeneration

Mechanisms of liver regeneration

The liver is unusual in its ability to regenerate from both mature cells and facultative stem cells, as shown diagrammatically in figure 1.1 (Duncan et al., 2009, Fausto, 2004). The mode of regeneration utilised varies according to the type and severity of injury.

Figure 1.1 Mechanisms of liver regeneration

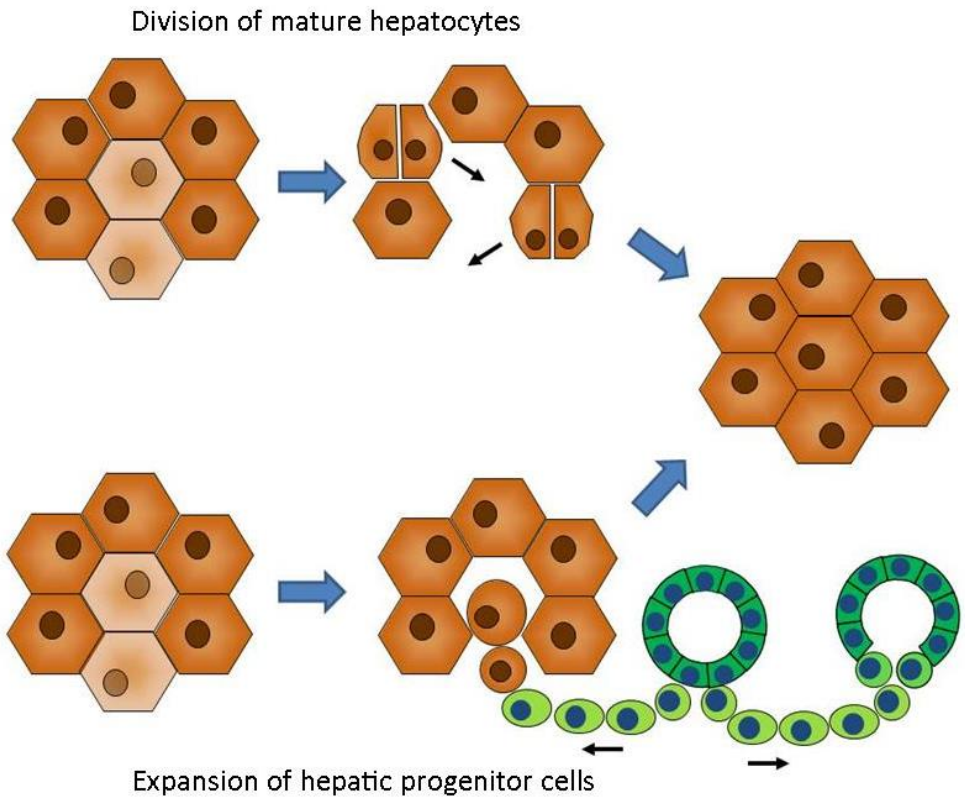

Figure 1.1 Pathways of liver regeneration

Following partial hepatectomy or acute hepatocellular injury, mature hepatocytes are able to re-enter the cell cycle and divide to restore the functional hepatocyte mass. Following chronic or severe acute injury, however, this mechanism appears to be impaired and hepatic progenitor cells (HPCs) located in the terminal bile ducts are able to expand and differentiate into hepatocytes instead. These HPCs are also capable of differentiating into biliary epithelial cells in the context of biliary injury.

Following surgical removal of up to two-thirds of the liver, the remaining uninjured liver is able to regenerate efficiently through division of mature hepatocytes (Higgins and Anderson, 1931, Michalopoulos, 2007). A similar mechanism is seen after acute toxic injury with acetaminophen or carbon tetrachloride (Lee et al., 1998). More recently, it has been shown that hepatocyte enlargement rather than simply division is also able to contribute significantly to recovery from acute liver injury (Miyaoka et al., 2012). Although hepatocyte-mediated regeneration is the predominant mechanism seen following partial hepatectomy, there is evidence that the ability of mature hepatocytes to replicate becomes compromised in advanced liver disease. In rodent models of fibrosis and cirrhosis, there is a reduction in hepatocyte DNA synthesis in response to partial hepatectomy (Kato et al., 2005, Kanta and Chlumska, 1991). Similarly in human cirrhosis, hepatocytes express markers of cell cycle arrest, suggesting that their ability to contribute to regeneration is impaired (Marshall et al., 2005).

After severe or chronic injury, therefore, it has been proposed that regeneration occurs through activation of a resident liver stem cell. This produces hepatic progenitor cells (HPCs) which are bipotential, capable of differentiating into either hepatocytes or biliary epithelial cells (Evarts et al., 1989, Forbes et al., 2002, Santoni-Rugiu et al., 2005, Vig et al., 2006). As these cells are only seen under certain conditions, they have also been referred to as facultative liver stem cells.

Some researchers have also suggested a potential contribution from mesenchymal cells to hepatocyte formation, via mesenchymal-epithelial transformation. Both glial fibrillary acidic protein (GFAP)-expressing cells and alpha smooth muscle actin (SMA)-expressing cells have been shown to contribute to hepatocytes under certain conditions (Yang et al., 2008, Swiderska-Syn et al., 2013). However, a recent lineage tracing report that marked nearly all hepatic stellate cells showed no evidence of epithelial progenitor function across a wide range of liver injury models (Mederacke et al., 2013).

In addition to hepatocyte self-renewal and HPC-mediated regeneration, recent work in cellular reprogramming has also suggested a greater degree of plasticity in liver

cell fate than was previously thought. Activation of Notch signalling within mature hepatocytes is capable of converting them into biliary epithelial cells, and lineage tracing studies suggest that this may occur spontaneously during biliary injury (Yanger et al., 2013). Similarly, ectopic activation of the Hippo/YAP pathway in hepatocytes results in de-differentiation and adoption of an HPC phenotype (Yimlamai et al., 2014). These studies suggest that the relationship between HPCs, hepatocytes and biliary epithelial cells may be more complex than we thought.

Defining hepatic progenitor cells

During fetal liver development, the foregut endoderm gives rise to a population of hepatoblasts, which can differentiate into both hepatocytes and biliary epithelial cells (Lemaigre, 2009). These fetal progenitors express the markers Dlk, E-cadherin and Liv2 (Tanimizu et al., 2003, Nitou et al., 2002, Watanabe et al., 2002). No cells equivalent to the fetal hepatoblast are seen in healthy adult liver. However, during regeneration after certain types of liver injury, a related cell emerges.

Oval cells, a population of small cells with an ovoid nucleus and a high nuclear-to-cytoplasmic ratio, were initially described in the portal areas of rat livers after chemical injury (Shinozuka et al., 1978, Sell, 1978). These cells were noted to co-express markers of hepatocytes (albumin) and biliary epithelial cells (keratin-19) in a similar manner to the fetal hepatoblasts, leading to speculation that oval cells may be common precursors for both lineages in the injured adult liver. These form ductular structures extending from the terminal biliary ductules (Paku et al., 2001). Similar but not identical cells are also seen in mice (Jelnes et al., 2007).

Cells with similar characteristics have also been seen in humans and have been called hepatic progenitor cells, or HPCs. The term ductular reaction (DR) refers to the proliferation of biliary epithelial cells (which are assumed to contain the hepatic progenitor cells) and the associated inflammatory reaction seen across a wide range of liver injuries. Three-dimensional reconstructions of the liver show that these cells arise from the interface between the hepatocyte canalicular system and the biliary

tree, known as the canals of Hering (Theise et al., 1999). This location is consistent with a common progenitor.

Although there are many similarities between fetal hepatoblasts and adult HPCs, it should not be assumed that the two will behave identically and care should be taken when discussing "liver stem (or progenitor) cells" to specify whether this is fetal or adult. In my thesis, I will use the term HPC to indicate only the adult hepatic progenitor cell.

Animal models of hepatic progenitor cells

A variety of animal models have been used to study HPCs. Progenitor-mediated regeneration has been modelled in the rat by combining with partial hepatectomy with chemical inhibition of hepatocyte proliferation using 2-acetylaminofluorene (2-AAF) or retrorsine (Laishes and Rolfe, 1981, Evarts et al., 1989). Although effective in inducing a progenitor cell response, the surgery was associated with pain, increased mortality and numerous changes in the physiological state of the animals. A similar oval cell response is seen in rats in response to the hepatotoxins D-galactosamine (Lemire et al., 1991) and allyl alcohol (Yin et al., 1999).

In mice, however, partial hepatectomy and 2-AAF fails to produce convincing activation of HPCs (Jelnes et al., 2007). Instead, several dietary or toxin models of mouse progenitor cell activation have been described: the choline-deficient, ethionine supplemented (CDE) diet (Akhurst et al., 2001), the 3,5-diethoxycarbonyl-1,4-dihydro-collidine-supplemented (DDC) diet (Wang et al., 2003) and phenobarbital/cocaine (Rosenberg et al., 2000). HPCs have also been shown after genetic induction of senescence in hepatocytes (Endo et al., 2012).

A novel transgenic mouse model has recently been described by our group which induces hepatic progenitor cells by conditional deletion of the Mdm2 gene in epithelial cells (Lu et al, under review). As this model induces very large numbers of HPCs within a short time period, it represents a useful model in which to study the laminin-progenitor cell interaction. Cyclic recombinase (Cre) is expressed under the

control of a cytochrome p450 promoter which is usually transcriptionally silent but is up-regulated in epithelial tissues in response to the xenobiotic beta-naphthoflavone, acting via the aryl hydrocarbon (Ah) receptor (Ireland et al., 2004). Mice carrying the AhCre transgene on a C57/Bl6 background were crossed with mice homozygous for the floxed murine double minute 2 (*Mdm2*) gene, a negative regulator of the tumour suppressor gene p53 (Grier et al., 2002). Uninduced animals develop normally until exposure to beta-naphthoflavone results in activation of Cre in epithelial tissues, with consequent loss of mdm2 and upregulation of p53. In the liver, this results in hepatocyte senescence and apoptosis, with a florid hepatic progenitor cell response.

Identification of progenitor cells

The distinction between stem cells and progenitor cells can be unclear at times (Tajbakhsh, 2009). The key properties of an adult stem cell are generally accepted to be the capacity for long-term self-renewal, and the ability for its progeny to differentiate into some or all of the main cell types within that organ. HPCs are thought to represent a transit amplifying population of proliferating committed progenitors that are not necessarily self-renewing. The identity of the presumed underlying self-renewing stem cell is not clear.

Attempts to identify putative HPCs have assessed both proliferation using clonogenic assays and the ability to differentiate towards hepatocytic and biliary lineages (Dorrell et al., 2011). The regenerative capacity of HPCs can also be assessed in vivo using liver repopulation assays (Wang et al., 2003, Suzuki et al., 2008).

One of the limitations of studies using adult liver progenitor cells is their lack of specific cell surface markers. Historically, progenitor cells were identified in tissue on the basis of morphology and location, as well as co-expression of hepatocytic and biliary markers. When attempting to isolate cells, however, there is no consensus between investigators on the molecular signature of the liver progenitor cell and no unique cell surface marker has been identified (Dolle et al., 2010). Many of the markers traditionally used to identify LPCs such as OV-6, keratin-19 (K19),

pancytokeratin (panCK) and Epithelial Cell Adhesion Molecule (EpCAM) are also expressed on mature cholangiocytes.

Epithelial Cell Adhesion Molecule (EpCAM) is a marker expressed on fetal hepatoblasts (Suzuki et al., 2000). EpCAM-positive cells derived from adult mouse liver can be differentiated into both lineages in culture (Suzuki et al., 2008, Okabe et al., 2009) and are capable of repopulating both hepatocytes and cholangiocytes in a transplant model (Yovchev et al., 2008).

Some markers usually associated with haematopoietic cells have also been demonstrated on hepatic progenitor cells. CD133+ CD45- cells coexpress markers of both hepatocytes and biliary epithelial cells and be differentiated into both lineages in culture (Rountree et al., 2007). CD13+ CD133+ CD49f+ cells from postnatal livers can differentiate into hepatocyte-like and cholangiocyte-like cells under appropriate culture conditions and have been shown to undergo self-renewal-like activity in serial sorted culture (Kamiya et al., 2009).

CD24 is expressed on both biliary epithelial cells and oval cells seen in the DDC model, and is associated with other progenitor markers such as K19 and EpCAM. CD24+ CD45- cells from adult liver have been shown to form hepatocytes in a transplantation model (Qiu et al., 2011).

More recently, a novel antibody identified by Markus Grompe's group (MIC1-1C3) is capable of isolating a population that contains clonogenic cells capable of generating both hepatocytes and biliary epithelial cells (Dorrell et al., 2011).

However, these markers are all expressed on normal uninjured bile ducts or haematopoietic cells and are not specific for progenitor cells. There is therefore no current marker which allows isolation of a pure hepatic progenitor cell population.

Small hepatocytes have been isolated from rat livers using selective culture conditions, which can be differentiated into mature hepatocytes and may represent an intermediate step in the differentiation of progenitor cells (Mitaka et al., 1999). CK19-positive and OV-6-positive cells are identified as the likely source of small

hepatocyte-like progenitors in rats treated with retrorsine/partial hepatectomy (Chen et al., 2013).

In humans, an equivalent hepatic progenitor cell population has been identified within the biliary tree that can form both hepatocytes and bile duct cells. These progenitors express EpCAM, NCAM, CXCR4 and CD44 (Cardinale et al., 2011).

In reality, there may be a range of overlapping phenotypes, from the most immature bipotential transit-amplifying cell through varying stages of commitment to either lineage (Sell, 1998). Ductular reactions in cirrhotic human livers have been shown to have distinct polarity, with hepatocytic and biliary differentiation at either end (Zhou et al., 2007). Indeed, some authors have described at least 8 stages of lineage maturation from stem cell through to fully mature pericentral hepatocyte (Turner et al., 2011). There are therefore likely to be differences in the behaviour of progenitor cells according to the marker used and the model from which the cells are obtained.

Relative contributions of hepatocytes and HPCs to liver regeneration

In order to study liver regeneration and the relative contributions of hepatocytes and HPCs, several techniques have been used. One early method for studying stem cells in other organs has been the label retention assay, in which a DNA marker such as tritiated thymidine or bromodeoxyuridine (BrdU) is incorporated by dividing cells. This label becomes gradually diluted by serial divisions in proliferating cells but remains detectable in slowly-dividing stem cells.

Tritiated thymidine labelling of dividing cells in the uninjured rat liver showed a gradual migration of labelled cells over several weeks from the periportal region towards the hepatic vein, suggesting hepatocyte turnover from a periportal source (Zajicek et al., 1985). This has been termed the “streaming liver” hypothesis. However, this is contradicted by an alternative study using retroviral labelling after partial hepatectomy, which did not demonstrate any migration of labelled cells (Bralet et al., 1994).

One of the difficulties with label-retaining studies in the uninjured liver is the slow rate of normal hepatocyte turnover, with BrdU incorporation rates of less than 1 in 20,000 cells. This technique has therefore been used in combination with repeated injury with paracetamol in mice, to increase turnover and stimulate regeneration (Kuwahara et al., 2008). This suggested 4 possible locations of label-retaining cells, including the terminal branches of the biliary tree (known as canals of Hering), the intralobular bile duct, the periductal monocyte and peribiliary hepatocyte. Work in the haematopoetic stem cell field, however, has suggested that BrdU label retention has a poor sensitivity and specificity for identifying stem cells (Kiel et al., 2007).

There is now evidence from animal models using genetic lineage tracing that HPCs can contribute, albeit modestly, to functional hepatocytes during injury. Using an osteopontin-linked Cre to label HPCs, it was shown that up to 3.26% of all hepatocytes were derived from progenitors in the CDE diet model (Espanol-Suner et al., 2012). This same study found a negligible contribution from HPCs to hepatocytes during normal liver homeostasis, after partial hepatectomy or carbon tetrachloride injury. Another lineage tracing study labelled hepatocytes using an adenoviral-associated vector-linked Cre (Malato et al., 2011). This showed that after chronic carbon tetrachloride injury, 1.3% of hepatocytes were derived from a non-hepatocyte source, presumed to represent HPCs. Again, there was little contribution to homeostasis after acute resection or toxic injury.

Although these numbers represent a minor proportion of mature hepatocytes, the injury models used are mild and short-term compared with chronic liver disease in humans. Further lineage tracing or transplantation experiments are required to determine the true functional regenerative capacity of HPCs over prolonged, repeated or severe liver injury that closely models human disease.

In humans, there is indirect evidence to suggest a lineage connection between HPCs and hepatocytes. Intraseptal hepatocytes in cirrhosis are strongly associated with K19-positive ductular reactions and can be shown by three-dimensional reconstructions to link to the biliary tree (Falkowski et al., 2003). Even in the uninjured human liver, non-pathogenic mutations in mitochondrial DNA have been

used to demonstrate clonal patches of hepatocytes abutting portal tracts and extending laterally towards the central veins (Fellous et al., 2009). Although this study is limited to single time points and so cannot demonstrate with certainty the direction of spread of these mutations, it does suggest that hepatocytes may be originating from a periportal source. Clearly, however, this does not identify the underlying cell of origin, and could be explained by the division of mature periportal hepatocytes just as readily as HPCs.

Hepatocytes that are positive for EpCAM are found close to ductular reactions and have a longer telomere length than EpCAM-negative hepatocytes, suggesting their origin from a slow-cycling stem cell (Yoon et al., 2011). However, the interpretation of this study relies on the assumption that EpCAM-positive hepatocytes have recently differentiated from HPCs, rather than having acquired EpCAM expression. It could be argued rather that biologically younger hepatocytes (as indicated by telomere length) may have greater plasticity to allow them to acquire EpCAM expression when exposed to paracrine signalling from a nearby ductular reaction. In short, the evidence for a functional role of HPCs in liver regeneration in humans is rather circumstantial, but is inferred from the similarities to HPCs in animal models.

HPCs and cancer

In addition to their role in regeneration, HPCs have also been implicated in the development of liver cancer. It is known that patients with cirrhosis and chronic viral hepatitis have an increased risk of developing primary liver cancers. In a series of 109 cases of hepatocellular cancer (HCC), more than a quarter expressed biliary/progenitor cell markers (Keratin-7 and/or Keratin-19), prompting speculation that they may have derived from malignant transformation of progenitor cells (Durnez et al., 2006). Expression of both hepatocellular and biliary markers does not necessarily imply origin from HPCs and could be explained by either de-differentiation or transdifferentiation. With the advent of a number of lineage tracing tools, it will hopefully be possible to answer this question more directly in the future. Nevertheless, the idea that dysregulation of HPCs may contribute to the development of primary liver malignancies remains a valid concern.

1.2 Extracellular matrix and cell behaviour

Cells in multicellular organisms are surrounded by a complex network of cross-linked proteins and polysaccharides. The composition of this matrix is dynamic and varies widely between tissues during both development and disease. The extracellular matrix (ECM) was initially thought of as an inert scaffold which simply provided physical support for cells. However, it is now recognised that in addition to structure, the matrix plays an important role in regulating cell behaviour (Hynes, 2009).

The extracellular matrix consists of a range of macromolecules composed of protein and carbohydrate elements. These include glycoproteins which are a predominantly protein core with the addition of carbohydrate elements, and proteoglycans which are mainly carbohydrate with some protein elements (Sharon, 1986). The main structural proteins include collagens which form helical fibrils that provide tensile strength, elastin which is heavily cross-linked to provide recoil, and laminins which can polymerise to form sheets. Glycoproteins such as fibronectin, nidogen and perlecan can form links between these main protein networks and also interact directly with cells themselves. In contrast, the proteoglycans bind large amounts of water and form a gel-like matrix. They are described according to the main disaccharides present (chondroitin, keratin, dermatin, heparin and hyaluronan) and their sulfation status.

These molecules can combine to form two main types of ECM: the thin dense basement membrane that underlies all epithelial cells, and the loose trabecular interstitial matrix that exists in the spaces between cells. Basement membranes are typically rich in laminin, type IV collagen, nidogen and perlecan, whereas interstitial matrix contains predominantly type I collagen, fibronectin and proteoglycans.

In contrast to all other epithelial tissues, the liver lacks a clearly-defined basement membrane underlying hepatocytes. Laminin-rich basement membranes occur around blood vessels and bile ducts but the normal liver parenchyma is almost devoid of laminins (Hahn et al., 1980). Instead, the gap between hepatocyte and endothelial

cell, known as the Space of Disse, has a sparse matrix composed mainly of fibronectin and type I collagen (Martinez-Hernandez and Amenta, 1993).

HPCs and the niche

The behaviour of stem cells has been shown to be critically influenced by their microenvironment, or niche (Voog and Jones, 2010, Fuchs et al., 2004). Within the niche, a stem cell may have direct contact with either a basal lamina or another cell type which are critical for their maintenance and function. The expression of high levels of cell-cell and cell-matrix adhesion molecules by mammalian stem cells is well-described, but the specific functions of these molecules are poorly understood (Marthiens et al., 2010). The stem cell niche is well-described in organs such as the bone marrow, brain, skin and intestine but not in liver.

HPCs are found in close association with a niche composed of other cells, including hepatic stellate cells and macrophages, and extracellular matrix (Kordes and Haussinger, 2013, Lorenzini et al., 2010), as illustrated in figure 1.2.

Figure 1.2 The hepatic progenitor cell niche

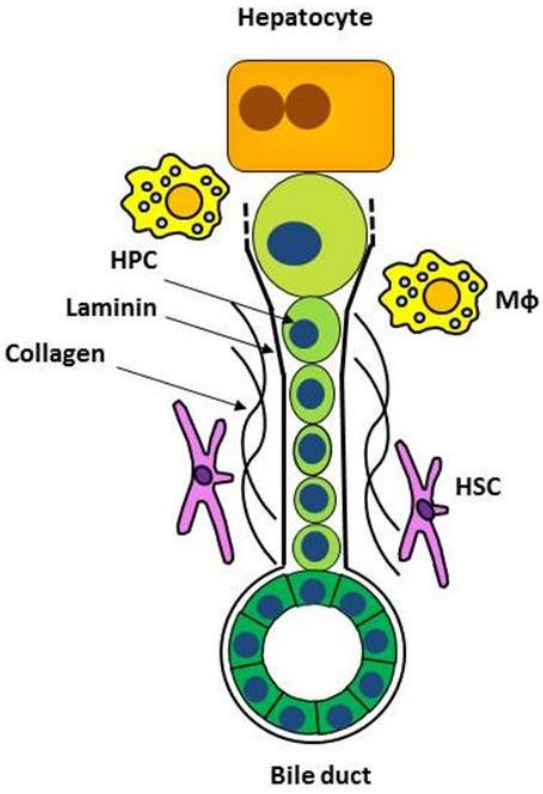

Figure 1.2 The hepatic progenitor cell niche

HPCs are located in the periportal region, arising from the canals of Hering. They are surrounded by an extracellular matrix rich in laminins and collagens. The laminin forms a basement membrane around the cells, and the collagen is located in front of the HPCs along the portovenous gradient as they migrate into the lobule. In close proximity, there are hepatic stellate cells (HSCs) and the resident liver macrophages (Mφs), or Kupffer cells. These cells may be important in influencing the matrix composition as well as providing direct cell-cell signalling.

The niche cells can influence HPCs directly via Wnt and Notch signalling (Boulter et al., 2012), but both stellate cells and macrophages can also alter the composition of the extracellular matrix. Hepatic stellate cells are the main matrix-producing cells of the liver (Maher et al., 1988, Arenson et al., 1988) and also produce matrix metalloproteinases (MMPs) and their inhibitors that regulate matrix degradation (Benyon and Arthur, 2001). Hepatic macrophages have been shown to be a source of MMPs during liver injury and regeneration (Knittel et al., 1999, Fallowfield et al., 2007). In chronic hepatitis C, macrophages expressing MMP-9 were confined to a portal subpopulation and their numbers correlated with portal fibrosis (Gadd et al., 2013). In addition, the HPCs themselves appear to be capable of matrix synthesis, at least in vitro (Lorenzini et al., 2010), and can produce MMPs (Pham Van et al., 2008). There are therefore a number of potential mechanisms for dynamic changes in matrix around HPCs during regeneration.

HPCs and matrix

There are strong associations between HPCs/DRs and changes in the matrix content of the liver (Zhu et al., 2012, Williams et al., 2014). In human liver disease, the ductular reaction correlates with the severity of fibrosis across a range of liver pathologies, including chronic hepatitis C, alcoholic and non-alcoholic steatohepatitis, and genetic haemochromatosis (Lowes et al., 1999, Clouston et al., 2005, Roskams et al., 2003, Wood et al., 2013).

Hepatic progenitor cells in rodent models are also associated with changes in matrix, and these models allow the link to be explored in more detail. In the mouse CDE dietary model of progenitor cell expansion, there is rapid upregulation of collagen I and laminin at a messenger RNA level, and an increase in Sirius Red staining (which stains collagens I and III) in the periportal area (Van Hul et al., 2009).

In the rat 2AAF/partial hepatectomy model, the liver progenitor cells are in direct contact with a basement membrane containing laminin, which is virtually absent from the normal liver sinusoids and disappears again following regeneration (Paku et

al., 2001). Laminin has also been demonstrated in association with progenitor cells in transgenic mice that express hepatitis B protein and were treated with retrorsine (Lorenzini et al., 2010) or mice treated with chronic carbon tetrachloride (Kallis et al., 2011). In humans, laminin has been shown to associate with progenitor cells in patients with chronic hepatitis B or C infection (Lorenzini et al., 2010).

The transition from progenitor cell to hepatocyte appears to correlate with the loss of contact with this basement membrane (Paku et al., 2004). Cells in contact with the basement membrane had low levels of the hepatocytic transcription factor Hepatocyte Nuclear Factor 4 (HNF4), whereas cells that lacked contact showed upregulation of HNF4.

The laminin is localised to areas of progenitor cell expansion. Transgenic mice that express urokinase-type plasminogen activator under the control of the albumin promoter (Alb-uPA) develop spontaneous liver injury, with evidence of a progenitor cell response (Braun et al., 2003). As the mice age, there is gradual emergence of clonal patches of hepatocytes which have lost expression of the transgene, resulting in mosaicism. Progenitor cells are restricted to areas of uPA-positive hepatocytes, and the extracellular laminin deposition is similarly localised.

In addition to changes in collagen and laminin, there is also a rapid increase in fibronectin following 2-AAF and partial hepatectomy. However, this is seen throughout the liver lobule and although fibronectin is found in association with the progenitor cells, it also has a much wider distribution beyond this (Zhang et al., 2009).

There is also indirect work to suggest a role for the matrix proteoglycan hyaluronan in HPC regulation. A number of proteoglycans including hyaluronan are over-expressed in cirrhosis (Murata et al., 1984). Rat small hepatocytes (an intermediate stage in the differentiation of HPCs towards hepatocytes) express the hyaluronan receptor CD44s (Chiu et al., 2009). When cultured on hyaluronan, the proliferation of small hepatocytes correlated with CD44s expression. However, when

differentiation was induced using Matrigel, CD44s expression was lost (Kon et al., 2006).

Chicken or egg?

It is clear then that a number of changes in the extracellular matrix accompany the proliferation and subsequent differentiation of HPCs, with altered levels of collagens, laminins and proteoglycans. However, it is not clear what role this plays in the regulation of the HPCs. Are matrix changes required to directly regulate HPCs, or are the matrix changes simply a consequence of HPC expansion or even a parallel response to injury? Is fibrosis beneficial for HPC-mediated regeneration or is fibrosis unintentionally exacerbated by the progenitor reaction (Clouston et al., 2009)? These questions clearly have major implications for both pro-regenerative and anti-fibrotic therapies.

In the CDE mouse model discussed earlier (Van Hul et al., 2009), the increase in Sirius Red staining is demonstrable as early as day 3 whereas the appearance of significant numbers of HPCs was only seen by day 7. Furthermore, the collagen I appears to precede the progenitor cells along the porto-venous gradient as they migrate into the liver lobule. This suggests that the matrix changes may be required for HPC expansion.

As well as a temporo-spatial association between progenitor cells and matrix, there is also evidence that impaired regeneration is associated with reduced matrix changes. Using an inbred strain of BALB/c mice that have deficient T-cell signalling, the reduced number of HPCs seen in response to the CDE diet was associated with a reduction in the amount of liver collagen, as assessed by Sirius Red staining (Knight et al., 2007a). Similarly, enhancing the regenerative response to the CDE diet by giving interferon gamma increases both the number of HPCs and the amount of liver fibrosis (Knight et al., 2007b). However, it is not clear from these studies whether the matrix changes are necessary for, or occur as a result of, progenitor cell activation.

Evidence for a functional effect of laminin on HPC behaviour comes from an in vitro study (Lorenzini et al., 2010). CD45-depleted non-parenchymal cells isolated from mice on the CDE diet were cultured for 7 days under conditions that positively select for HPCs. The resulting cells were small and rounded with a high nuclear-to-cytoplasmic ratio and demonstrated positive staining with a pancytokeratin antibody. These cells remained positive for pancytokeratin staining when cultured for 7 days on laminin, but lost this on collagen I, collagen IV or fibronectin. Cells cultured on laminin also upregulated gene expression of biliary markers (GGT, aquaporin) and downregulated the hepatocytic transcription factor C/EBP alpha. In contrast, fibronectin led to hepatocytic differentiation, as demonstrated by cytochrome p450 staining. This supports the hypothesis that contact with laminin is necessary for adult HPCs to maintain a naive phenotype, and suggested that fibronectin may be important in promoting differentiation.

Extracellular matrix has also been used a factor to aid the differentiation of human liver progenitors in vitro. Human HPCs cultured on a matrix containing a mixture of collagen IV and laminin adopted a hepatocytic fate, whereas those cultured on collagen I resembled biliary cells (Cardinale et al., 2011). Although this supports the idea that matrix can contribute to cell fate, it should be noted though that there were also significant differences between the media used in these two groups, making it impossible to determine the relative contribution of the matrix to this process.

Perhaps the strongest in vivo evidence so far of an effect of matrix on progenitor cell function comes from a recent lineage tracing experiment (Espanol-Suner et al., 2012). This used an inducible Cre recombinase under the control of osteopontin to selectively label progenitor/biliary cells and demonstrate differentiation into hepatocytes. This model was used to study the effects of Iloprost, a prostacyclin analogue that causes a reduction in connective tissue growth factor (CTGF) production with a subsequent reduction in matrix deposition (Pi et al., 2005). When Iloprost was given during the CDE diet, there was a reduction in both the collagen and laminin content of the liver. This was associated with a reduction in the number of progenitor/biliary cells and an increase in the number of progenitor-derived hepatocytes, suggesting premature differentiation. Although the authors argue that

the reduction in HPCs is due to the altered matrix, it is known that Iloprost has other effects on stellate cells (Kawada et al., 1992). It is therefore possible that Iloprost may be having other direct cellular effects rather than necessarily acting through the alteration in matrix.

As well as matrix influencing HPC behaviour, it has been suggested that HPCs may promote fibrosis. Tumor necrosis factor-like weak inducer of apoptosis (TWEAK) is a mitogen for HPCs, acting via the Fn14 receptor (Jakubowski et al., 2005). A recent study showed that administration of recombinant TWEAK to fibrotic mice undergoing partial hepatectomy caused an increase in both the number of HPCs and the amount of collagen (Kuramitsu et al., 2013). The authors conclude that HPCs are driving the fibrosis. However, there is evidence from other organs that TWEAK acts directly on myofibroblasts to promote activation and collagen production (Novoyatleva et al., 2013, Dohi and Burkly, 2012). It is therefore possible that TWEAK is having parallel effects on myofibroblasts and HPCs.

HPCs and matrix remodelling

Further insight into the role of collagen in HPC regulation comes from a transgenic mouse (r/r mouse) that produces mutated collagen I that is resistant to MMP degradation. In the r/r mouse model, liver progenitor cell numbers were reduced compared to wild-type mice in response to both chronic carbon tetrachloride injury and the CDE diet (Kallis et al., 2011). Although there was an increase in liver collagen content in the r/r mouse, the impaired HPC response was associated with a reduction in laminin deposition. This suggests that laminin may be more closely related to HPCs than collagen.

The same investigators also showed a non-significant trend towards a reduction in progenitor cell numbers in MMP-13 (collagenase) knock-out mice compared to wild-type mice. This suggests that the presence of collagen I in itself does not promote HPC expansion but that rather the turnover of collagen I is required. It remains

unclear whether this is due to a physical barrier or is mediated by either growth factor release or direct matrix-cell signalling.

1.3 Laminins

Laminins are a family of large ECM proteins that are a major component of basement membranes (Durbeej, 2010). Laminins have been shown to play key roles in a range of cell behaviours including survival, migration and differentiation (Paulsson, 1992, Colognato and Yurchenco, 2000).

Laminins are trimers composed of 3 different polypeptide chains, termed α, β and γ (Aumailley et al., 2005). Each trimer is composed of one α, one β and one γ chain, as shown in figure 1.3. The heterotrimeric proteins are able to further polymerise to form continuous sheets, and are the main matrix component in many basement membranes. Laminins bind also several other matrix proteins, including nidogen, agrin, perlecan, fibulin-1 and fibulin-2, and sulfatides.

At present, 5α, 4β and 3γ chains are known for mouse and human (Miner and Yurchenco, 2004) which represent distinct gene products. These can combine to form at least 18 different trimers. Basement membranes will often contain several different isoforms in combination.

A variety of nomenclatures have been used to identify the different laminin isoforms. Although each trimer was initially allocated a single number to reflect the order in which they were described and some have individual names, it is now recommended that they should be referred to by three-digit numbers that reflect their chain composition (Aumailley et al., 2005). For instance, the trimer formed by the α3, β3 and γ2 chains which was formerly known as laminin-5 or kalinin is laminin-332. This is the nomenclature which I will use in this thesis.

Figure 1.3 Structure of laminin

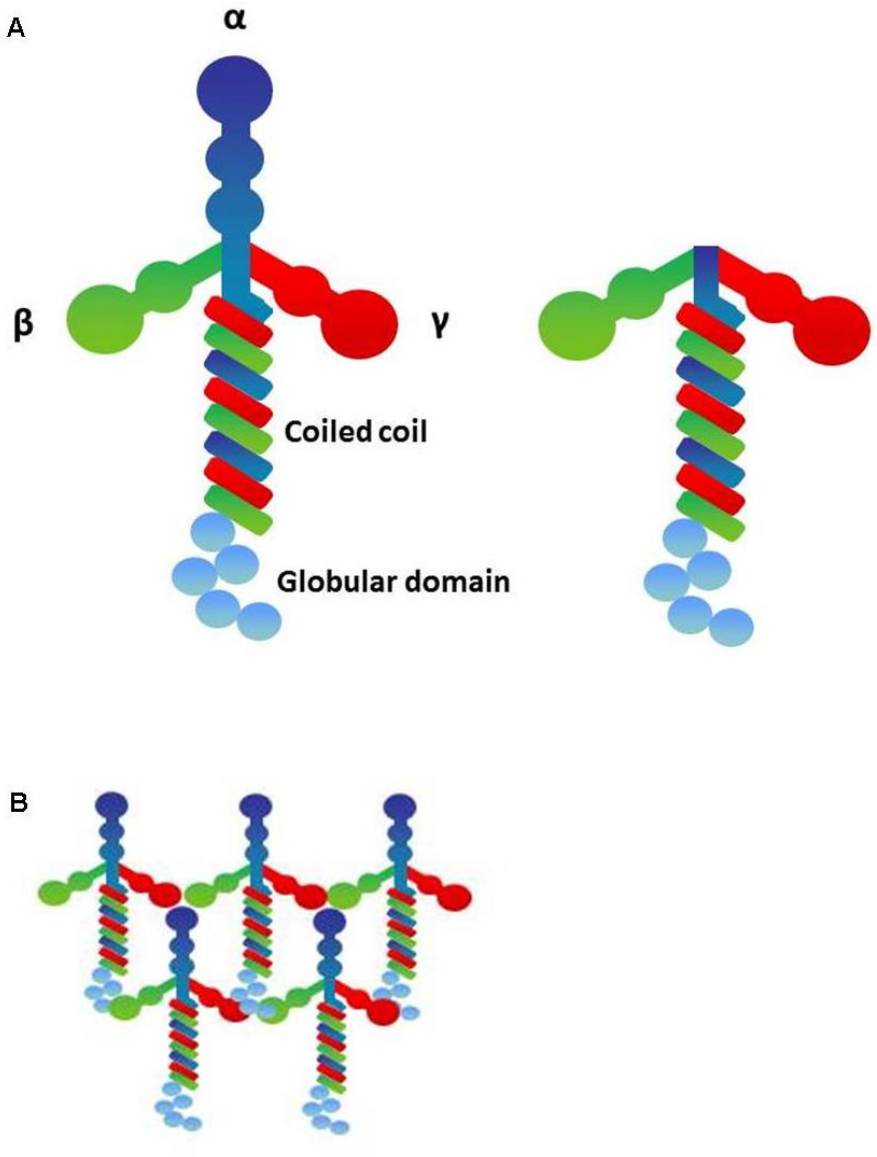

Figure 1.3 Laminin structure

A. Each laminin molecule is formed as an obligate heterotrimer, with an alpha, a beta and a gamma chain. These usually combine to form a cross-shaped molecule (left), although the truncated short arms of the alpha 3A and alpha 4 chains results in a T-shaped structure (right). **B**. The trimers are then able to polymerise further to form a sheet-like structure which forms the basis of basement membranes.

Different isoforms have different distributions

It has been shown that expression of different laminin chains varies between organs and at different stages of development (Yurchenco et al., 2004, Miner et al., 1997). These differences are mainly (although not exclusively) determined by variation in expression of α chains, with other chains (such as β1 and γ1) being ubiquitously expressed. This is perhaps reflective of the fact that laminin α chains display greater sequence divergence than the β and γ chains (Tryggvason, 1993). The main distribution of laminin isoforms is shown in table 1.1.

As well as different tissue distributions, there are also different temporal patterns of laminin expression during development. During in vitro skin morphogenesis, there is differential expression of the laminin α chains. Laminin α1 is up-regulated during the early proliferative phase, whereas laminin α2 and α5 chains were expressed during the later differentiation phase (Fleischmajer et al., 2000).

This led to speculation that individual isoforms may have unique functions in specific tissues (Vachon and Beaulieu, 1995, Turck et al., 2005, Nguyen and Senior, 2006). The observation that laminin alpha chains have different tissue distributions is supported by evidence from mouse models that show different effects of knock-out of specific laminin alpha chains (Scheele et al., 2007). Loss of either laminin α1 or α5 results in a non-viable embryo. However, mutations in some of the other laminin chains lead to discrete pathologies in mice that survive until after birth, despite compensatory up-regulation of other laminin chains.

Table 1.1 Laminin isoforms and their expression.

Laminin isoform	**Main site of expression** (modified from Durbeej, 2010)
111	Embryonic epithelium, some adult epithelium (kidney, liver, testis, ovary), brain blood vessels
121	Placenta
211	Muscle, heart, peripheral nerve, testis
221	Muscle, heart, peripheral nerve, neuromuscular junction
213	Placenta, testis
212/222	Peripheral nerve
3A11, 3A21	Epidermis, amnion
3A32	Epidermis, placenta, mammary gland
3A33	Testis
3B32	Skin, uterus, lung
411	Endothelium, smooth muscle, fat, peripheral nerve
421	Endothelium, smooth muscle, neuromuscular junction
423	Retina/central nervous system
511	Developing/mature epithelium, endothelium, smooth muscle
521	Mature epithelium, mature endothelium, smooth muscle, neuromuscular junction, glomerular basement membrane
523	Retina/central nervous system

Laminin α1 deficiency results in the absence of Reichert's membrane and death by E6.5 (Miner et al., 2004). Loss of α2 results in severe congenital muscular dystrophy and peripheral neuropathy (Miyagoe et al., 1997). Loss of α3 results in skin blistering and glomerular problems (Ryan et al., 1999). Loss of α4 causes abnormalities in blood vessels, neuromuscular junctions, the peripheral nervous system and heart (Patton et al., 2001, Thyboll et al., 2002, Wallquist et al., 2005, Wang et al., 2006). Loss of laminin α5 is lethal by E16.5, with defects in neural tube closure, digit septation and placentation (Miner et al., 1998). Loss of laminin α5 also results in defects in kidney development including failed vascularisation of the glomerulus (Miner and Li, 2000).

It is clear that specific laminin isoforms provide crucial signals to cells in multiple developmental processes. However, as well as their role in embryonic development, laminins are also found in a range of adult stem cell niches. The alpha chain composition of laminins in this setting varies between tissues.

The adult neural stem cell niche in the mouse subependymal zone is characterised by expression of laminin α2, α4 and α5 (Kazanis et al., 2010).

Within the eye, there are adult stem cells located in the limbal epithelium. There are marked variations in laminin alpha chain expression. Laminin α3 is expressed throughout the ocular epithelium and α5 is restricted to both limbal and conjunctival epithelium. In contrast, the laminin α1 and α2 chains are only expressed in the limbal region (Schlotzer-Schrehardt et al., 2007).

Different effects of laminin isoforms on cell behaviour in vitro

Much of the original in vitro work on the effects of laminin on cell behaviour have used laminin purified from the Engelbreth-Holm-Swarm sarcoma, which is laminin-111. There is increasing evidence that there are differences between laminin isoforms in their ability to influence cell function. Until relatively recently, this work has been limited by the difficulties in obtaining sufficient quantities of purified forms of many

laminin isoforms to perform functional assays. However, it has now become possible to compare the effects of different laminin trimers in vitro.

As well as demonstrating changes in transcription during development, in vitro experiments have now also shown a direct effect of specific laminin isoforms on cell behaviour. In mouse embryonic stem (ES) cells cultured on different matrix components, laminin-511 supported self-renewal and retention of pluripotency markers such as OCT-4, SOX-2 and Nanog. In contrast, laminin-332 enabled proliferation but loss of pluripotency; laminin-111 caused rapid differentiation and laminin-411 did not support survival (Domogatskaya et al., 2008).

Similarly, using a cell line derived from human colonic adenocarcinoma, laminin-211, -332 and -511 supported proliferation, whereas laminin-111 promoted intestinal cell differentiation (Turck et al., 2005).

Evidence for effects of specific laminin isoforms within the liver

Many of the descriptive studies looking at matrix composition of the niche have used a pan-laminin antibody that recognises a shared epitope common to all of the isoforms. However, there is some limited data on specific laminin isoforms within the liver.

Laminin alpha chains have been studied following partial hepatectomy, a situation where regeneration occurs via mature hepatocytes rather than progenitor cells. In this case, there was a transient increase in laminin alpha 1 chain within the sinusoids, peaking at 6 days after partial hepatectomy (Kikkawa et al., 2005). Laminin alpha 1 was produced by stellate cells. In vitro studies showed that laminin-111 promoted spreading of both sinusoidal endothelial cells and stellate cells more than laminin-411 suggesting a functional effect.

Laminin alpha 5 is expressed in hepatocellular carcinomas (Kikkawa et al., 2008). HCC cells express the laminin-binding receptors α3β1 and α6β1 integrins, as well as Lutheran. HCC cells attach to laminin alpha 5 more avidly than healthy hepatocytes.

Finally, in embryonic development, it has been shown that α1 and α5 have different effects in vitro with regard to bile duct formation. Researchers used a cell line derived from hepatoblasts from mouse fetal liver (Tanimizu et al., 2004). HPPL cells form cysts with a central lumen, a process which is believed to parallel developmental bile duct morphogenesis. Exogenous laminin α1 was necessary for the initial formation of cysts but not for their maintenance. By this stage, the cells produced their own laminin α5. Interference with laminin α5 production using small interfering RNA (siRNA) inhibited lumen formation (Tanimizu et al., 2012). This suggests that laminin α1 and α5 have sequential roles in initiating and completing bile duct morphogenesis.

There is a lack of data on the specific laminin isoforms associated with HPC-mediated regeneration.

1.4 Laminin receptors

There are a number of mechanisms by which changes in matrix can influence cell behaviour. Changes in the matrix content may affect cells indirectly by changing local concentrations of growth factors and altering physical properties of the tissue such as stiffness. However, the most direct mechanism of action is the binding of individual matrix components to cell surface receptors, resulting in intracellular signal transduction.

Integrins

The main group of cell-surface receptors which interact with the ECM are the integrins (Hynes, 1992, Barczyk et al., 2010). These are involved in a wide range of cellular processes including attachment, movement, differentiation and death. The integrins are a family of heterodimeric transmembrane proteins, each composed of an α and a β subunit. 18 alpha and 8 beta chains have been described in mammals. Not all subunits can combine with every other, with some restricted to a single partner. At present, there are 24 recognised combinations. The integrins can be grouped together according to ligand-binding specificity (Humphries et al., 2006). The ligand-

receptor relationship is often promiscuous: several integrins can recognise the same ECM ligand, and similarly each integrin may bind a range of ECM components. The largest subgroups of integrins are those sharing the β1 and αv subunits. Integrins that bind laminin include α3β1, α6β1, α6β4 and α7β1 (Kikkawa et al., 2000).

Binding of integrins to matrix can initiate a number of intracellular signalling pathways, including focal adhesion kinase (FAK), integrin-linked kinase (ILK) and phosphoinositide-3 kinase (PI3K) (Giancotti and Ruoslahti, 1999). Integrins can also interact with growth factor receptors, ion channels and the actin cytoskeleton. The activation of such intracellular pathways by integrins is termed "outside-in" signalling. Each alpha-beta integrin combination has its own signalling properties. Different cell types have unique integrin profiles which will determine not only which ECM they can bind, but also the downstream signalling pathways that will be activated. Further control is made possible by the ability of cells to regulate the affinity of integrin binding in response to intracellular changes, so-called "inside-out" signalling (Hynes, 2002).

Beta-1 integrin

Although there a variety of receptors capable of interacting with laminin, the beta-1 subunit is found in the majority of laminin-binding integrins. In particular, the α6β1 integrin has been shown to be highly expressed on a number of stem cells (Nagato et al., 2005, Tate et al., 2004). Inhibiting α6β1 integrin function with blocking antibodies disrupts the behaviour of neuronal progenitor cells in mice (Shen et al., 2008).

As with laminins, the use of transgenic mice to study the role of integrins in cell behaviour has been limited by the critical role played during embryogenesis. Constitutive deletion of β1 integrin leads to embryonic death, long before any effect in the regenerating liver can be adequately assessed (Fassler and Meyer, 1995). Similarly, deletion of the α6 integrin subunit leads to a severe detachment of the

epidermis and death shortly after birth, and α3-null mice die shortly after birth due to defective kidney and lung development (Bouvard et al., 2001).

Mutations can be induced in adult Drosophila flies using a flippase recombinase. In the Drosophila ovary, mutations in either laminin A or its corresponding integrins resulted in a loss of follicular stem cell renewal and affects the development of their progeny (O'Reilly et al., 2008). However, Drosophila have significantly less variation in either their laminin chains or integrin subunits. Studies in mice (which have the same laminin isoforms and integrins as humans) have used Cre-mediated recombination to demonstrate the role of β1-integrin in a number of specific cell types (Jones et al., 2006, Benninger et al., 2006, Lei et al., 2008, Raghavan et al., 2000).

Conditional deletion of beta-1 integrin in the intestinal epithelium causes a profound increase in proliferation and inhibited differentiation (Jones et al., 2006). Hedgehog expression was markedly reduced in the integrin knockout mice and transfection of intestinal epithelial cells with beta-1 integrin stimulates Hedgehog expression, suggesting that loss of Hedgehog signalling may be a mediator of this effect.

Integrin expression in the liver

In normal liver, human hepatocytes express only α1β1 (collagen-binding), α5β1 (fibronectin-binding) and α9β1 (tenascin-binding) integrins (Volpes et al., 1991, Palmer et al., 1993, Scoazec, 1996). Cholangiocytes, which are in contact with a laminin basement membrane, express α3β1 and α6β1 (both laminin-binding) integrins. In inflammatory conditions, however, there is increased expression of α3β1 and α6β1 integrins in the liver (Quondamatteo et al., 2004). Furthermore, in patients with chronic hepatitis C, the degree of upregulation of α6β1 integrin was closely related to the deposition of perisinusoidal laminin (Nejjari et al., 2001). In the CDE diet mouse model, as oval cell numbers increased, there was increased expression of mRNA for the α6 integrin subunit (Van Hul et al., 2009).

Non-integrin laminin receptors

In addition to integrins, there are a number of other cell surface receptors which can interact with laminin. Syndecans are transmembrane glycoproteins which interact with the extracellular matrix (Couchman, 2003) and may modulate integrin signalling (Streuli and Akhtar, 2009). Non-integrin laminin-binding receptors also include dystroglycan and Lutheran blood group glycoprotein/basal cell adhesion molecule (BCAM). α-dystroglycan has a high affinity for laminin α1 and α2, whereas Lutheran/BCAM binds only to laminin α5.

Physical characteristics of matrix

As well as signalling pathways linked to specific cell surface receptors, the physical characteristics of the matrix, such as stiffness, can regulate cell behaviour. Culturing a hepatocellular carcinoma cell line on a gel of increasing stiffness led to increased proliferation, regardless of the overlying matrix coating (Schrader et al., 2011). The extracellular matrix can also bind to soluble growth factors, regulating their distribution, activation and presentation to cells. Hepatocyte growth factor (HGF), one of the key mitogens for hepatocytes, binds to collagen (Schuppan et al., 1998). Collagen-bound HGF was still able to induce proliferation of cultured hepatocytes, suggesting that it retains its biological activity. Collagen also sequesters MMPs and modulates their activity (Freise et al., 2009).

1.5 Cre-lox recombination

The use of transgenic animal studies to understand the role of laminins in adult stem cell behaviour has been limited by the critical role played during early embryonic development. Knock-out mice have demonstrated the requirement for specific ECM components in early embryonic development (Tsang et al., 2010). A major advance in the study of gene function has been the development of transgenic mice that allow site-specific DNA recombination.

Newly-emerging technologies such as flippase recombination enzyme (Flp) or cyclic recombinase (Cre) allow conditional gene deletion in a tissue-specific and/or time-specific manner (Branda and Dymecki, 2004). Using these techniques, the effects of gene deletion can be studied after a period of normal development.

Cyclic recombinase (Cre) is a bacteriophage-derived enzyme that catalyses site-specific recombination of DNA. Cre acts at specific 34 base pair target sequences known as loxP sites. Where 2 loxP sites occur in a cis arrangement, Cre recombinase will mediate the deletion of the intervening segment, and can be used to inactivate a gene of interest. By deleting a segment within a STOP codon, Cre recombinase can be used to activate a gene. A gene that is flanked by loxP sites is said to be floxed. As neither Cre nor loxP sites occur naturally in mammalian systems, they need to be introduced into the mouse genome using transgenic technology. By targeting the gene for Cre recombinase to a specific non-critical integration site using a knock-in strategy, gene deletion can be controlled by specific promoters to target specific tissues or cell types.

A further level of control can be added by the use of fusion proteins, in which Cre recombinase is given a ligand binding domain that regulates access to the nucleus. Cre-ERT is a construct which requires the presence of exogenous tamoxifen in order to induce recombination.

1.6 Summary

Stem cells are frequently associated with a specialised extracellular matrix or niche which is believed to be important in regulating their behaviour. Progenitor cells in regenerating adult liver have been shown to be closely associated with laminins, although the pattern of laminin isoforms has not been fully characterised. Work in other organs has demonstrated a functional role for laminins in regulating stem cell behaviour, but has highlighted the importance of specific isoforms in this process. The relevance of individual laminin isoforms as a potential mechanism of regulating LPC behaviour has not been assessed. Understanding the mechanisms by which extracellular matrix regulates progenitor cell behaviour may allow therapeutic interventions to enhance intrinsic regeneration in chronic liver disease, as well as having implications for the development or treatment of liver cancers.

1.7 Hypothesis

My central hypothesis is that interaction between specific laminin isoforms and cell-surface laminin receptors is required for the regulation of liver progenitor cell behaviour.

This hypothesis makes the following predictions:

1. Alteration of the matrix composition or blocking of cell-surface receptors will affect HPC behaviour *in vitro*.
2. Perturbation of this interaction will disrupt the hepatic progenitor cell response *in vivo*.

1.8 Aims of the project

1. To define the specific laminin alpha chains associated with the hepatic progenitor cell response in the mouse liver.
2. To examine the functional effect of specific laminin alpha chains on the hepatic progenitor cell response *in vitro* and *in vivo*.

Chapter 2: Methods and Materials

2.1 Animal models

Wild-type mice were supplied by Harlan (UK). Transgenic mice were bred in house. All animals were maintained in 12 hour light/dark cycles with free access to food and water. All procedures were performed in accordance with UK Home Office guidelines as described in the Animals (Scientific Procedures) Act 1986.

AhCre-Mdm2^{flox} model

The AhCre-Mdm2^{flox} mouse colony was kindly provided by Owen Sansom (Beatson Institute, Glasgow). Genotyping was performed on ear notches, following digestion overnight in 50 mM Tris pH 8.5 with 12 mM $MgCl_2$ and 500 μg/mL proteinase K (Sigma) at 60°C. The primers are listed in table 2.1. The PCR product was run on a 1.5% agarose gel containing gel red dye for 40 minutes at 70V, and viewed under a VersaDoc Imaging System.

Table 2.1 Primer sequences for genotyping

Gene	***Primer sequence***
Ah-Cre forward	CCTGACTAGCATGGCGATAC
Ah-Cre reverse	ATTGCCCCTGTTTCACTATC
Mdm2 forward	TGTGGAGAAACAGTTACTTC
Mdm2 reverse	CTGTGCTCCTTCACAGAG

AhCre^{+} Mdm2$^{flox/flox}$ mice aged 12 - 16 weeks were given intraperitoneal injections of either 40mg/kg or 20mg/kg of β-naphthoflavone (Sigma Aldrich) dissolved in corn oil at a concentration of 10mg/ml. Mice were culled by exposure to rising concentration of carbon dioxide.

DDC model

In the initial descriptive work in chapter 3, I have used liver sections and frozen tissue generated previously by another member of the Forbes group, Dr Luke Boulter. In his original experiments, S129 S2 mice aged 6-8 weeks were given 0.1% w/w 3,5-diethoxycarbonyl-1,4-dihydrocollidine (DDC) in chow for 8, 12 or 18 days, and culled as above. This has been shown to cause a biliary injury via accumulation of porphyrins and results in marked HPC expansion.

2.2 Transgenic models

K19Cre

The K19Cre^{ERT} R26R-EYFP mouse colony was kindly provided by Prof Guoqiang Gu (Vanderbilt University School of Medicine, Nashville) and was bred in-house. This mouse strain has the transgene Cre recombinase fused with a tamoxifen response element, under the control of the cytokeratin-19 promoter. This is combined with an enhanced yellow fluorescent protein (EYFP) reporter located in the ROSA26 locus that is preceded by a flox-stop-flox sequence, so that EYFP is expressed only after activation of the Cre (Srinivas et al., 2001). Genotyping was performed on ear notches by Transnetyx (Cordova, United States).

K19Cre Lama5flox

The Lama5flox mouse colony was kindly provided by Prof Jeffrey Miner (Washington University, Saint Louis) and bred in-house. The generation of this allele has been described previously (Nguyen et al., 2005). This was crossed with the K19Cre mouse to generate K19Cre^{+} Lama5$^{flox/flox}$ R26R-EYFP$^{+/+}$ mice for experimental use.

K19Cre-Itgb1flox

The Itgb1flox mouse colony was purchased from the Jackson Laboratory (Bar Harbor, Maine, USA) and bred in-house. This was crossed with the K19Cre mouse to generate K19Cre^{+} Itgb1$^{flox/flox}$ R26R-EYFP$^{+/+}$ mice for experimental use.

rdTomato reporter

For cell isolation, the R26R-EYFP reporter was bred out and replaced with the brighter rdTomato reporter from the Ai14 strain (Jackson laboratory, Bar Harbor, Maine, USA).

Tamoxifen induction

1g of tamoxifen (Sigma) was dissolved in 5ml of ethanol and suspended in 10ml cremophor. The resulting suspension was diluted in 35ml sterile PBS to give a final concentration of 20 mg/ml. 6 week old mice were given 3 doses of 4mg tamoxifen (200 µl) via intraperitoneal injection over a period of 5 days.

Transgenic diets

For the choline-deficient, ethionine supplemented (CDE) diet, transgenic mice were fed a diet of choline-deficient chow (MP Biomedicals) with sweetened drinking water containing 0.15% w/v ethionine (Sigma Aldrich). This was commenced 14 days after the first tamoxifen injection and animals were harvested after 21 days of diet.

For the DDC diet, transgenic mice were fed a diet of 0.1% DDC with normal drinking water. This was commenced 21 days after the first tamoxifen injection and animals were harvested after 14 days of diet.

Tissue harvest

Blood was collected by cardiac puncture at the time of tissue harvest. Liver tissue was fixed in either 10% formalin solution or methacarn (60% methanol, 30% chloroform, 10% glacial acetic acid) overnight. Fixed tissue was transferred to 70% ethanol prior to paraffin embedding. In addition, tissue was snap-frozen on dry-ice and stored at -80°C for RNA extraction, and embedded in OCT embedding matrix

(CellPath) prior to immersion in a bath of isopentane surrounded by dry ice for frozen sections.

2.3 Immunohistochemistry

3 µm sections of paraffin-embedded tissue were dewaxed in xylene and rehydrated through decreasing concentrations of ethanol (100%, 90%, 80%, 65% and water). Where required, antigen retrieval was performed by either microwaving in either 0.01M sodium citrate pH6, Tris-EDTA pH9 or treating with 125 µg/ml proteinase K in a waterbath at 37°C.

For diaminobenzidine (DAB) staining, endogenous peroxidase activity was quenched by immersion in 1% hydrogen peroxide for 15 minutes prior to blocking with avidin and biotin. Non-specific binding was blocked by incubation with protein block (Spring Bioscience) for 30 minutes. Sections were incubated with primary antibody in Antibody Diluent Reagent Solution (Invitrogen), for either 1 hour at room temperature or overnight at 4°C. To confirm the specificity of staining, appropriate isotype controls were used for each primary antibody where available; where isotype controls were not available (eg. the laminin alpha 5 antibody provided by Prof Watts), a control was performed using no primary antibody instead. A list of all primary antibodies is given in table 2.2.

Following washing, sections were incubated with a biotinylated secondary antibody for 30 minutes, followed by ABC reagent (Vector) for 30 minutes. Finally, sections were treated with DAB (Liquid DAB Substrate Chromogen System, DAKO) for 5 minutes, prior to counterstaining with haematoxylin, dehydration through alcohols and xylene, and mounting in Pertex hard setting mounting medium.

For immunofluorescence, sections were incubated with protein block prior to the primary antibody. Secondary antibodies were conjugated to Alexa Fluor 488 or 555 (Invitrogen). Where further signal amplification was required or additional antigen retrieval was required for dual immunofluorescence, a Tyramide Signal Amplification kit was used (PerkinElmer). Slides were mounted using DAPI Fluoromount-G (Southern Biotech).

For frozen sections, 10 µm sections were air-dried and stored at -20°C prior to fixation in ice-cold methanol and acetone.

Table 2.2. Antibodies used in imnunohistochemistry

Antigen	Host species	Manufacturer (Cat No)	Antigen retrieval	Dilution
A6	Rat	Gift from V Factor	Frozen	1/200
Alpha-smooth muscle actin	Mouse	Sigma A5228	Sodium citrate	1/2000
Collagen I	Goat	SouthernBiotech 1310-01	Sodium citrate	1/400
Collagen III	Goat	SouthernBiotech 1330-01	Sodium citrate	1/400
F4/80	Rat	Abcam ab6640	Proteinase K	1/100
GFP	Chicken	Abcam ab13970	Tris-EDTA	1/500
HNF4a	Goat	Santa-Cruz sc-6556	Sodium citrate	1/100
Integrin alpha 3	Rabbit	Millipore AB1920	Frozen	1/500
Integrin alpha 6	Rat	Millipore MAB 1378	Frozen	1/100
Integrin beta 1	Rat	Millipore MAB1997	Frozen	1/100
Keratin 19	Rabbit	Abcam	Tris-EDTA	1/100

		ab15463		
Ki67	Rabbit	Novocastra Ki67p	Tris-EDTA	1/500
Laminin	Rabbit	Abcam ab11575	Sodium citrate	1/25
Laminin alpha 1	Rat	Santa Cruz sc-65645	Frozen	1/100
Laminin alpha 2	Rat	Axxora ALX-804-190-C100	Frozen	1/2000
Laminin alpha 5	Rabbit	CRUK-1186-018	Sodium citrate / frozen	1/3500
MIC1-1C3	Rat	Novus NBP1-18961	Frozen	1/100
Osteopontin	Goat	R&D AF808	Tris-EDTA	1/250
Pancytokeratin	Rabbit	DAKO Z0622	Sodium citrate	1/200
P53	Mouse	Abcam ab26	Sodium citrate	1/500
Sox9	Rabbit	Santa Cruz sc20095	Sodium citrate	1/100

Assessment of tissue sections

Stained slides were blinded and randomised prior to photographing for quantification. For panCK quantification, a minimum of 20 serial, non-overlapping fields were photographed at x200 magnification. For YFP quantification, 20 consecutive portal tracts were photographed at x400 magnification.

2.4 Quantitative PCR analysis

Total RNA was extracted from snap-frozen liver tissue using TriReagent (Amersham). Following homogenisation, chloroform was added in a ratio of 1 part chloroform: 5 parts Trizol, mixed well and centrifuged at 12000 rpm for 15 minutes at 4°C. The aqueous layer was then mixed with an equal volume of 70% ethanol in RNase-free water, prior to use of RNeasy Mini Kit (Qiagen, UK) elution columns. The resulting RNA concentration was measured using a NanoDrop (ThermoFisher).

RNA extraction from cells was performed using RLT lysis buffer (Qiagen) in place of TriReagent.

Reverse transcription was performed using the Qiagen kit according to manufacturer's instructions. Pre-designed validated primer sets were purchased from Qiagen (listed in table 2.3).

qPCR reaction mixtures were prepared using SYBR-Green. Each reaction consisted of 5 µl of cDNA, 6.25 µl of SYBR mastermix and 1.25 µl of primers. Samples were prepared in 384 well plates and run using a LightCycler480. Data was analysed using the LightCycler480 software. All reactions were performed in triplicate. Gene expression was internally controlled by measuring expression of the housekeeping gene peptidylprolyl isomerase A (PPIA) in the same sample.

Table 2.3 qPCR primers used

Gene	***Code***
Albumin	QT00115570
E-cadherin	QT00121163
EpCAM	QT00248276
Integrin alpha 3	QT00125678
Integrin alpha 6	QT00144354
Integrin alpha 7	QT00136990
Integrin beta 1	QT00155855
Integrin beta 4	QT01065729
Keratin-19	QT00156667
Laminin alpha 1	QT00163394
Laminin alpha 2	QT00155589
Laminin alpha 3	QT01889104
Laminin alpha 4	QT00149583
Laminin alpha 5	QT01750637
PPIA	QT00247709

2.5 Cell culture

The Bmol cell line was kindly provided by George Yeoh, University of Western Australia. The derivation and characterisation of these cells is discussed in more

detail in chapter 4. Bmol cells were cultured in William's E + GlutaMAX-1 medium (Gibco) supplemented with 100 units/ml penicillin and 100 µg/ml streptomycin (PAA) and 2% fetal calf serum, unless stated otherwise. Cells were cultured in a humidified atmosphere with 5% carbon dioxide at 37°C.

2.6 Matrix coating of plates

Recombinant human laminin-111, -211, -411 and -511 (Biolamina) were diluted in sterile phosphate buffered saline (PBS) to a concentration of 20 µg/ml. Wells were coated for 1 hour at 37°C, or overnight at 4°C, and then washed with PBS.

2.7 Attachment assay

Cells were trypsinised and suspended at $1x10^5$ cells/ml. A 96-well plate was coated with matrices as above, and incubated with 3% bovine serum albumin (BSA) to block non-specific binding. 100 µl of cell suspension was added to each well and incubated for 30 minutes at 37°C. The wells were then washed twice with PBS to remove any unattached or loosely attached cells. The remaining cells were fixed with 5% glutaraldehyde, stained with crystal violet, and solubilised in 10% acetic acid. A spectrophotometer was used to determine absorbance at 570nm. Blank wells without cells were used as controls. Each experiment was performed using a minimum of 5 wells per condition, and was repeated at least once.

2.8 Spreading assay

Cells were trypsinised and suspended at $2\ x10^4$ cells/ml. A 96-well plate was coated with matrices and blocked with BSA. 100 µl of cell suspension was added to each well and incubated for 60 minutes at 37°C. The cells were fixed directly by the addition of 25% glutaraldehyde to the wells without any washing. Cells were washed, stained with crystal violet and photographed using a x40 objective lens. Image analysis software (ImageJ) was used to measure the area of 100 cells per well.

2.9 Migration assay

Cells were trypsinised and incubated with 5 µg/ml mitomycin C for 2 hours, and re-suspended at 5 x10^5 cells/ml. 100 µl of cell suspension was added per well of an Oris migration plate, and incubated overnight to allow confluent cell attachment. The stoppers were removed to create a standardised central defect. Control wells were fixed immediately with 5% glutaraldehyde. The remaining wells were fixed at 24 hours. Cells were stained with crystal violet and photographed. Quantification of cell migration was performed using ImageJ. Integrin-blocking antibodies (MCA699X2 and MCA2298EC) were used at 25 µg/ml.

2.10 MTT assay

Cells were trypsinised and suspended at 5x10^4 cells/ml. 100 µl of cell suspension was added per well of a 96-well plate. Cells were incubated at 37°C for 48 hours. 20 µl of MTT solution was added per well to the medium. After 3 hours, the medium was aspirated and 100 µl of DMSO was added and the plate was placed on an orbital shaker at 200rpm for 5 minutes. A spectrophotometer was used to determine absorbance at 570nm.

2.11 EdU assay

Cells were cultured in 48 well plates at 1 x10^5 cells/ml. After 48 hours on matrix, 100 µl of 20 µM EdU was added to each well and cells were incubated for 3 hours. Cells were fixed with 4% formaldehyde prior to washing with 3% BSA in PBS and permeabilising with 0.1% TritonX in PBS. The Click-It reaction was used as per manufacturer's instructions and photographed for quantification.

2.12 siRNA transfection

Small interfering RNA (siRNA) against laminin alpha 5 was obtained from Qiagen (FlexiTube GeneSolution, Cat No GS16776). Oligonucleotides were suspended in 100 µl of RNAse-free water. Cells were suspended at 1 x 10^5 cells/ml and plated. Cells were transfected using HiPerFect reagent (Qiagen) as per manufacturer's instructions. A mastermix of siRNA was prepared in serum-free medium with 37.5ng of siRNA and HiPerFect reagent. This was vortexed and left for 10 minutes to form complexes before adding dropwise to the cells.

Efficiency of transfection was assessed using an ELISA kit against mouse laminin alpha 5 (AMS Biotechnology).

2.13 Isolation of cells

Livers were perfused in situ with 10ml of Gibco Liver Perfusion medium, followed by 20ml of Gibco Liver Digestion medium. Following this, the livers were excised, chopped and homogenised using a gentleMACS Dissociator (Miltenyi Biotec). The resulting homogenate was incubated for 30 minutes at 37°C, before being passed through a 70 µm filter. This was spun at 50G for 5 minutes to remove hepatocytes, and the supernatant containing the non-parenchymal fraction was then pelleted at 300G for 5 minutes.

HPCs

The non-parenchymal fraction was resuspended and spun over a discontinuous Percoll gradient (Sigma). Cells isolated from the 20%/50% boundary were washed and plated in HPC selective medium (Okabe et al., 2009): Williams' Medium E (Gibco) containing 10% FCS, 17.6 mM NaHCO3, 20mM HEPES pH 7.5, 10 mM nicotinamide, 1 mM sodium pyruvate, 1x insulin transferrin selenium (ITS) solution (Gibco), 100 nM dexamethasone, 0.2 mM ascorbic acid, 14 mM glucose, 10 ng/mL IL-6 (Peprotech), 10 ng/mL HGF (Peprotech), 10 ng/mL EGF (Sigma-Aldrich). Cells were washed after 24 hours to remove unattached or dead cells and cultured for 14 days.

Hepatic stellate cells

The non-parenchymal fraction was resuspended and spun over a discontinuous OptiPrep gradient (Sigma). Cells isolated from the 40%/60% boundary were plated in DMEM containing 20% FCS, L-glutamine and sodium pyruvate for a minimum of 3 passages until a typical stellate morphology was observed.

Recombined cells for gene array

The non-parenchymal fraction was incubated with 1/100 dilution of anti-mouse CD45-PE conjugated antibody (eBioscience, 12-0451-82) and 7-amino-actinomycin D (7-AAD) (eBioscience, 00-6993-50) for 10 minutes prior to washing and sorting using a BD FACS Aria II.

2.14 Statistical analysis

Statistical analysis was performed using GraphPad Prism 5 (GraphPad Software). Parametric data were analysed by Student's t-test or one-way ANOVA, whilst non-parametric data were analysed by Mann-Whitney or Kruskal-Wallis tests.

Chapter 3: Characterisation of laminin isoforms in the adult hepatic progenitor cell response

3.1 Introduction

Although an association between hepatic progenitor cells and extracellular laminins has been demonstrated previously by several groups (Lorenzini et al., 2010, Van Hul et al., 2009), the subunit composition of the laminins in this setting has never been described. As the various laminin isoforms can have different effects on cell behaviour, I sought to define the changes in specific laminin chains during the progenitor cell response.

Liver progenitor cells are bipotential and occur in response to both hepatocytic and biliary injury. I have therefore chosen to examine two models of progenitor-mediated injury to reflect these two different regenerative responses. The AhCre-Mdm2^{flox} mouse (which I will hereafter refer to as the 'Mdm2 mouse' for brevity) is a recently described transgenic model that induces hepatocyte-specific injury and induces a robust progenitor cell response (Lu et al, under review). In contrast, DDC is an orally-administered toxin that produces a predominantly biliary injury accompanied by HPCs.

As the Mdm2 mouse is a novel model that was still being developed by our group, I first set out to optimise the induction dosage and to characterise the time-course of progenitor cell expansion.

Using both models, I aimed to characterise the laminin alpha chain expression using a combination of qPCR and immunohistochemistry. I then compared stellate cells and HPCs in culture to identify the cell type responsible for the synthesis of the predominant isoforms. I also aimed to examine the expression of laminin-binding integrins, as potential mediators of the effect of altered matrix on cell behaviour.

3.2 Results

Refinement of a model of hepatocellular injury via conditional deletion of Mdm2

In the transgenic AhCre mouse strain, Cre recombinase is conditionally expressed under the regulation of a rat cytochrome p450 (Cyp1a1) promoter element. This is up-regulated in many of the epithelia of the gastrointestinal tract, including hepatocytes, in response to the xenobiotic beta-naphthoflavone (Ireland et al., 2004). This strain was crossed with a floxed *Mdm2* (murine double minute 2) gene (Grier et al., 2002), resulting in an inducible loss of MDM2 within hepatocytes and other epithelia. This is shown diagrammatically in figure 3.1A. A representative genotyping gel in figure 3.1B shows the amplification products of the AhCre and both wild-type and floxed *Mdm2* alleles. In the following experiments, all mice used had a single copy of the AhCre transgene and were homozygous for the floxed *Mdm2* gene.

MDM2 is a negative regulator of the tumour suppressor gene p53, and loss of MDM2 results in rapid up-regulation of p53. High p53 levels result in cell cycle arrest and can initiate apoptosis.

The initial characterisation of this transgenic model was performed by Thomas Bird, who demonstrated that a single dose of 80 mg/kg of beta-naphthoflavone administered intraperitoneally (i.p.) induced a florid HPC response. However, this model was associated with an unacceptably high mortality. I therefore set out to modify the model, in order to develop a robust model of progenitor-mediated hepatocellular regeneration that remained within moderate severity limits, in which to study the changes in extracellular matrix.

A single dose of 40 mg/kg of beta-naphthoflavone still resulted in significant mortality, with five out of six mice dying or requiring euthanasia by day 7. A further dose reduction to 20 mg/kg was much better tolerated, with the majority of animals surviving to 14 days (figure 3.1C). The 20mg/kg dose was associated with less weight loss at days 5 and 6 after the beta-naphthoflavone injection, and the mice started to gain weight again by day 7 (figure 3.1D). By day 6 after induction, mice

had fallen to 85.5% of their starting weight with the lower dose, compared with 78.0% in the higher dose group.

Having established tolerability, I wanted to assess whether the lower 20 mg/kg dose would still induce adequate liver injury to be a useful model for studying progenitor cells.

As described earlier, genetic recombination will result in loss of MDM2 and subsequent up-regulation of p53. Using p53 immunostaining, Thomas Bird had shown that the 80 mg/kg dose resulted in recombination in more than 99% of hepatocytes. I have shown that the 20 mg/kg dose still resulted in high levels of p53-positive hepatocytes, with approximately 80% of hepatocytes showing nuclear staining 3 days after induction (figure 3.1E).

Figure 3.1 Dose-finding study for the AhCre-Mdm2^{flox} model

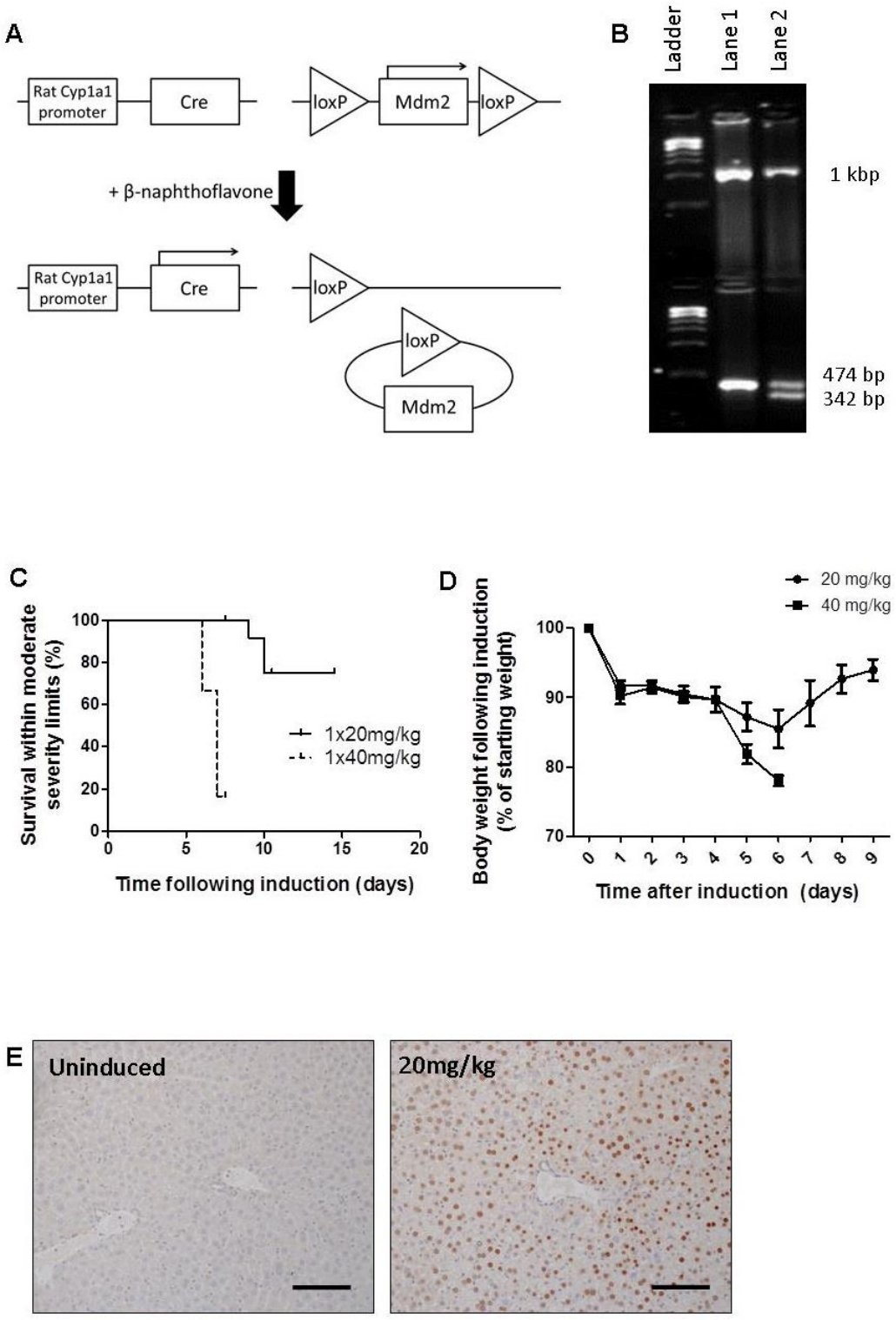

Figure 3.1 – Dose-finding study for the AhCre-Mdm2^{flox} model

A. Activation of the *AhCre* transgene by beta-naphthoflavone results in deletion of the floxed *Mdm2* gene in hepatocytes and other gut epithelial tissues. **B.** A representative genotyping gel shows the amplification products of the *AhCre* transgene (top band, 1 kbp) and both wild-type (342 bp) and floxed (474 bp) *Mdm2* alleles. Lane 1 shows a homozygous flox/flox mouse (experimental animal) and lane 2 shows a heterozygote flox/wild-type (for comparison). **C.** Kaplan-Meier survival curves for high dose (40mg/kg) and low dose (20mg/kg) beta-napthoflavone show significantly lower mortality with the lower dose. Log-rank (Mantel-Cox) test $p<0.0001$. **D.** Weight loss following induction was initially similar between the two groups but there appeared to be a trend towards greater weight loss with the higher dose at later time points. **E.** p53 staining is not seen in an uninduced mouse liver but is seen in the majority of hepatocytes at day 3 after induction with 20 mg/kg, suggesting efficient loss of MDM2. Original magnification x200, scale bars represent 100 μm.

Characterisation of the HPC response in the AhCre-Mdm2 model

Having demonstrated an improved tolerability at the expense of a modest reduction in recombination, I then wanted to see whether this still resulted in liver injury and expansion of the HPCs. I characterised the response to a 20 mg/kg dose of beta-naphthoflavone at days 0, 3, 5, 7, 10 and 14 (figure 3.2A). I measured serum alanine transaminase (ALT) as a measure of hepatocellular injury. Even at the reduced dose, there is still a rapid and statistically significant rise in ALT (figure 3.2B). The median ALT increases from 37 IU/L at day 0 to 508 IU/L at day 7.

To identify HPCs, I stained liver sections for pancytokeratin, a marker of both mature bile ducts and HPCs (figure 3.2C). In the uninjured liver, pancytokeratin staining is mostly limited to the portal tracts and represents bile ducts with very few HPCs. Following induction with beta-naphthoflavone, there is a steady increase in periportal staining, with cords of cells extending into the liver parenchmya. These cells are morphologically typical for HPCs.

For quantification, I counted pancytokeratin-positive cells but excluded those obviously associated with well-defined lumens which represent interlobular bile ducts. There is a significant increase in panCK-positive cells (figure 3.2D), rising from 10.3 cells per field at day 0 to a peak of 53.8 cells per field at day 10.

Because of a lack of consensus for HPC markers, I also stained the livers from the day 10 time point for the alternative HPC markers keratin-19 (figure 3.2E) and osteopontin (figure 3.2F). Both markers show the same pattern of periportal cells extending into the parenchyma, further supporting the claim that these are HPCs.

This model produces a rapid and robust expansion of HPCs following a single defined hepatocellular injury that is greater than that seen with the CDE diet. This also offers the unique opportunity to look at the timecourse of HPC expansion and differentiation in a way that cannot be achieved with the CDE or DDC dietary models, as these will have ongoing injury over a prolonged period with ongoing generation of progenitors.

Figure 3.2 Characterisation of the HPC response in the AhCre-Mdm2^{flox} model

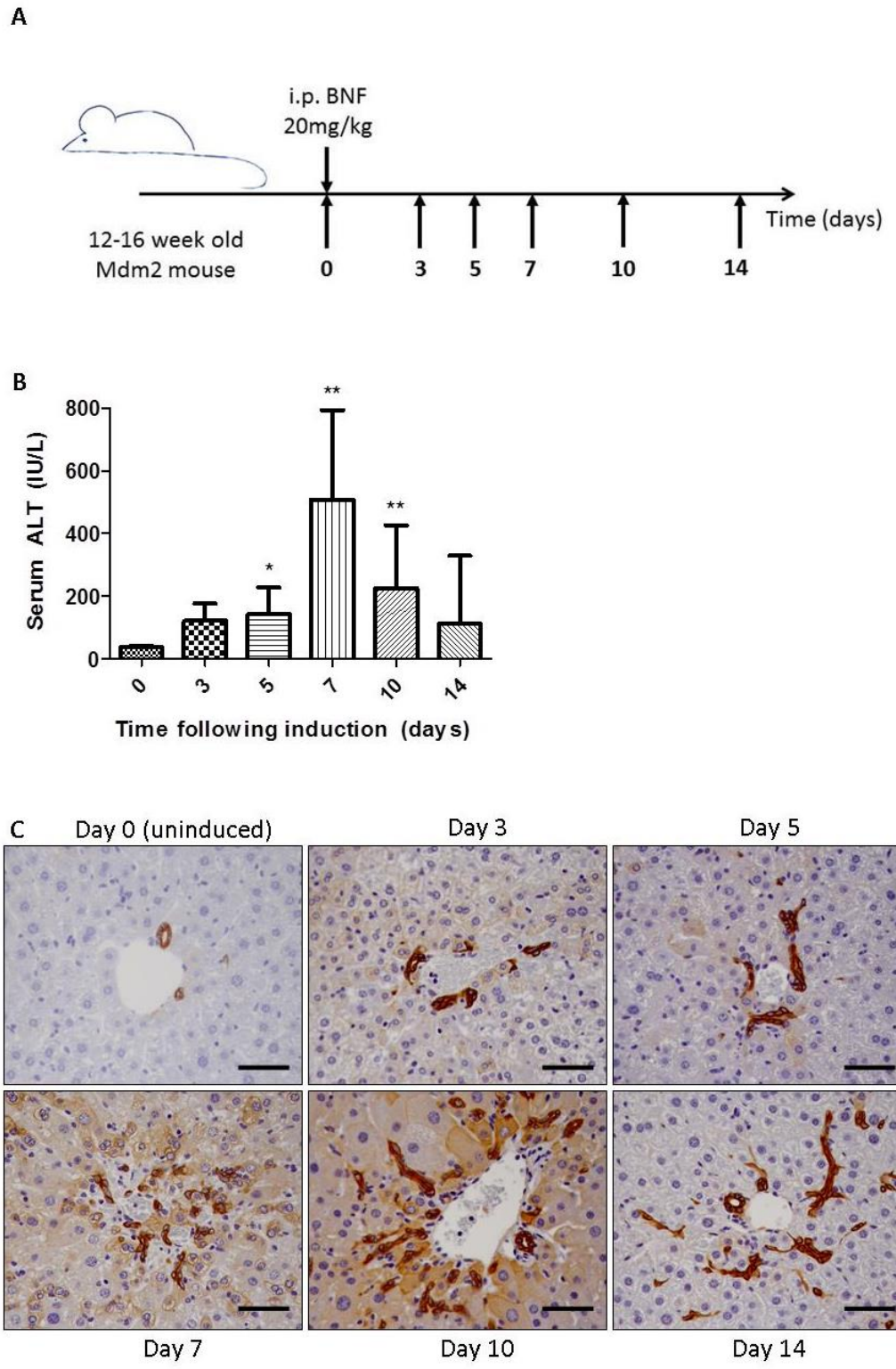

Figure 3.2 Characterisation of the HPC response in the AhCre-Mdm2^{flox} model (cont)

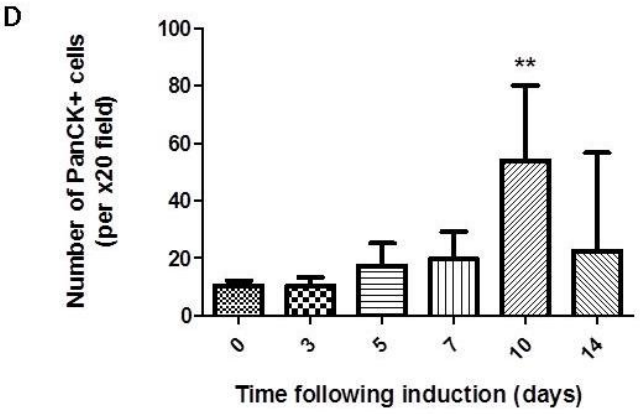

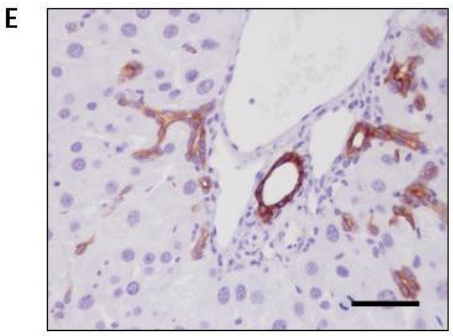

K19

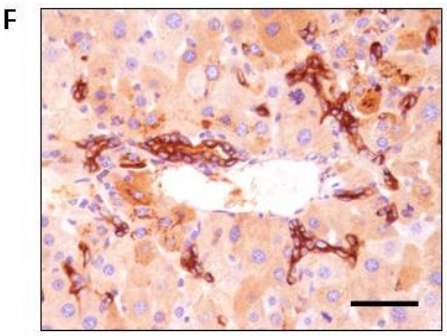

Osteopontin

Figure 3.2 – Characterisation of the HPC response in the AhCre-Mdm2^{flox} model

A. Schematic of experimental design. A single 20 mg/kg dose of beta-naphthoflavone was given intraperitoneally to adult AhCre-Mdm2flox mice, and tissues were harvested at days 0, 3, 5, 7, 10 and 14. **B**. There was a significant elevation of serum alanine transaminase (ALT) levels after induction, with a peak at 7 days. Bars represent median and interquartile range; n=3-6 animals per group, Kruskal-Wallis test p0.007, Dunnett's multiple comparison test for each time point vs day 0 *p<0.05, **p<0.01. **C.** Pancytokeratin (panCK) staining in the normal liver is found predominantly in the bile ducts with very few HPCs seen. Following induction, there is a progressive increase in panCK-positive cells in the periportal areas which then extend into the lobule. **D.** Quantification of panCK-positive cells shows a significant peak at day 10 after induction. Bars represent median and interquartile range; n=4-6 animals per timepoint, Kruskal-Wallis test p0.02, Dunnett's multiple comparison test for individual time points compared to day 0. **E-F.** Staining for keratin-19 and osteopontin shows the same pattern of periportal HPC expansion at day 10. Original magnification x400. Scale bars represent 50 μm.

Characterisation of the HPC niche in the Mdm2 model

HPCs occur in association with a stereotypical niche (Lorenzini et al., 2010, Van Hul et al., 2009). This consists of other cell types (hepatic stellate cells and macrophages) and extracellular matrix (collagen and laminin). As the Mdm2 model is novel, I wanted to confirm that the niche constituents seen in other HPC models are present here too.

Using immunohistochemistry, I compared the livers from the point of maximal HPC numbers (day 10 post-induction) with uninduced livers. Alpha smooth muscle actin staining shows the presence of very few activated myofibroblasts in the uninduced liver (figure 3.3A), contrasted with a marked increase in myofibroblasts in the periportal region at day 10 following induction (figure 3.3B). F4/80 staining shows an even distribution of macrophages throughout the lobule in the uninduced liver (figure 3.3C), with periportal expansion of macrophage numbers at day 10 (figure 3.3D).

Collagen I staining in the uninduced liver (figure 3.3E) is focussed mainly around blood vessels and bile ducts, with minimal sinusoidal staining. At day 10 following induction (figure 3.3F) there is an increase in periportal staining, extending into the lobule. Collagen III staining is very restricted in uninduced liver with minimal blood vessel staining only (figure 3.3G) but is also expanded in the periportal region at day 10 (figure 3.3H).

Figure 3.3 Characterisation of the HPC niche in the AhCre-Mdm2^{flox} model

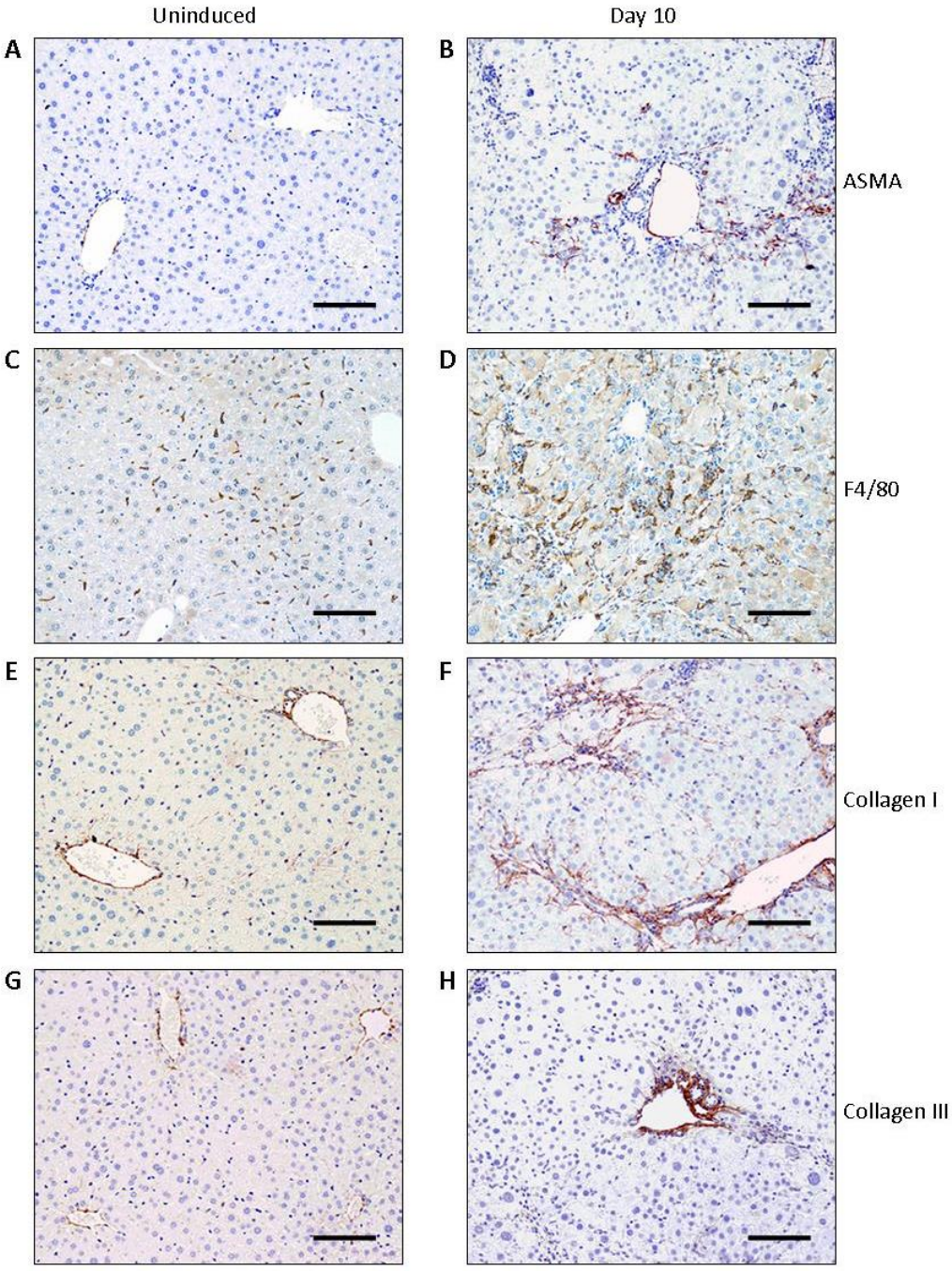

Figure 3.3 Characterisation of the HPC niche in the Mdm2 model

Immunohistochemistry of liver sections from uninduced AhCre-Mdm2^{flox} mice (**A,C,E,G**) and at 10 days after induction with 20mg/kg beta-naphthoflavone (**B,D,F,H**). HPC expansion is accompanied by an increase in both activated myofibroblasts and macrophages, as demonstrated by alpha smooth muscle actin (**A-B**) and F4/80 (**C-D**) staining respectively. There is also an increase in both collagen I (**E-F**) and collagen III (**G-H**) staining. Original magnification x200. Scale bars represent 100 μm.

Biliary injury with DDC triggers a hepatic progenitor cell response

Having established a model of HPC expansion in the setting of hepatocyte injury, I also wanted to examine a model of biliary injury. A well-established paradigm in the literature is the DDC diet. Using archival tissue kindly provided by Luke Boulter, I compared adult mice fed normal chow with those fed 8, 12 or 18 days of DDC-containing diet (figure 3.4A). Using pancytokeratin staining, I was able to demonstrate HPC expansion with increasing duration of diet (figure 3.4B). In the AhCre-Mdm2^{flox} model, the HPCs appeared as infiltrating cords extending into the liver parenchyma. In contrast, in the DDC model, the HPCs retain a ductular appearance and are mostly in contact with a lumen.

As before, these cells also stain for keratin-19 (figure 3.4C) and osteopontin (figure 3.4D), consistent with HPCs.

Figure 3.4 DDC diet induces an HPC response

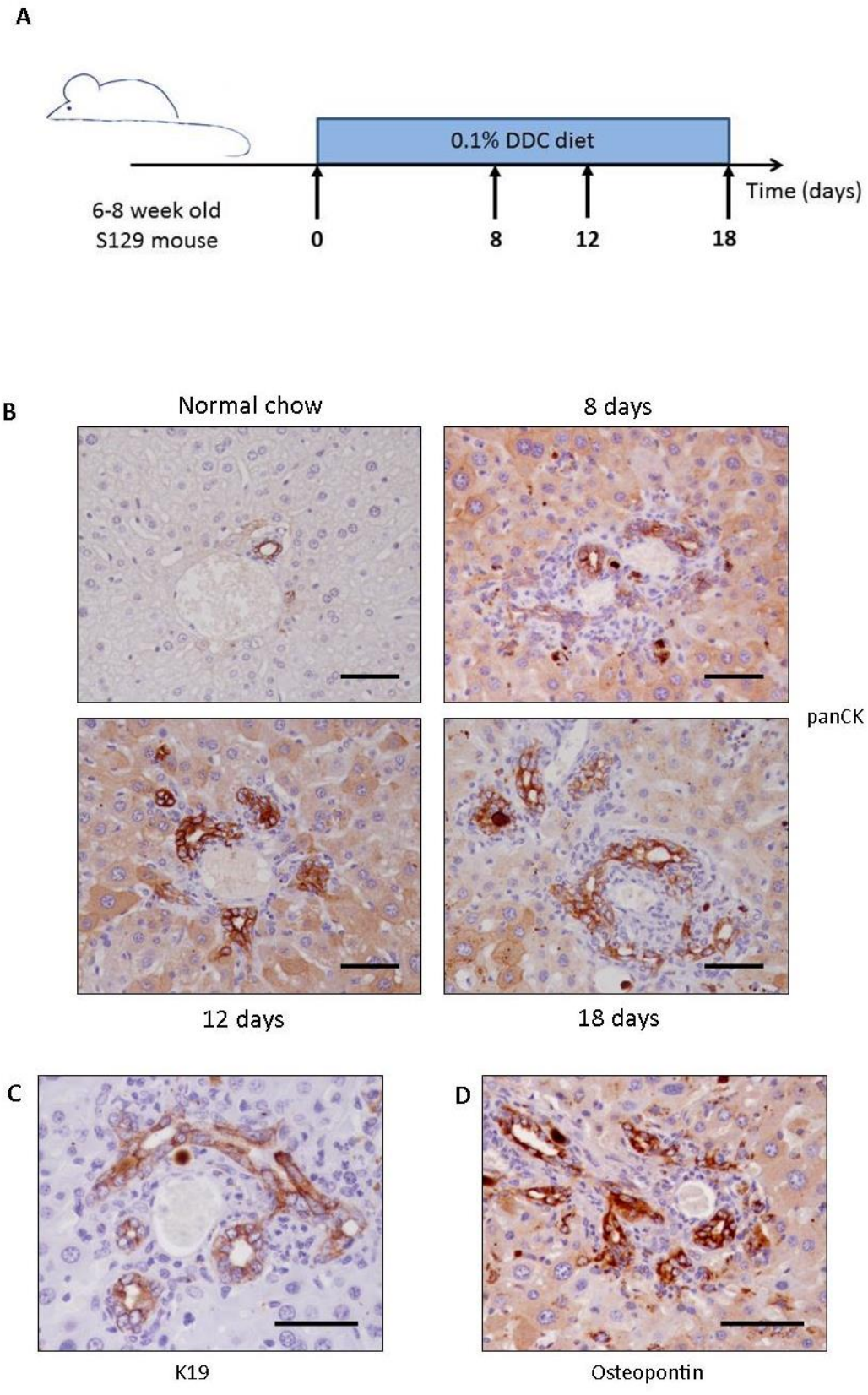

Figure 3.4 – HPC expansion in DDC model

A. Schematic of experimental design. S129 mice aged 6-8 weeks were fed diet containing 0.1% DDC and culled after 0, 8, 12 or 18 days. **B.** Immunohistochemistry for pancytokeratin (panCK) shows a progressive increase in periportal panCK-positive cells with DDC-containing diet. Original magnification x400. Scale bars represent 50 μm. These periportal cells also stain for keratin-19 (**C**) and osteopontin (**D**), consistent with HPCs. Original magnification x600. Scale bars represent 50 μm.

Both models of HPC expansion are associated with increased laminin

Having demonstrated HPC expansion in both of my models, I then sought to confirm the association with extracellular laminin that has been described elsewhere. Using a pan-laminin antibody that binds all isoforms, I performed immunohistochemistry on liver sections from both models. In the normal liver, laminin expression is expected to be mostly restricted to the basement membrane around bile ducts and blood vessels with very little sinusoidal laminin. This is indeed the pattern seen in both the uninduced Mdm2 mice (figure 3.5A,C) and S129 mice fed normal chow (figure 3.5E). Following induction with beta-naphthoflavone, the Mdm2 mice show marked expansion of laminin in the periportal region (figure 3.5B,D). This appears to form a discrete basement membrane-like structure around the HPCs. A similar increase in laminin staining is seen in the S129 mice exposed to DDC-containing diet (figure 3.5F).

In order to better demonstrate the association between HPCs and laminin, I performed dual colour immunofluorescence. In figure 3.5G, the HPCs are shown in red and laminin is shown in green. It can be seen that laminin forms a basement membrane around the bile ducts with projections extending into the parenchyma alongside the HPCs.

Figure 3.5 HPCs are associated with laminin in both models

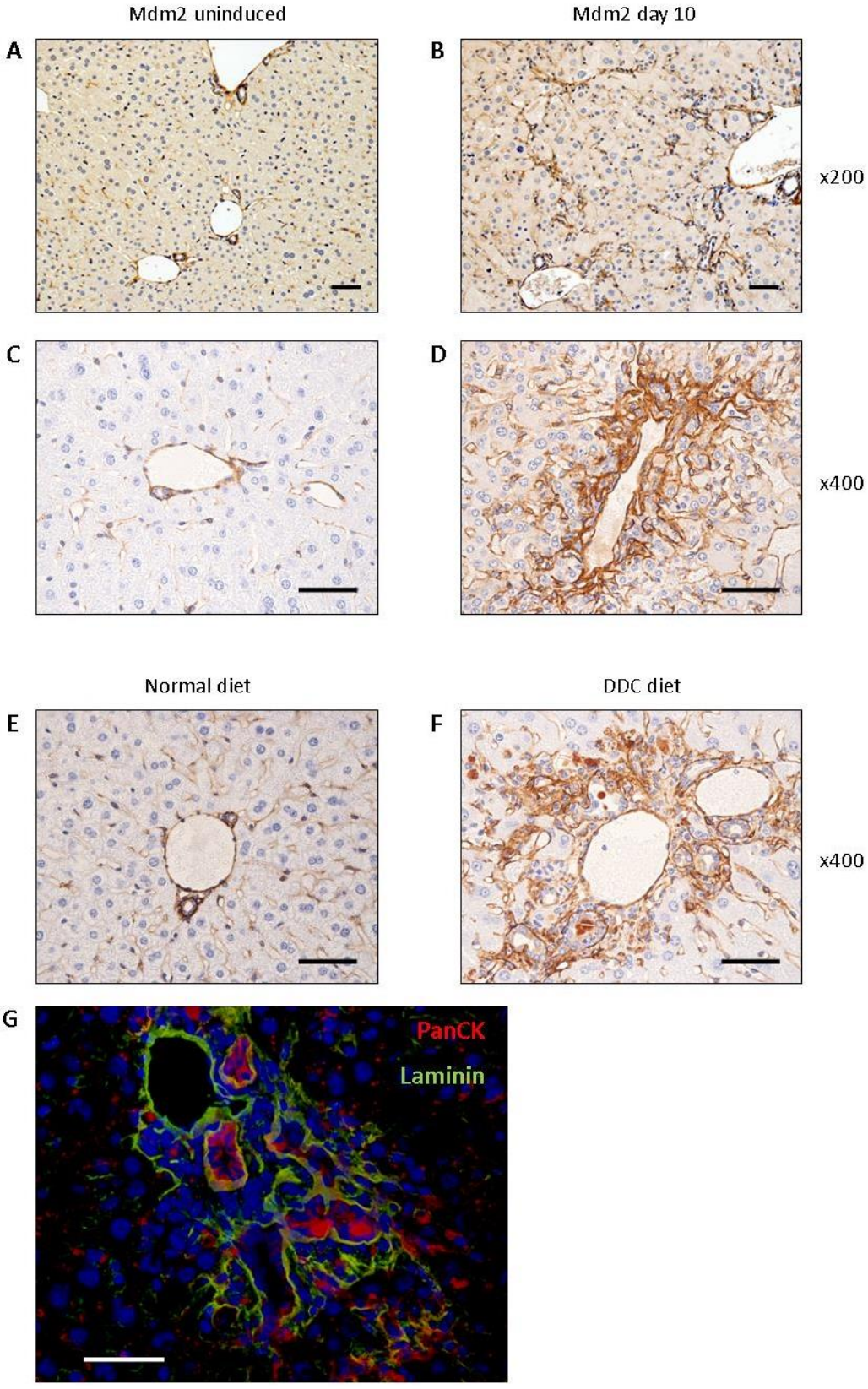

Figure 3.5 –HPCs are associated with laminin in both models

A-F. Immunohistochemistry for laminin. Laminin staining in the uninduced Mdm2 mouse liver (**A** x200 magnification**, C** x400) is restricted to the basement membrane of bile ducts and blood vessels, with no sinusoidal staining. 10 days after induction with 20 mg/kg of beta-naphthoflavone (**B** x200**, D** x400), there is marked expansion of laminin staining in the periportal region. **E-F.** A similar pattern is seen when comparing S129 mice fed normal chow (**E**) and after 18 days of DDC-containing diet (**F**). **G.** Dual colour immunofluorescence shows co-localisation of laminin (green) and panCK (red), with laminin closely surrounding the HPCs in the DDC model. Original magnification x400. Scale bars represent 50 μm.

Laminin alpha 5 chain is upregulated during the HPC response

Having established an increase in laminins in both models of HPC expansion, I then wanted to identify whether specific laminin isoforms were predominant. Extracellular matrix proteins can be regulated by both the rate of synthesis and the rate of degradation. However, given the low levels of laminin expression in the normal liver, I felt it was most likely that the change is due to an increase in synthesis and I therefore started by looking at laminin gene transcription. The alpha chains are believed to be the main determinant of cell surface receptor binding. I therefore performed qPCR on whole liver tissue at multiple time points during the HPC response, looking for mRNA for each of the 5 alpha chains.

The changes in alpha chain transcription in the Mdm2 model are shown in figure 3.6. I firstly looked at the multiple time points after low dose (20 mg/kg) beta-naphthoflavone (figure 3.6A-E). Significant increases were seen in laminin alpha 1 (Figure 3.6A, peak increase of 3.3-fold at day 7) and alpha 5 (Figure 3.6E, peak increase of 13.6-fold at day 7). In contrast, alpha 3 was significantly reduced (Figure 3.6C, peak reduction of 9.4-fold at day 10). There was no significant change from baseline in either laminin alpha 2 or alpha 4.

I also looked at the two time points available from the higher dose (40 mg/kg) of beta-naphthoflavone (figure 3.6F). This showed significant increases in laminin alpha 2 and alpha 5, to 11.5 and 16.5 times their values in the uninjured liver respectively.

The changes in alpha chain transcription in the DDC model are shown in figure 3.7. In this case, significant increases were seen in laminin alpha 2 (Figure 3.7B, 4.7-fold increase at day 12) and alpha 5 (figure 3.7E, 4.2-fold increase at day 12). There was a significant reduction in alpha 3 (figure 3.7C, 17.1-fold reduction at day 18). There was no significant change in laminin alpha 1 or alpha 4.

The consistent change across both models was therefore an increase in laminin alpha 5 (and possibly alpha 2) and a reduction in alpha 3 gene transcription.

Figure 3.6 Laminin alpha chain transcription in the Mdm2 model

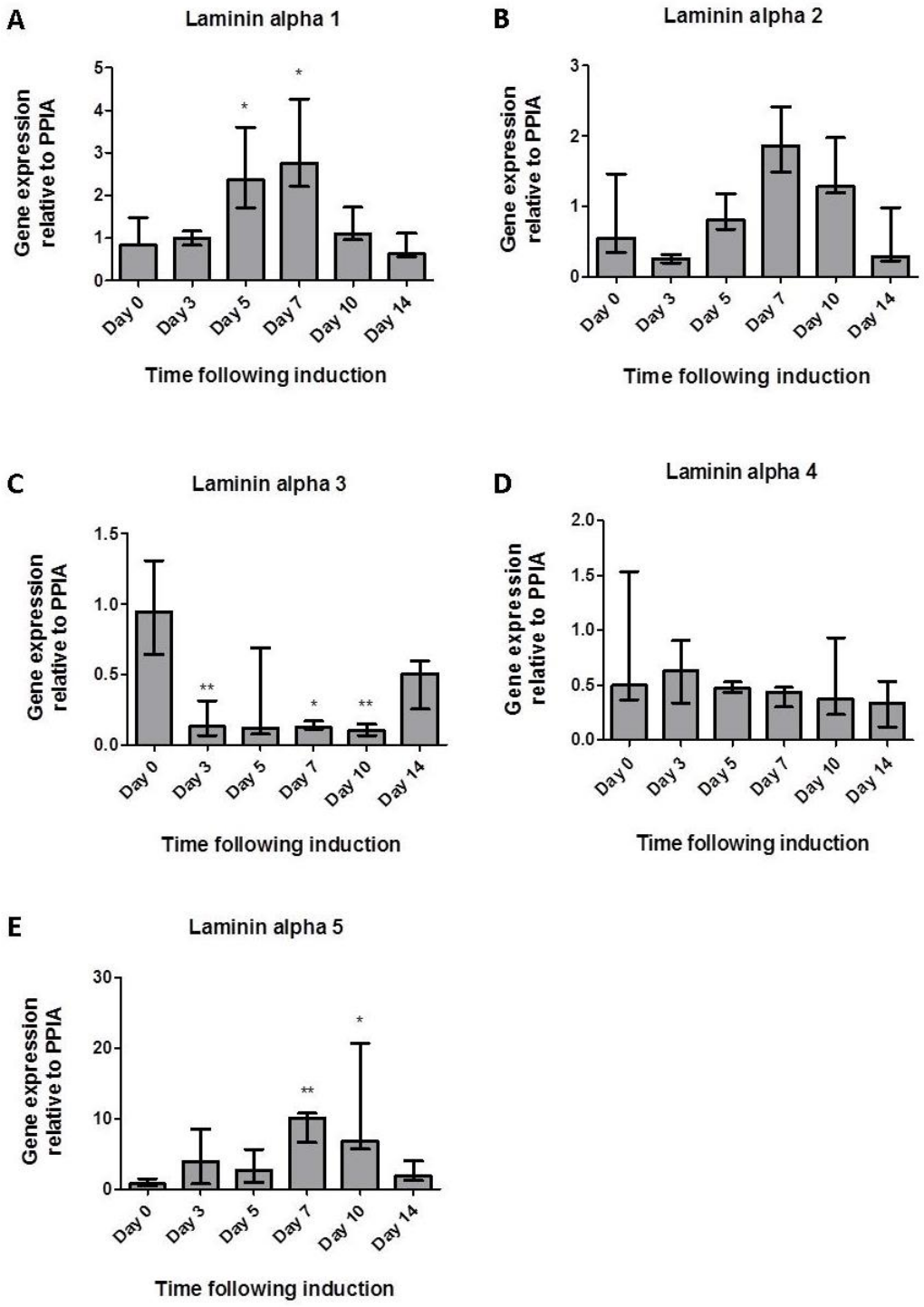

Figure 3.6 Laminin alpha chain transcription in the Mdm2 model

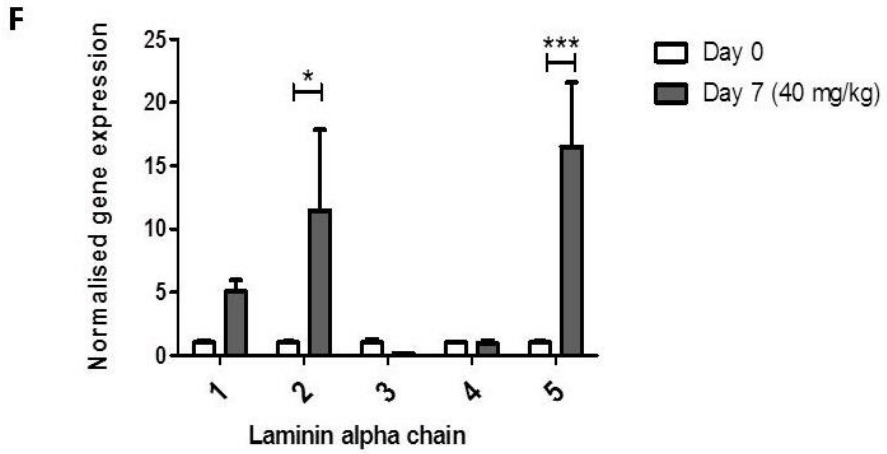

Figure 3.6 – Laminin alpha chain qPCR in Mdm2 model

A-E. AhCre+ Mdm2flox/flox mice aged 12-16 weeks were given a single dose of 20 mg/kg beta-napthoflavone by i.p. injection. Laminin alpha chains were assessed by qPCR of whole liver tissue. Values were normalised to the housekeeping gene PPIA and expressed relative to the expression at day 0. Data are shown as median +/- interquartile range, and were analysed by a Kruskal-Wallis test. Where significant differences were found, Dunnett's multiple comparison test was used to compare each time-point with day 0. * $p<0.05$, ** $p<0.01$. n=3-6 animals per group. **A.** Alpha 1, Kruskal-Wallis, p 0.0018. **B.** Alpha 2, Kruskal-Wallis p NS. **C.** Alpha 3, Kruskal-Wallis p 0.0048. **D.** Alpha 4, Kruskal-Wallis p NS. **E.** Alpha 5, Kruskal-Wallis p 0.0197. **F.** Laminin alpha chain gene expression following high dose (40 mg/kg) beta-naphthoflavone.

Figure 3.7 Laminin alpha chain transcription in the DDC model

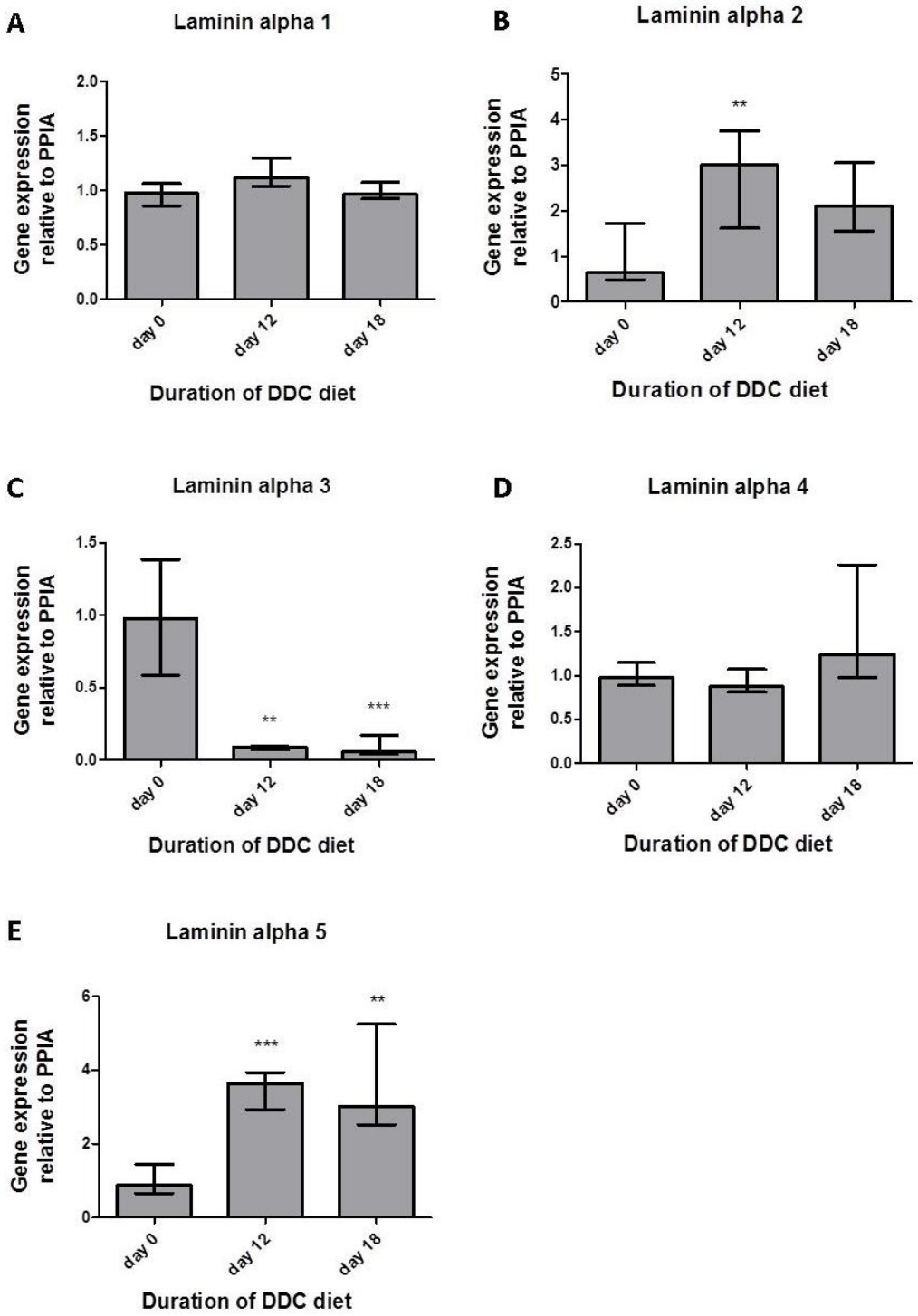

Figure 3.7 – Laminin alpha chain qPCR in DDC model

A-E. S129 mice aged 6-8 weeks were given diet containing 0.1% DDC. Laminin alpha chains were assessed by qPCR of whole liver tissue. Data are shown as median +/- interquartile range, and were analysed by a Kruskal-Wallis test. n=8 animals per group. **A.** Alpha 1, Kruskal-Wallis, p NS. **B.** Alpha 2, Kruskal-Wallis p 0.0048. **C.** Alpha 3, Kruskal-Wallis p 0.0004. **D.** Alpha 4, Kruskal-Wallis p NS. **E.** Alpha 5, Kruskal-Wallis p 0.0005. Where significant differences were found, Dunn's multiple comparison test was used to compare each time point with day 0. *p<0.05, **p<0.01, ***p<0.001.

Laminin alpha 5 chain closely associates with the HPCs

Having shown differential gene expression for the laminin alpha chains during the HPC response, I wanted to confirm these changes at a protein level. I therefore performed immunohistochemistry using antibodies specific for laminin alpha 1, alpha 2 and alpha 5 chains in both the Mdm2 (figure 3.8A) and DDC (figure 3.8B) models. It can be seen that there is a slight increase in laminin alpha 1 and 2 chains, but the most striking increases are seen in laminin alpha 5.

Dual immunofluorescence was used to confirm the colocalisation of laminin alpha 5 with the HPCs (figure 3.8C). As the previously described markers (panCK, K19, osteopontin) are all stained for using antibodies raised in the same species as the laminin alpha 5 antibody (rabbit), I used an alternative HPC marker called A6 which is raised in a different species (rat) to avoid any cross-reactivity. This marker is well-described in the DDC model (Preisegger et al., 1999). It can be seen that the HPCs are closely associated with the laminin alpha 5.

Figure 3.8 Laminin alpha 5 closely associates with HPCs

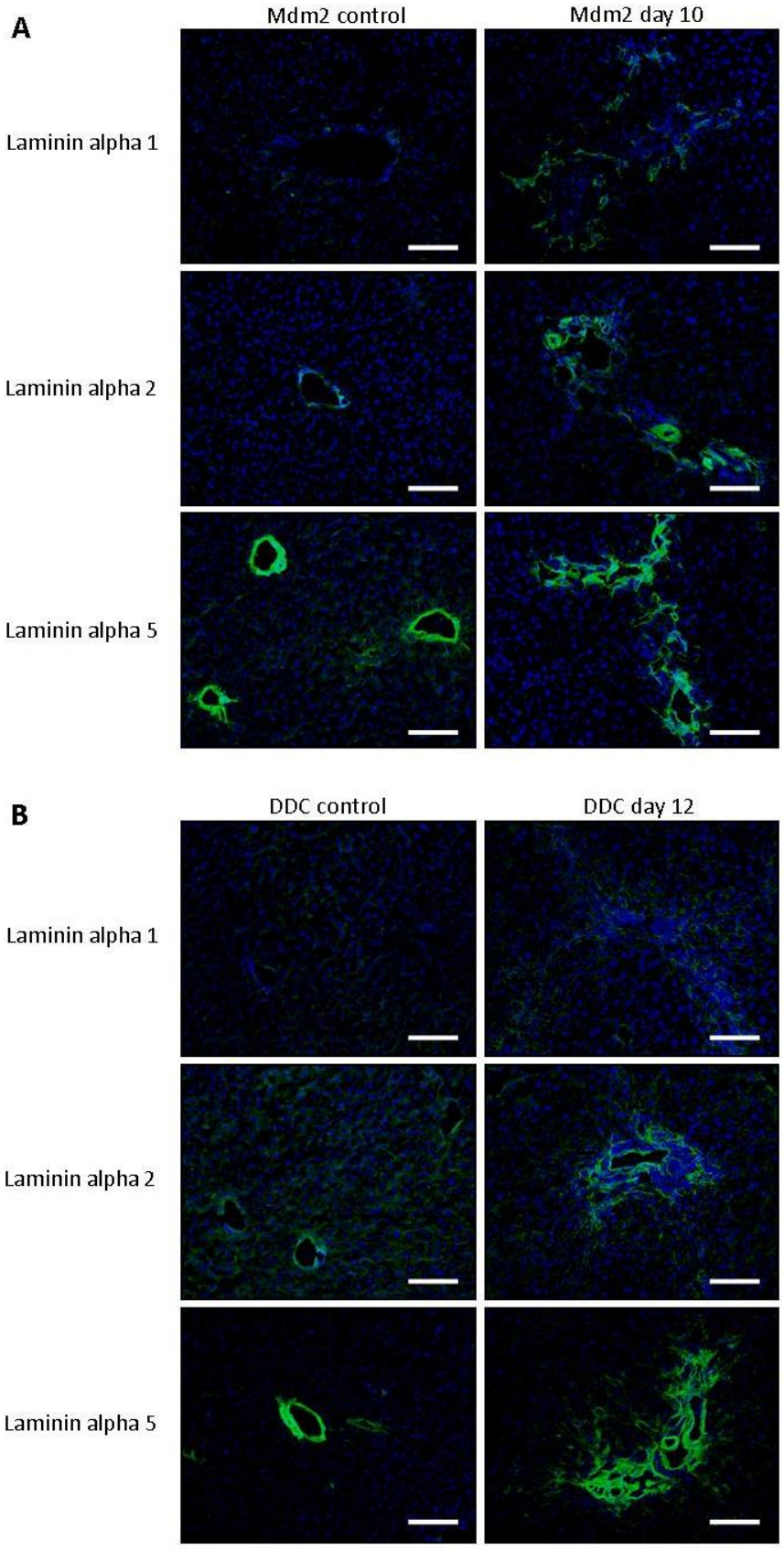

Figure 3.8 Laminin alpha 5 closely associates with HPCs

C

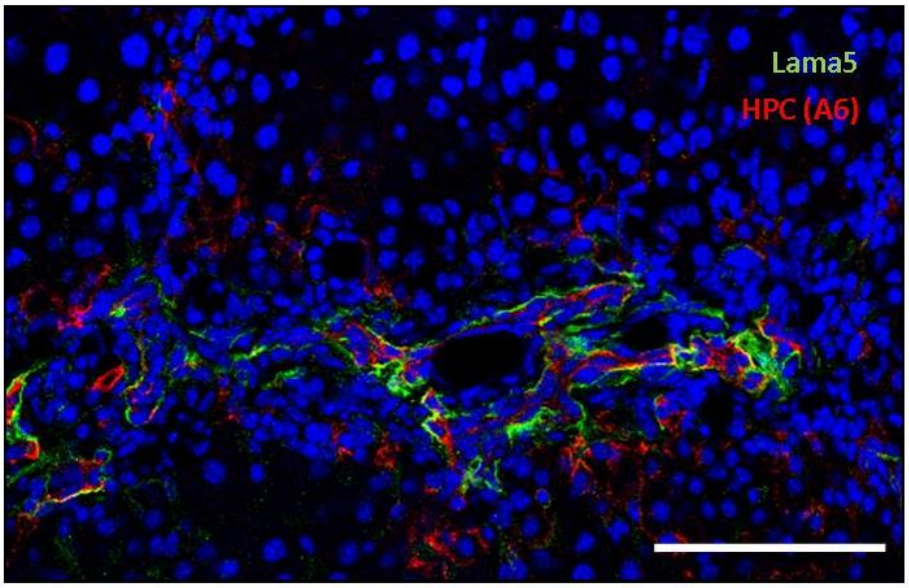

Figure 3.8 – Lama5 co-localises with HPCs

A. Immunofluorescence for laminin alpha 1, 2 and 5 on frozen sections from Mdm2 model. Panels on the left show the control livers and those on the right show regenerating livers, at day 10 after induction with beta-naphthoflavone. Although there are slight increases in alpha 1 and alpha 2 chains, the most striking change is an increase in laminin alpha 5 deposition in the periportal region. Original magnification x200. Scale bars represent 50 micrometers. **B**. Immunofluorescence for the same laminin chains in the DDC model, after 12 days of diet shows a similar pattern of changes. Original magnification x200. **C**. Confocal microscopy showing colocalisation of laminin alpha 5 with the hepatic progenitor cell marker A6. Scale bar represents 100 micrometres.

Laminin alpha 5 is seen in human liver disease

In order to confirm the relevance of these findings in mouse models to human disease, human liver tissue was obtained from the NHS Lothian Tissue Bank. Sections were obtained from explanted livers of patients undergoing liver transplantation for cirrhosis secondary to alcoholic liver disease, hepatitis C and primary sclerosing cholangitis. Sections were stained for pancytokeratin to demonstrate the presence of a ductular reaction (figure 3.8 A,C and E). Sections from the same livers were also stained for laminin alpha 5 (figure 3.8 B, D, F and G). Laminin alpha 5 expression is seen in each of the livers with a predominantly ductular distribution, suggesting its association with HPCs.

Figure 3.9 Laminin alpha 5 is seen in human liver disease with ductular reactions

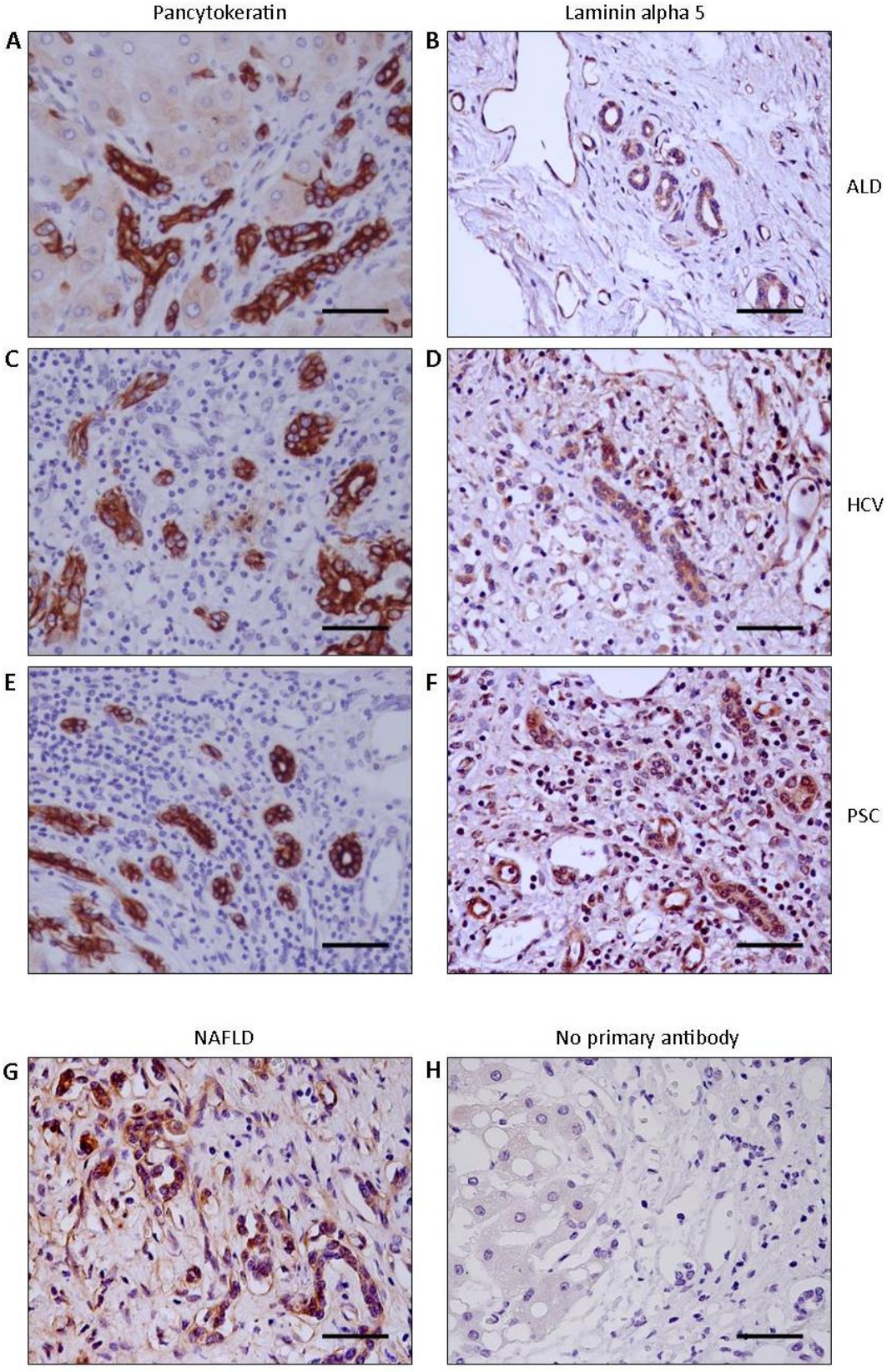

Figure 3.9 – Laminin alpha 5 is seen in human liver disease with ductular reactions

Human liver sections from patients with alcoholic liver disease (**A-B**), hepatitis C (**C-D**), primary sclerosing cholangitis (**E-F**) and non-alcoholic fatty liver disease (**G**). Pancytokeratin staining (**A,C,E**) confirms the presence of ductular reactions in all livers. Staining for laminin alpha 5 (**B,D,F,G**) shows the same ductular pattern of staining. A negative control performed without primary antibody did not show any staining (**H**). Original magnification x400 for all images, scale bar represents 50 μm.

HPCs synthesise laminin alpha 5

Having confirmed increased expression of laminin alpha 5 during regeneration, I wanted to identify the cellular source of the matrix. Hepatic stellate cells are the main matrix-producing cells in the liver, and are the predominant source of collagen during liver injury. Given the close association between HPCs and stellate cells, they would seem a likely candidate for the source of the laminin. However, as fetal hepatoblasts synthesise laminin during liver development, it is also possible that HPCs produce their own laminin niche.

In order to address this question, I isolated both stellate cells and HPCs from the Mdm2 mouse model using density centrifugation and selective culture conditions (figure 3.10A). I then compared their transcription patterns for the different laminin alpha chains using qPCR. Figure 3.10B shows that laminin alpha 1 mRNA expression is 10-fold higher in stellate cells than progenitors, and alpha 2 expression is 21-fold higher in stellate cells. Both of these just fail to reach statistical significance with p values of 0.06. Conversely, laminin alpha 5 is the only chain which appears to be produced predominantly by progenitor cells rather than stellate cells, with 2.5-fold higher mRNA levels (p 0.11). Although none of these changes reached statistical significance, there were only 3-4 samples per group. Furthermore, the cell populations were enriched for stellate cells or HPCs through selective culture conditions but were not exclusive populations. There is likely to have been contamination from other cell types that will tend to reduce any differences.

In order to confirm this result, I therefore also examined data that I extracted from a published gene array (Dorrell et al., 2011). The data are accessible at the NCBI GEO database (Edgar et al., 2002), accession number GSE29121. In this study, adult hepatic progenitor cells were isolated from DDC-treated mice using flow-assisted cell sorting for the cell surface markers CD133 and MIC1-1C3. A progenitor-enriched population (CD133+, MIC-1C3+) was compared with the progenitor-depleted (CD133-, MIC1-1C3-) non-parenchymal cells. Gene expression profiling was perfomed using Agilent Whole Mouse Genome Arrays. As shown in figure 3.10C, the progenitor cells expressed significantly higher levels of the laminin alpha

5 chain (13.8-fold higher, $p<0.05$), whereas the progenitor-depleted cells expressed higher levels of laminin alpha 1 and 2.

These data suggest that laminin alpha 5 is being synthesised predominantly by the progenitor cells themselves, in contrast to other laminin alpha chains which are being produced mainly by stellate cells.

This is in keeping with the situation in intestinal development, where it has been shown that laminin alpha 2 comes from mesenchymal cells whereas laminin alpha 5 comes from epithelial cells (Lefebvre et al., 1999).

Figure 3.10 HPCs synthesise laminin alpha 5

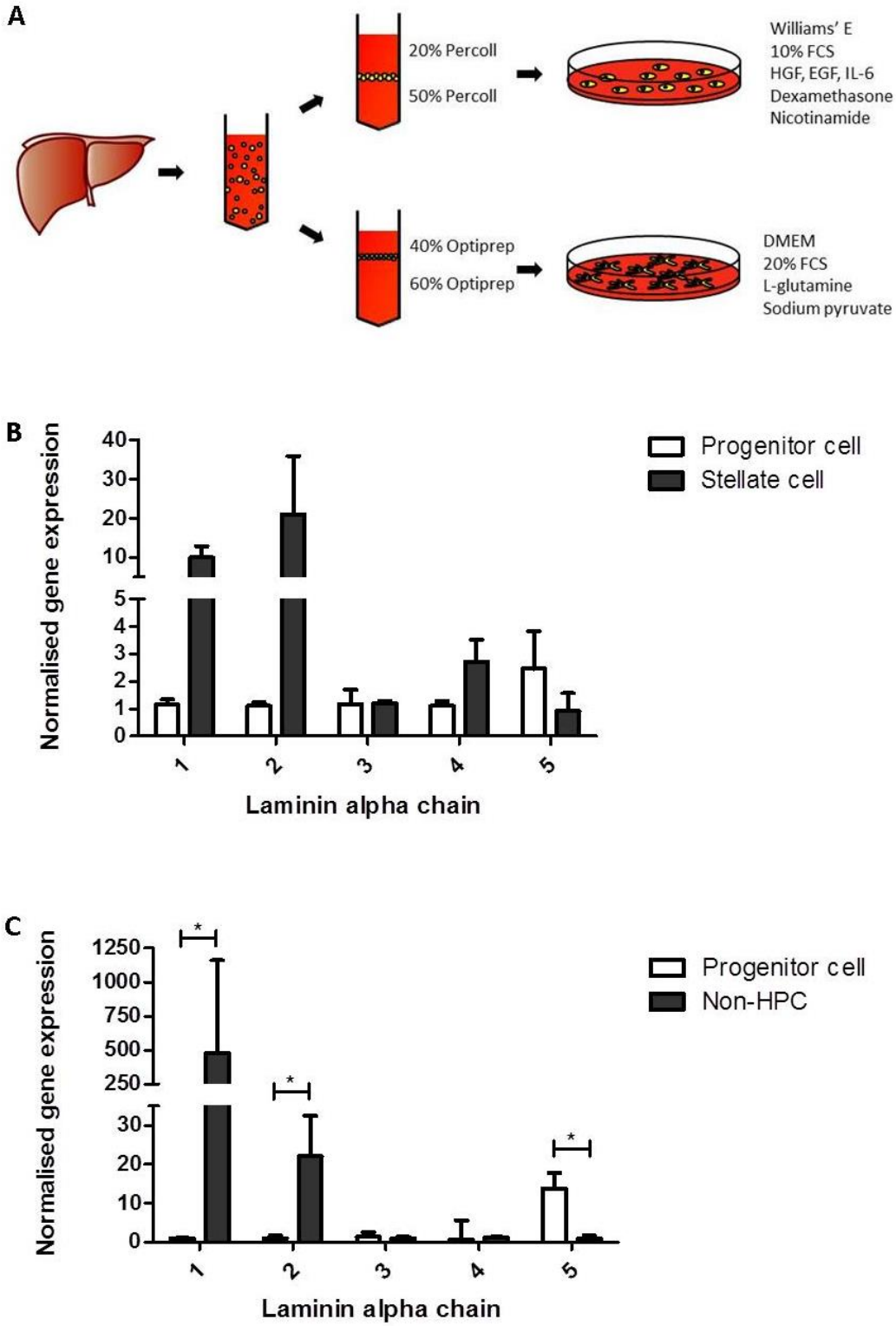

Figure 3.10 – Cellular source of laminin alpha 5

A. Livers from Mdm2 mice 7 days after induction were digested and purified using two protocols of density centrifugation followed by selective culture conditions to enrich for stellate cells and progenitor cells respectively. **B**. qPCR for laminin alpha chain gene expression from stellate cells and hepatic progenitor cells. Gene expression is normalised to the house-keeping gene PPIA. n=4 samples for progenitor cells, n=3 samples for stellate cells. No differences reached statistical significance by Mann-Whitney test but there was a trend towards higher laminin alpha 5 expression by the progenitor cells rather than stellate cells. **C.** Analysis of gene microarray data extracted from the GEO database from an original experiment by Dorrell et al (2011). Progenitor cells were isolated from the DDC model using flow-activated cell sorting for CD133+ and MIC1-1C3+ cells, and compared with progenitor-depleted (CD133- MIC1-1C3-) non-parenchymal cells. n=4 samples for both groups. This showed laminin alpha 1 and 2 expression was greater in the progenitor-depleted population and alpha 5 expression was greater in the progenitor-enriched population. Expression of each gene was compared using a Mann-Whitney test. *$p<0.05$.

Laminin-binding integrins are upregulated during HPC expansion

Laminin can interact with a range of cell surface receptors to influence cell behaviour. The best described of these are the integrin family. These are heterodimers, consisting of an alpha and beta subunit. The integrins that are most widely accepted as laminin receptors are α3β1, α6β1, α7β1 and α6β4. I therefore looked at the transcription of these subunits in the models that I have already described. I selected the time points of maximal gene transcription for laminin alpha 5 (day 7 in the Mdm2 model and day 12 in the DDC model) and performed qPCR using whole liver tissue.

In the Mdm2 model (figure 3.11A), both the α3 and α6 integrin subunits are upregulated approximately 10-fold during regeneration, with no change in α7 expression. The β1 integrin subunit is upregulated 2.7-fold, and there is a trend towards an increase in β4 integrin (p 0.11).

In the DDC model (figure 3.11B), both α3 and α6 integrins are again upregulated (1.8 and 4.9-fold, respectively), whereas α7 integrin is down-regulated. There is no change in β1 expression and a 3.0-fold increase in β4 integrin.

Alpha 3 integrin only associates with beta 1 integrin, and has no other known binding partners. The failure to demonstrate upregulation of the corresponding beta 1 subunit in the DDC model may be due to a switch of existing beta 1 integrin from one or more of its other binding partners to favour alpha 3 integrin, rather than requiring increased synthesis.

Alpha 6 integrin may associate with either beta 1 or beta 4 integrin. It is not clear from the data presented which of these is the main binding partner in this context, and it is possible that both are present.

Although these data suggest an increase in gene expression for various laminin-binding integrins at a time that corresponds to HPC expansion, it is not clear whether the integrins are expressed on the HPCs. It is also worth acknowledging here that integrin function is not necessarily regulated at a transcriptional level. Integrin affinity can be regulated by intracellular signals that result in conformational

changes, so-called inside-out signalling. Therefore an increase in gene transcription is not equivalent to an increase in integrin signalling. Nevertheless, this data identifies potential laminin-binding receptors to investigate further.

Figure 3.11 Laminin-binding integrins are upregulated in regeneration

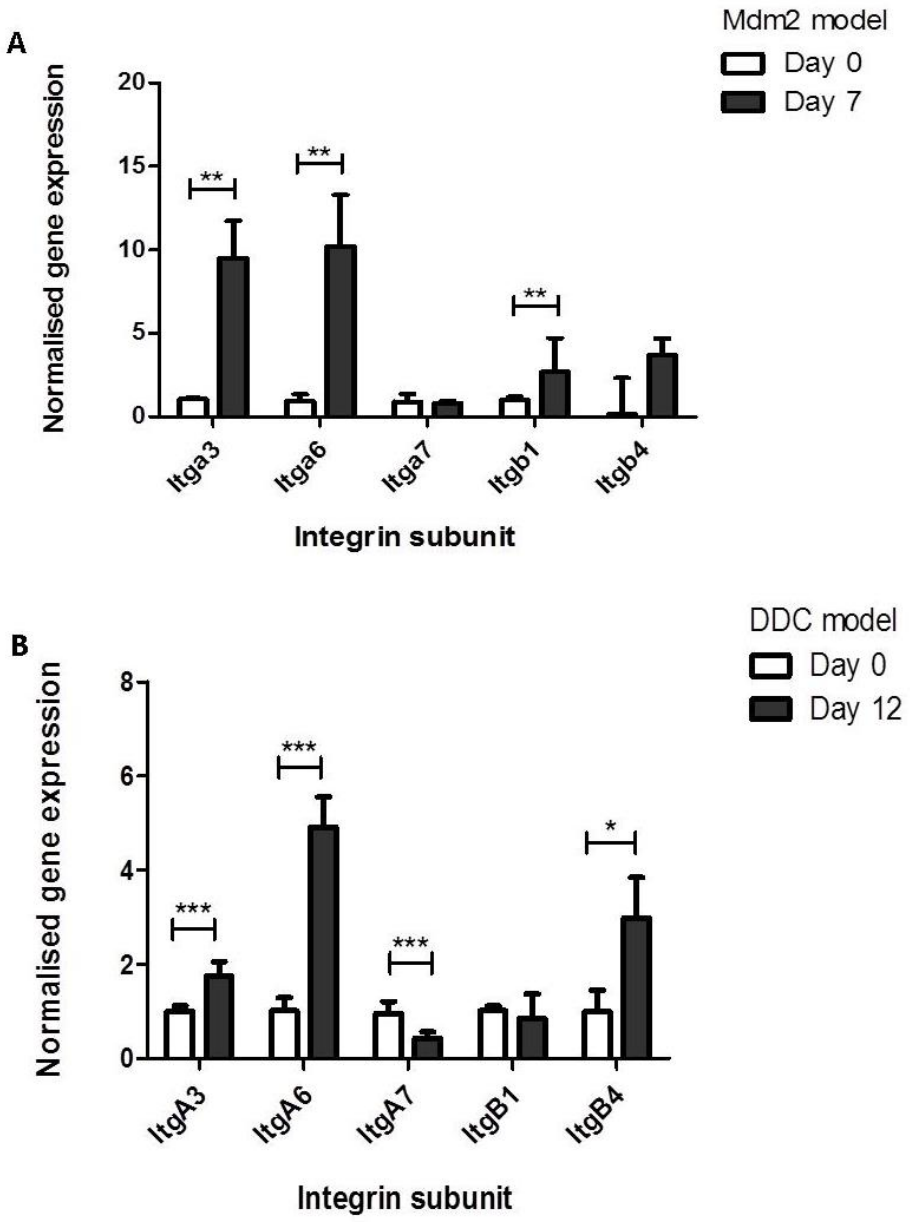

Figure 3.11 – Expression of laminin-binding integrins during regeneration

A. AhCre+ Mdm2flox/flox mice aged 12-16 weeks were given a single dose of 20 mg/kg beta-napthoflavone by i.p. injection. Integrin subunits were assessed by qPCR of whole liver tissue, which showed upregulation of alpha 3, alpha 6 and beta 1 subunits during HPC expansion. n=6 animals at day 0, n=4 animals at day 7. **B.** The same analysis was performed in S129 mice aged 6-8 weeks given diet containing 0.1% DDC. n=8 animals per group. In this case, there was upregulation of alpha 3, alpha 6 and beta 4 subunits during the HPC response. All data are shown as median +/- interquartile range, and were analysed by a Mann-Whitney test. * $p<0.05$, ** $p<0.01$, ***$p<0.001$.

HPCs express laminin-binding integrins

Having demonstrated an increased expression of various integrin subunits at the whole tissue level, I wanted to establish whether any of these were expressed on the HPCs themselves. I therefore performed immunohistochemistry on liver sections from the Mdm2 model. Alpha 3 integrin did not appear to be expressed on HPCs, whereas both alpha 6 integrin and beta 1 integrin do appear to colocalise with HPCs. Attempts to stain for beta 4 integrin were unsuccessful.

Figure 3.12 HPCs express laminin-binding integrins

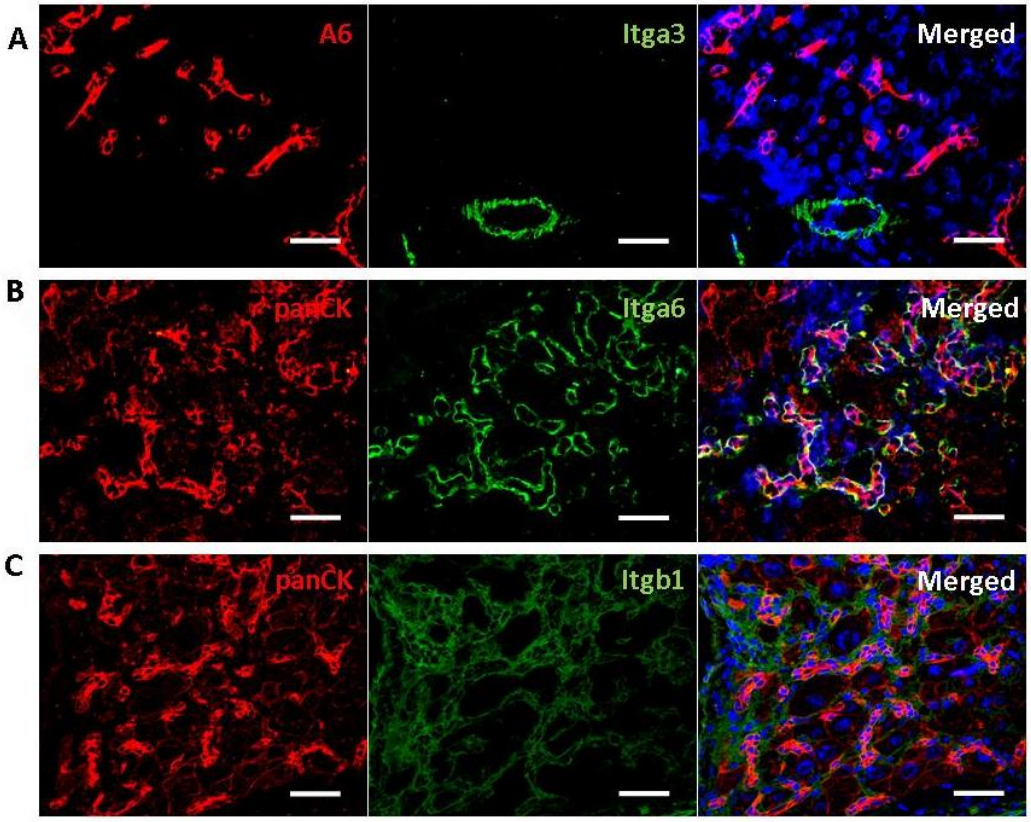

Figure 3.12 – HPCs express laminin-binding integrins

A-C. Immunohistochemistry on frozen sections from the Mdm2 model. Livers harvested 10 days after induction with 20mg/kg beta-naphthoflavone. **A.** HPC marker A6 (red) and integrin alpha 3 (green) show separate non-overlapping staining patterns. **B.** HPC marker panCK (red) and integrin alpha 6 (green) appear to co-localise. **C.** HPC marker panCK (red) and integrin beta 1 (green) also appear to be co-expressed, although beta 1 integrin is also expressed across the other non-progenitor cells. Original magnification x200. Scale bar represents 50 μm.

3.3 Discussion

Although the association between HPCs and extracellular laminins is well-described, the detailed composition of the laminin isoforms in this setting has not been described.

In order to study this further, I have first refined a model of HPC expansion in the context of hepatocellular injury. The Mdm2 mouse model allows conditional deletion of MDM2 within hepatocytes in response to the xenobiotic beta-naphthoflavone. I have demonstrated that a single low dose of beta-naphthoflavone (20 mg/kg) administered intraperitoneally is sufficient to stimulate robust progenitor cell expansion that peaks 7-10 days after induction. I have compared this with the DDC model, in which mice are fed a diet containing the toxin DDC to stimulate progenitor cell expansion associated with biliary regeneration.

In both mouse models, there is upregulation of laminin alpha 5 gene transcription, with increased deposition in the periportal region. This laminin alpha 5 closely associates with the HPCs, forming a basement membrane-like structure around the ductules. Laminin alpha 5 is also shown in the ductular reaction seen in human liver disease.

The laminin alpha 5 chain occurs predominantly as laminin-511, which is found in epithelia, endothelia and smooth muscle. It can also form laminin-521 which has a similar distribution but is also found at the neuromuscular junction and in the glomerular basement membrane within the kidney. Lastly, it can occur as laminin-523 which is described in the retina and central nervous system. As the beta and gamma chains tend to have less marked variation, I have not characterised these to date. However, both the beta and gamma chains are capable of influencing receptor binding to some degree (Taniguchi et al., 2009, Ido et al., 2008). It would therefore be of interest to further delineate the other laminin chains involved in HPC expansion.

Laminin alpha 5 is the main alpha chain seen around mature bile ducts (Kikkawa et al., 2005). Given the origin of HPCs from the canals of Hering and the continued

expression of a number of biliary markers, it is perhaps not surprising that this is the main isoform expressed during HPC expansion. However, this is in contrast to the laminin which is transiently expressed in the liver following partial hepatectomy, which is predominantly laminin alpha 1.

Laminin alpha 5 has been shown to have an important role in the morphogenesis of a number of tissues, including teeth (Fukumoto et al., 2006), hair (Li et al., 2003a), small intestine (Mahoney et al., 2008), lung (Nguyen et al., 2005) and submandibular gland (Rebustini et al., 2007). There is also work showing increased expression of laminin alpha 5 in human malignancies, including colorectal and breast cancers (Hewitt et al., 1997). However, there is little work looking at laminin-511 in relation to adult tissue stem cells.

I have isolated both stellate cells and hepatic progenitor cells from the Mdm2 model, using density centrifugation and selective culture conditions. There was a non-significant trend towards higher expression of laminin alpha 1 and alpha 2 mRNA by cultured stellate cells compared to progenitors, in comparison to higher laminin alpha 5 mRNA expression by progenitors. Similar results are seen using a published microarray result, using FACS-isolated cells from mice fed a DDC diet. A progenitor-enriched population showed significantly higher expression of laminin alpha 5 and lower levels of alpha 1 and alpha 2 than the progenitor-depleted population.

These results are consistent with other related work in the field. During regeneration after partial hepatectomy, the increase in laminin alpha 1 was produced by stellate cells (Kikkawa et al., 2005). During fetal liver development where laminin alpha 5 has been shown to play a role, this is produced by the hepatoblasts themselves (Tanimizu et al., 2012). Although my work suggests that HPCs represent a significant source of laminin alpha 5 during regeneration, this is not proven beyond doubt. The methods of cell purification are not completely specific and there is likely to be a degree of contamination with other cell types. Furthermore, I did not look at other cell types such as endothelial cells. This could be addressed by using in situ hybridisation on liver sections from both models to provide a more accurate

comparison of all of the possible cellular sources of laminin alpha 5, but it was felt that this was beyond the scope of this thesis.

Finally, I have shown that there is increased expression of certain subunits of laminin-binding integrins (α3, α6, β1 and β4) during HPC expansion. It is important to note when considering the qPCR data that integrin function may not relate directly to transcription levels, as conformational changes play a significant role in regulating their activity. Furthermore, some subunits (especially β1) exist in multiple pairings and so a switch in binding partner may occur without requiring an increase in transcription. The α6 and β1 subunits appear to co-localise with the HPCs, suggesting a possible mechanism by which the extracellular laminin could modulate HPC behaviour.

The descriptive work outlined in this chapter identifies laminin alpha 5 as the predominant alpha chain expressed around HPCs, and led me to perform further experiments to compare the effects of the different laminin alpha chains on HPC behaviour.

Chapter 4: Defining the effects of laminin isoforms on hepatic progenitor cell behaviour in vitro

4.1 Introduction

Having established a specific pattern of laminin alpha chain expression, I then wanted to investigate the ability of the different laminin alpha chains to influence hepatic progenitor cell behaviour. In order to assess this, I have performed a number of in vitro experiments.

I have used the Bmol cell line which is derived from adult hepatic progenitor cells isolated from mice fed a CDE diet and which have undergone spontaneous immortalisation (Tirnitz-Parker et al., 2007). Following liver digestion, a Percoll density centrifugation gradient was used to generate primary cultures that were 50-80% pure for A6-positive and K19-positive cells by day 7. Colonies were trypsinised and serially diluted to obtain single cell cultures, some of which overcame growth inhibition to form clonally-derived lines. Bmol cells express phenotypic markers of both biliary and hepatocytic lineages, and can be differentiated towards hepatocytes using dexamethasone with insulin-transferrin-selenium and nicotinamide.

To look at specific laminin chains, I have used commercially-available recombinant laminins. These are produced from transfected human embryonic kidney cancer cells (HEK293) and purified using chromatography (Doi et al., 2002). In order to selectively study the effects of the alpha chains, I compared isoforms that all shared the common beta-1 and gamma-1 chains: laminin-111, -211, -411 and -511. The laminin-311 isoform is not available commercially and is relatively uncommon, as the alpha-3 chain occurs predominantly as the trimer laminin-332. In the previous chapter, I have shown that the alpha 3 chain is down-regulated in both models of HPC expansion so I felt that this was not a major omission.

In this chapter, I briefly compare the laminin alpha chain expression profile of the Bmol cell line with the HPC models presented in the previous chapter. I then use

exogenous recombinant laminins to examine the effect of specific laminin alpha chains on cell adhesion, migration, proliferation and differentiation. In order to demonstrate the effect of endogenous laminin synthesis on proliferation and differentiation, I also use small interfering RNA (siRNA) to laminin alpha 5.

4.2 Results

Validation of the progenitor characteristics of the Bmol cell line

Prior to using this cell line for experiments, I first established that they showed the expected characteristics of adult hepatic progenitor cells. As there is no universal specific marker for HPCs, I have tested for a panel of markers that have been shown to be present on progenitors. Bmols all express the HPC markers that I used in the previous chapter, namely pancytokeratin, keratin-19 and osteopontin (figure 4.1A-C). Bmols also stained for MIC1-1C3 (figure 4.1D), an antibody that enriches for bipotential clonogenic adult progenitors (Dorrell et al., 2011), and sox9 (figure 4.1E), a nuclear transcription factor that has been shown to label HPCs in a lineage tracing experiment (Furuyama et al., 2011).

Figure 4.1 Bmols express adult hepatic progenitor cell markers

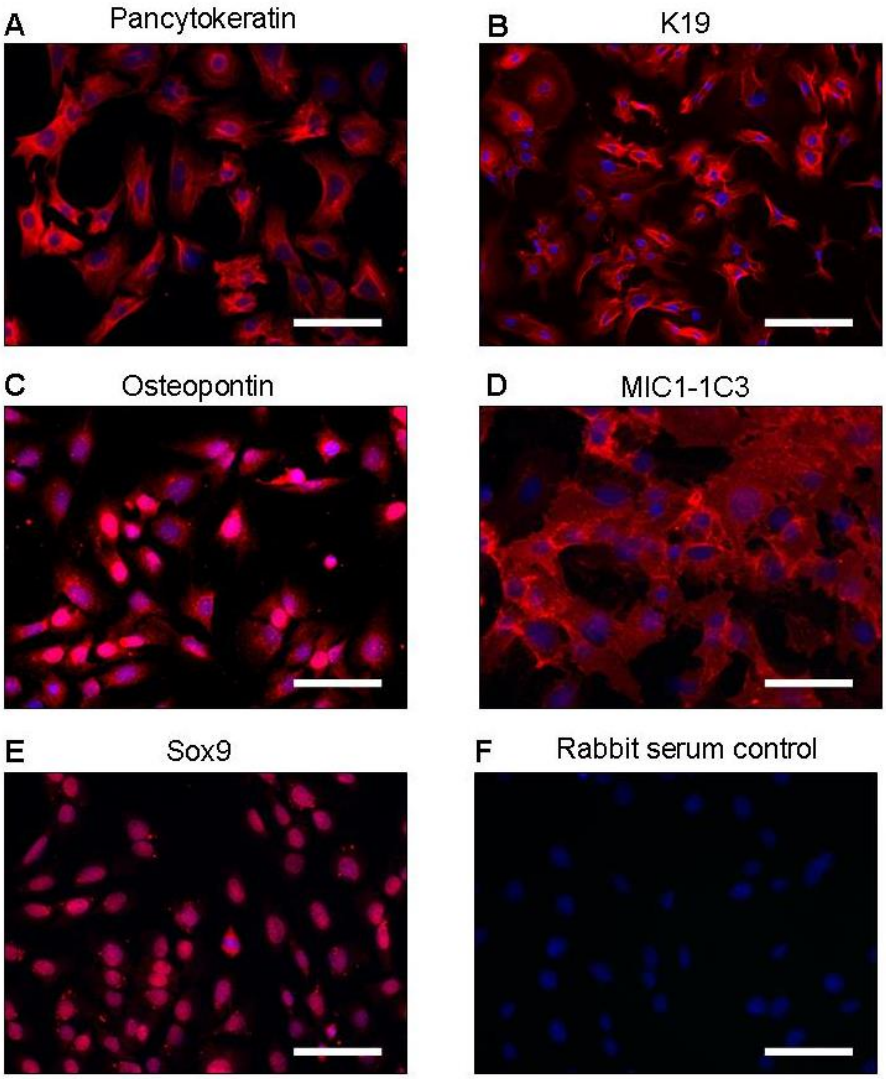

Figure 4.1 – Bmols express adult hepatic progenitor cell markers

Bmol cells grown on tissue culture plastic were stained using immunofluorescence for the liver progenitor cell markers pancytokeratin (A), keratin-19 (B), osteopontin (C), MIC1-1C3 (D) and sox9 (E). Controls performed for each antibody using species-matched serum in place of the primary antibody and photographed on the same exposure showed no staining. A representative example is shown for pancytokeratin (F). Original magnification x400. Scale bars represent 25 μm.

Bmols show a similar pattern of laminin expression to primary HPCs

I have shown in the previous chapter that primary HPCs in culture express laminin alpha 5. I wanted to see whether Bmols shared the same pattern of laminin expression.

I performed qPCR on cell lysate from Bmols grown on tissue culture plastic, looking at the five laminin alpha chains (figure 4.2A). In order to provide a relative level to aid interpretation, I have compared this to the baseline level of expression of each chain in normal mouse liver. It can be seen that laminin alpha 1, alpha 2 and alpha 3 are expressed at much lower levels by Bmols than in normal liver. In contrast, laminin alpha 5 is expressed at a higher level in Bmols than in normal liver. Furthermore, laminin alpha 5 synthesis by Bmols can be demonstrated by immunocytochemistry (figure 4.2B). This suggests that Bmols do express laminin alpha 5 in a similar manner to primary HPCs.

Figure 4.2 Bmols synthesise laminin alpha 5

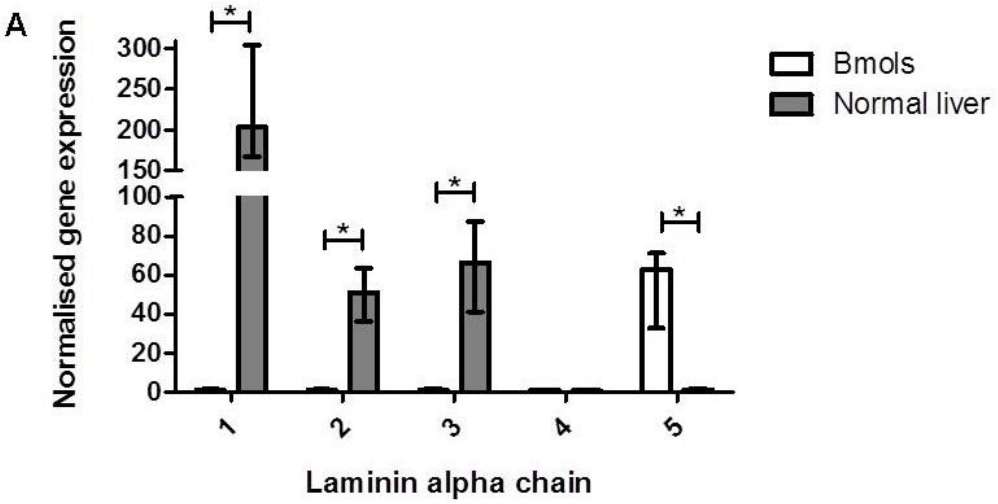

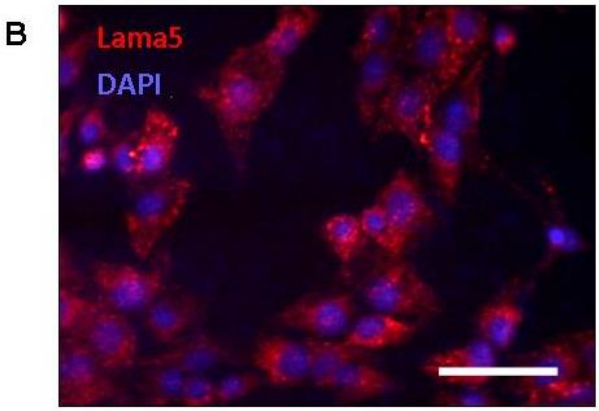

Figure 4.2 – Bmols synthesise laminin alpha 5

A. qPCR for laminin alpha chains, comparing cell lysate from Bmols cultured on plastic to expression levels in normal liver. Laminin alpha 5 is expressed at higher levels by Bmols than in normal liver, in contrast to all of the other laminin alpha chains. n=4 samples per group. Bars represent median +/- interquartile range. Data analysed by Mann Whitney test. *$p<0.05$. **B.** Bmols grown on tissue culture plastic. Immunofluorescence for laminin alpha 5 (red) and DAPI (blue) confirms laminin alpha 5 production at a protein level. Original magnification x320. Scale bar represents 25 µm.

Adhesion of HPCs to laminins

Adhesion of cells to a substrate can be measured in a number of ways (Humphries, 2009). I have chosen two assays to quantify the adhesion of Bmols to the different laminin isoforms: a spreading assay which measures the extent of flattening of adherent cells using image analysis, and an attachment assay which uses a colorimetric detection of the number of bound cells after washing.

When Bmols are plated onto either untreated tissue culture plastic, the majority of cells remain rounded after an hour (figure 4.3A). The same is observed when cells are plated on laminin-111, -211 and -411 (figure 4.3B-D). When plated on laminin-511, however, Bmols rapidly flatten and spread (figure 4.3E). Average cell area was quantified using image analysis software, and was significantly greater on laminin-511 than any of the other matrices (figure 4.3F).

As discussed earlier, a number of cell surface receptors can mediate the interaction between cells and extracellular laminin. The majority of laminin-binding integrins share the common beta-1 subunit. The addition of a blocking antibody against beta-1 integrin reduces cell spreading on laminin-511 (figure 4.3G), although it did not return it to the level seen on plastic. In contrast, an alpha-6 integrin blocking antibody did not have a significant effect on cell spreading.

An attachment assay measured the number of cells that remained adherent after washing. This confirmed significantly greater adhesion to laminin-511 than other matrices (figure 4.3H). Again, cell attachment to laminin-511 was reduced by a blocking antibody to beta-1 integrin, but not by a blocking antibody to alpha-6 integrin (figure 4.3I). Although a formal dose-response curve was not performed, doubling the concentration of the blocking antibody did not increase the level of attachment, suggesting that other receptors are likely to be involved.

Figure 4.3 Bmols adhere preferentially to laminin-511.

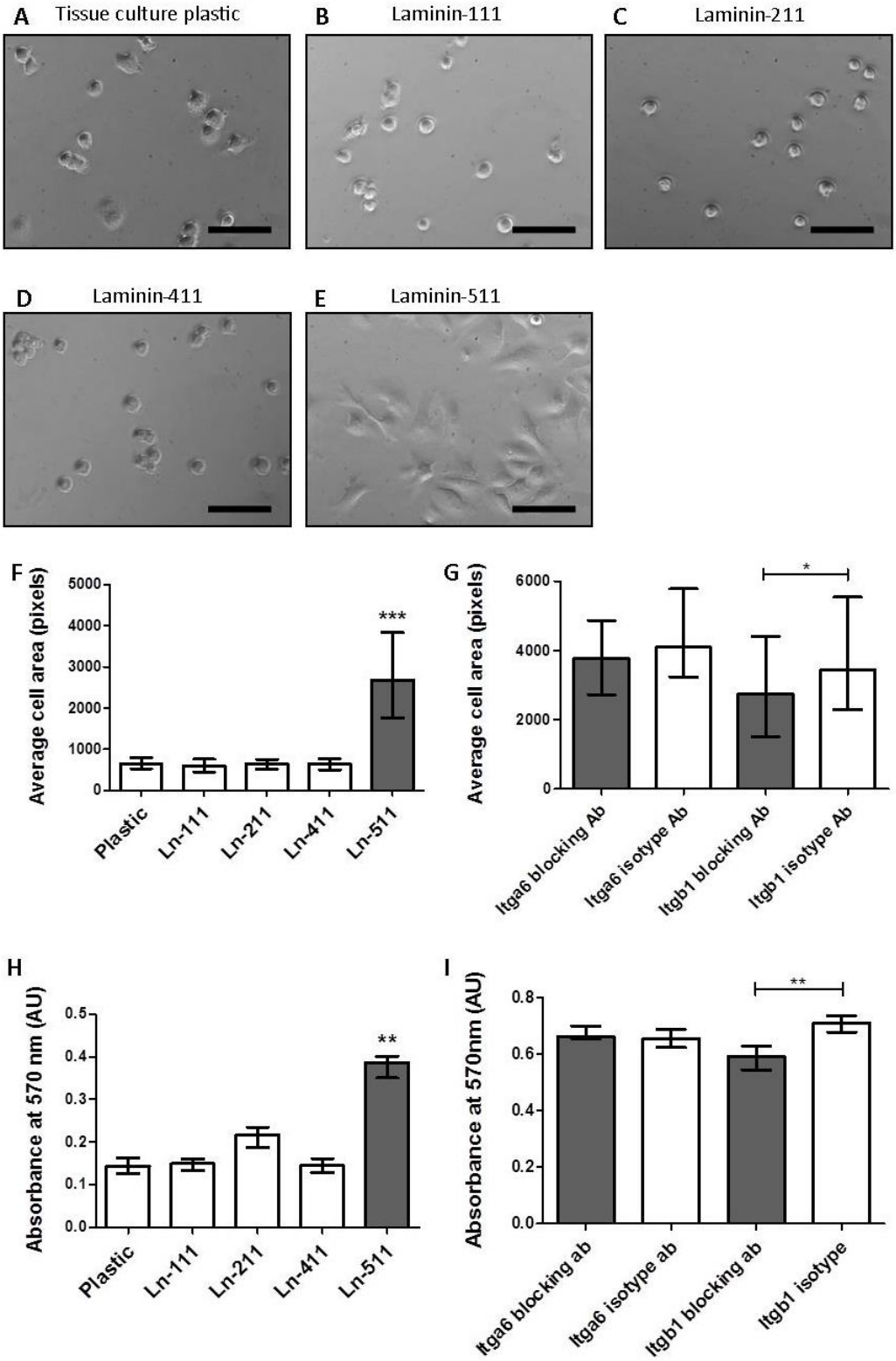

Figure 4.3 - Bmols adhere preferentially to laminin-511

Tissue culture wells were coated with 20 µg/ml of the various recombinant laminins. One hour after plating, phase contrast microscopy shows that Bmols remain small and rounded on plastic (**A**), laminin-111 (**B**), laminin-211 (**C**) and laminin-411 (**D**). In contrast, cells plated on laminin-511 (**E**) show evidence of flattening and spreading. Original magnification x400 for all conditions. Scale bars represent 25 µm. **F**. Image analysis of cell spreading confirms a significantly larger cell area on laminin-511 than any of the other matrices. Results show the average area of 100 cells per group. **G.** Cell spreading of Bmols plated on laminin-511 after pre-incubation with blocking antibodies to α6 and β1 integrin subunits or their isotype controls. Results show the average area of 100 cells per group. **H.** A colorimetric assay to assess the number of bound cells shows significantly greater cell attachment on laminin-511 relative to the other matrices. n=4 wells per group. **I.** Attachment of Bmols to laminin-511 after pre-incubation with blocking antibodies to α6 and β1 integrin subunits or isotype controls. n=4 wells per group.

In all graphs, bars represent median +/- interquartile range. Data comparing matrices were analysed by Kruskal-Wallis test, with Dunn's post-test comparison for each group against plastic. Data comparing integrin-blocking antibodies used Mann Whitney tests for each antibody and its isotype, *$p<0.05$, **$p<0.01$, ***$P<0.001$. Data shown in each graph represents the results from a single experiment but all results were confirmed in at least one independent replicate.

Migration of HPCs on laminins

In order to assess migration, cells were pre-treated with mitomycin C to inhibit proliferation and plated at a confluent density around a central plug. Removal of the plug created a standardised circular area into which cells could migrate (figure 4.4A). After 24 hours, cells were fixed, stained and photographed. Although there was some migration of cells on untreated plastic (figure 4.4B), this was enhanced on laminin-511 (4.4C). The extent of cell migration was then quantified using image analysis software. Migration was significantly greater on laminin-511 than any of the other laminin isoforms (figure 4.4D-E). Pre-treatment with blocking antibodies against alpha-6 or beta-1 integrin did not significantly affect this, although there was an apparent trend towards a reduction with both antibodies (figure 4.4F).

Figure 4.4 Bmols migrate preferentially on laminin-511

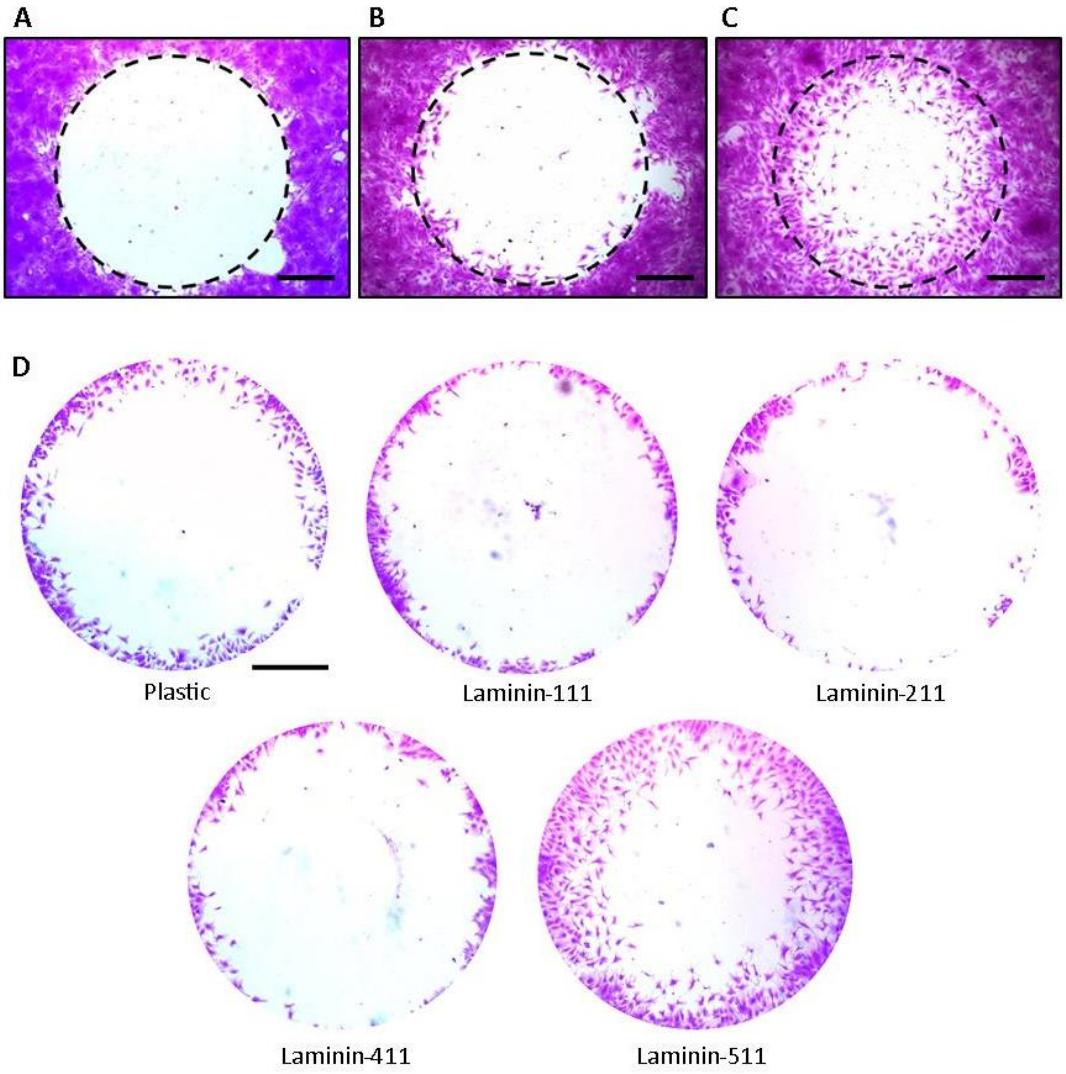

Figure 4.4 Bmols migrate preferentially on laminin-511 (cont)

F

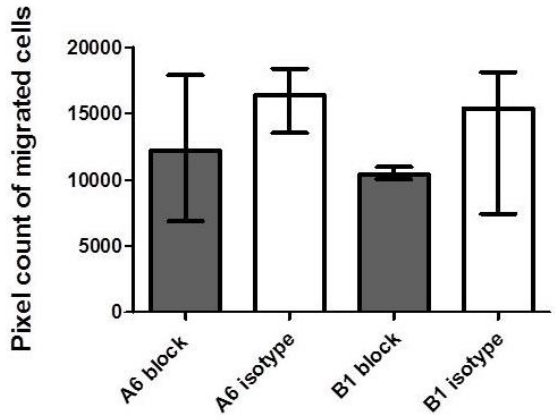

Figure 4.4 – Bmols migrate preferentially on laminin-511

A-C. Cells fixed and stained at the start of the migration assay (**A**) show a central defect into which cells migrate over 24 hours on both plastic (**B**) and laminin-511 (**C**). Original magnification x40. Scale bars represent 500 µm. **D.** Migration occurs significantly more on laminin-511 than on any of the other surfaces. n=4 wells per group. Analysed by Kruskal-Wallis test with Dunnett's post-test analysis to compare each matrix against untreated plastic. **p<0.01. Data shown represent the results from a single experiment but were confirmed in two independent replicates. Scale bar represents 500 µm. **E**. Although there was a trend towards a reduction in migration with both alpha 6 and beta 1 integrin-blocking antibodies, neither reached statistical significance consistently. The graph shows the combined results of 3 independent replicates, with n=4 wells per group in each experiment.

Proliferation of HPCs on recombinant laminins

In order to assess for differences in proliferation, I first used an MTT assay. This test utilises the ability of cells to convert the yellow dye 3-(4,5-dimethylthiazol-2-yl)-2,5-diphenyltetrazolium bromide (MTT) to purple formazan. The rate of conversion under defined conditions relates to the number of viable cells present. This has the advantage of being a simple colorometric assay that can be readily performed in multiple wells. However, it should be noted that it will be affected by both cell proliferation and cell death. I therefore went on to also use 5-ethynyl-2'-deoxyuridine (EdU) incorporation as a more specific measure of cell proliferation.

To determine the appropriate number of cells to use for the MTT assay for the Bmol cell line, I performed an optimisation experiment. Figure 4.5A compares 3 different cell numbers (2500, 5000 and 10,000) assessed at 4 timepoints (0, 24, 48 and 72 hours after plating). It can be seen that an initial population of 5000 cells per well expands over 48-72 hours to provide easily detected colour change in the MTT assay. Increasing the starting cell number to 10,000 does increase the absorbance reading further but with an apparent levelling off between 48 and 72 hours. This may be due either to saturation of the read-out or contact inhibition of cells. I therefore decided to use 5000 cells per well as the starting number for subsequent experiments.

I then performed the MTT assay in wells coated with the recombinant laminin isoforms. Culturing Bmols on different laminin isoforms under standard conditions did not result in any measurable difference in cell number (figure 4.5B).

As the MTT assay measures the number of viable cells rather than proliferation *per se,* it is possible that an effect on proliferation is masked by changes in cell loss. I therefore went on to assess proliferation directly by measuring DNA synthesis. 5-ethynyl-2'-deoxyuridine (EdU) is a nucleoside analogue of thymidine that is incorporated into DNA during S-phase, which can be detected using a click reaction. Figure 4.5C shows an example of EdU staining. All nuclei are stained blue by DAPI, and those of cells in S-phase will also appear green as a result of EdU staining.

Figure 4.5D shows the effect of culturing cells on different laminin alpha chains on EdU incorporation. The proportion of cells incorporating EdU was not significantly affected by culturing cells for 48 hours on recombinant laminins prior to EdU administration.

Figure 4.5 Proliferation of Bmols on laminins

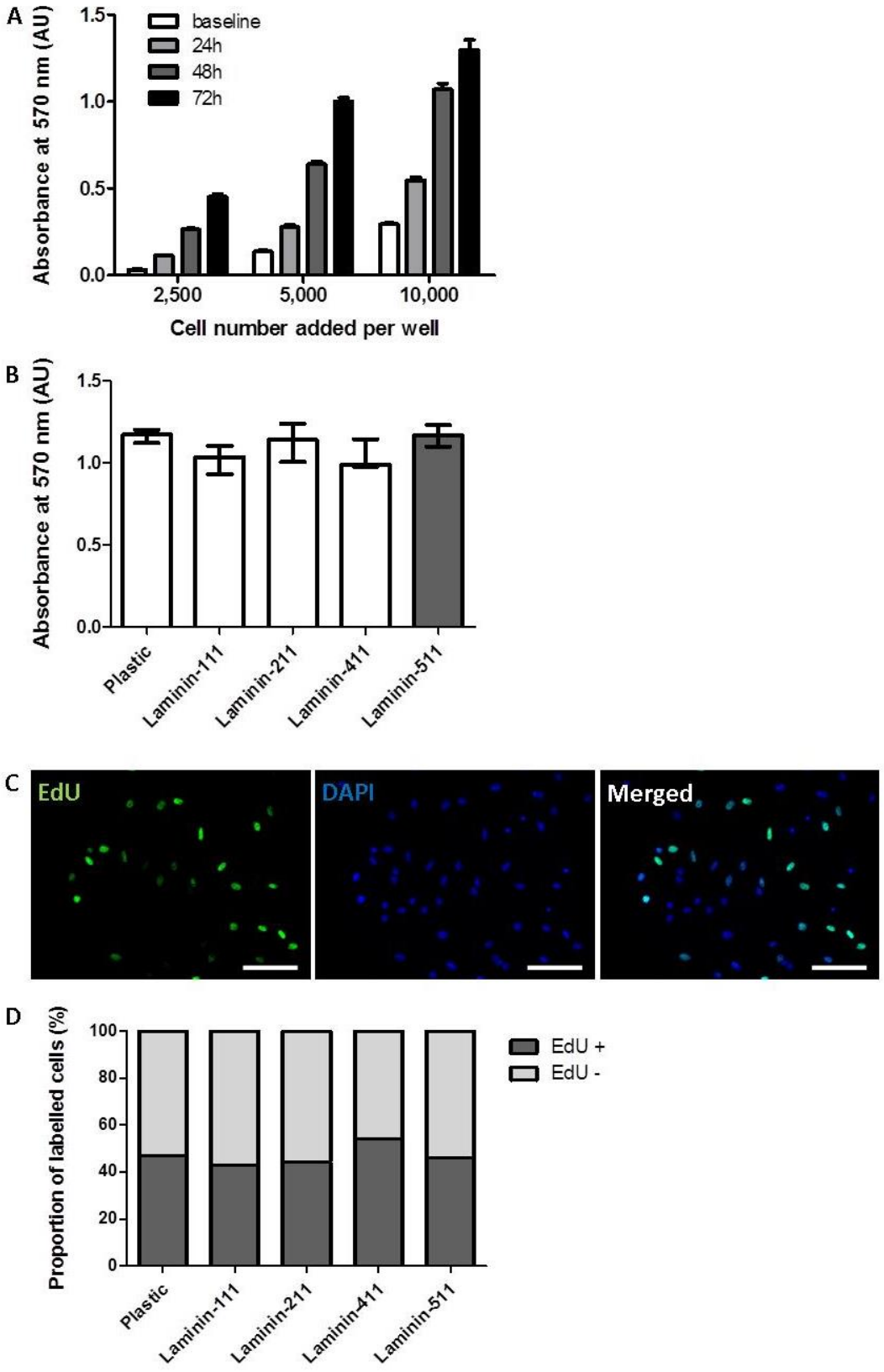

Figure 4.5 Proliferation of HPCs on recombinant laminins

A. Optimisation of the MTT assay for Bmols, comparing the effects of starting cell number and duration of culture on MTT dye conversion. A starting population of 5000 cells per well was selected for the optimal change in read-out after 48-72 hours. n=6 wells per group. **B**. Coating the wells with recombinant laminins did not produce any detectable change in the rate of MTT dye conversion. n=6 wells per group, Kruskal-Wallis p 0.07. Results are shown for a single experiment but this was confirmed in an independent replicate. **C**. Fluorescent staining of EdU incorporation by Bmols (EdU, green; DAPI, blue) was used to detect actively proliferating cells. Original magnification x200. Scale bars represent 50 μm. **D**. Quantification of EdU incorporation by Bmols after 48 hour incubation on recombinant laminin chains did not show any significant difference in rates of proliferation, Chi-squared test p 0.56. Cells were quantified in 5 low-powered (x20) fields per group. Data shown represent the results from a single experiment but these results were confirmed in an independent replicate.

Effect of serum concentration on Bmol response to recombinant laminins

It has been suggested that using high concentrations of serum in cell culture experiments may mask an effect of extracellular matrix. I therefore looked at the effect of reducing the serum concentration on cell viability in cells grown both on tissue culture plastic and on recombinant laminins.

Figure 4.6A shows the effect of reducing serum concentration on cells cultured on tissue culture plastic. It can be seen that there is only mild loss of cell viability with serum as low as 0.5%, but a marked drop in viability in serum-free conditions.

I therefore re-assessed the effect of recombinant laminins on Bmols in both low-serum (0.5%) and serum-free conditions. In low-serum conditions (figure 4.6B-C), cell number appears to be reduced in the presence of laminin-111, -211 and -411 compared to untreated tissue culture plastic, but maintained on laminin-511. In serum-free conditions (figure 4.6D), there is marked cell death on all matrices but this is most marked on laminin-111 and -411, and the highest level of cell viability is seen on laminin-511.

Figure 4.6 Effect of serum concentration on Bmol response to laminins

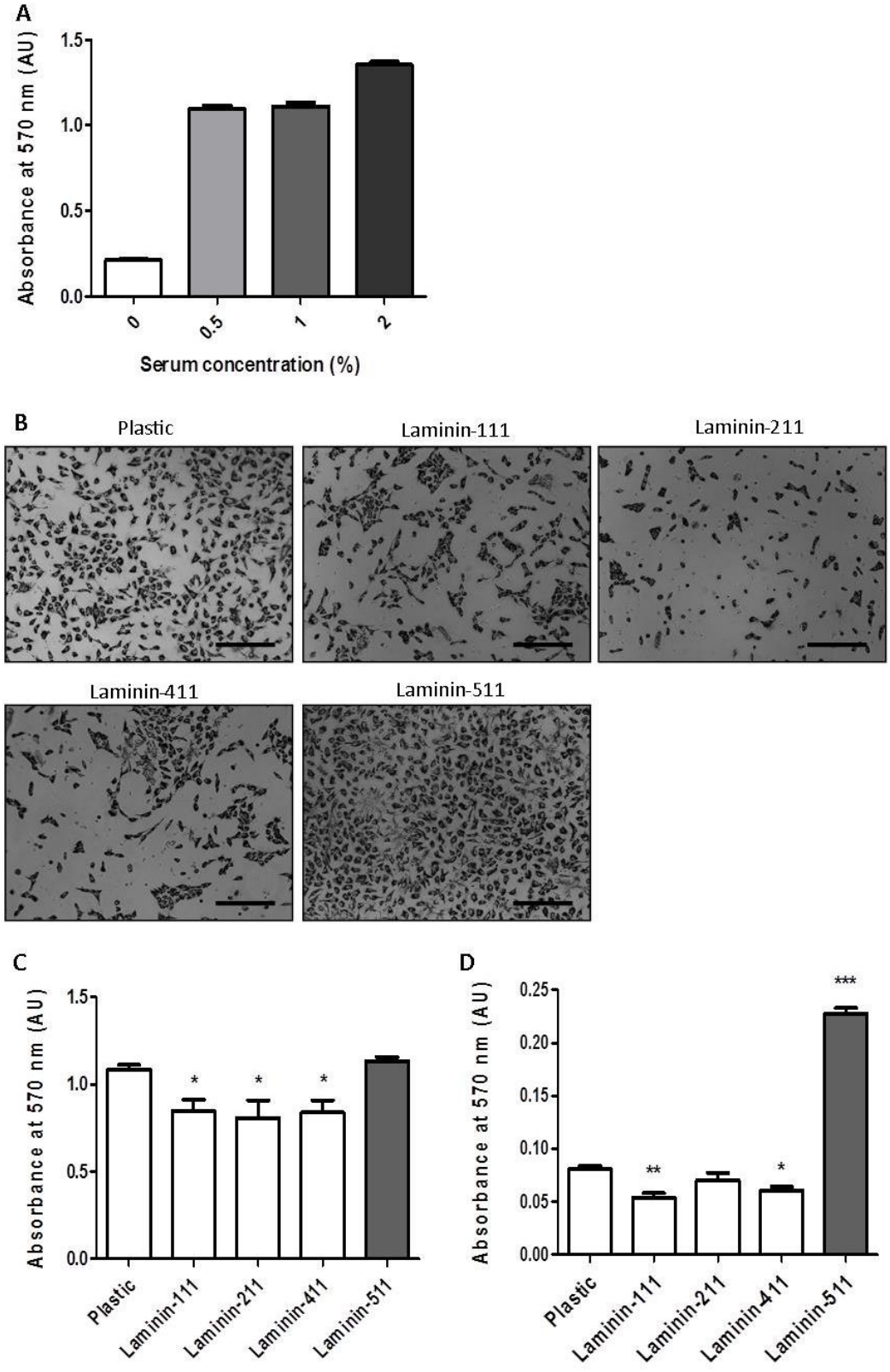

Figure 4.6 Effect of varying serum concentration on proliferation

A. MTT assay performed on Bmols cultured on plastic with varying concentrations of fetal calf serum (FCS) shows a marked drop in cell viability in serum-free conditions. n=6 wells per group in a single experiment. **B**. Representative pictures of phase microscopy of cells cultured on recombinant laminins in the presence of 0.5% FCS, following administration of MTT. There are appear to be fewer cells on laminin-111, -211 and -411. Original magnification x40. Scale bars represent 250 µm. **C**. This was quantified using the colorimetric MTT assay, confirming lower numbers of viable cells on laminins other than laminin-511. n=12 wells per condition in a single experiment. One-way ANOVA p 0.0009, post-test Dunnett's comparison of each column versus plastic, *$p<0.05$. **D**. MTT assay on Bmols cultured on recombinant laminins in serum-free medium showed a higher number of viable cells on laminin-511 than either plastic or other recombinant laminins. n=6 wells per condition in a single experiment. One-way ANOVA $p<0.001$, post-test Dunnett's comparison of each column versus plastic, *$p<0.05$. All columns represent mean, error bars represent standard error of mean.

Proliferation of HPCs following knock-down of laminin alpha 5

As I have already demonstrated that Bmols synthesise laminin alpha 5, it is possible that an effect of exogenous matrix is being masked by endogenous matrix production. This is unlikely to be significant over the one hour time-frame of the adhesion assays but may well influence outcome over the longer periods of culture (48-72 hours) required for proliferation assays. To investigate this possibility, I used small interfering RNA (siRNA) to knock-down endogenous laminin alpha 5 production.

I initially compared 4 siRNA sequences directed specifically against laminin alpha 5, a scrambled sequence and untransfected cells. Figure 4.7A shows the efficiency of knock-down for each of the sequences, as determined by qPCR. It can be seen that there is a degree of non-specific knock-down with the scrambled sequence. Knock-down efficiencies assessed at 24 hours after transfection were expressed as a proportion of the level of gene expression seen with the scrambled sequence. Knock-down of 65% and 79% were seen with sequences 2 and 3. Increasing the concentration of siRNA and the concentration of transfection reagent did not significantly alter the transfection efficiency. These sequences were then evaluated at a protein level, using an ELISA against laminin alpha 5. The results are shown in figure 4.7B, and confirmed a marked reduction in laminin alpha 5 synthesis following the siRNA treatment.

Figure 4.7C shows the effect of laminin alpha 5 knock-down on the number of viable cells, as determined by an MTT assay. There was a significant reduction in the cell number with both sequences, when compared to the scrambled sequence.

As discussed previously, the change in MTT could reflect an alteration in either cell proliferation or cell death. I therefore used EdU incorporation to determine cell proliferation rates in response to the siRNA. Figure 4.7D shows a marked reduction in the proportion of EdU-positive cells following siRNA against laminin alpha 5 (12% and 20%, compared with 51% in those treated with the scrambled sequence). This suggests that endogenous laminin alpha 5 production supports cell proliferation.

Figure 4.7 Effect of knock-down of laminin alpha 5 on proliferation

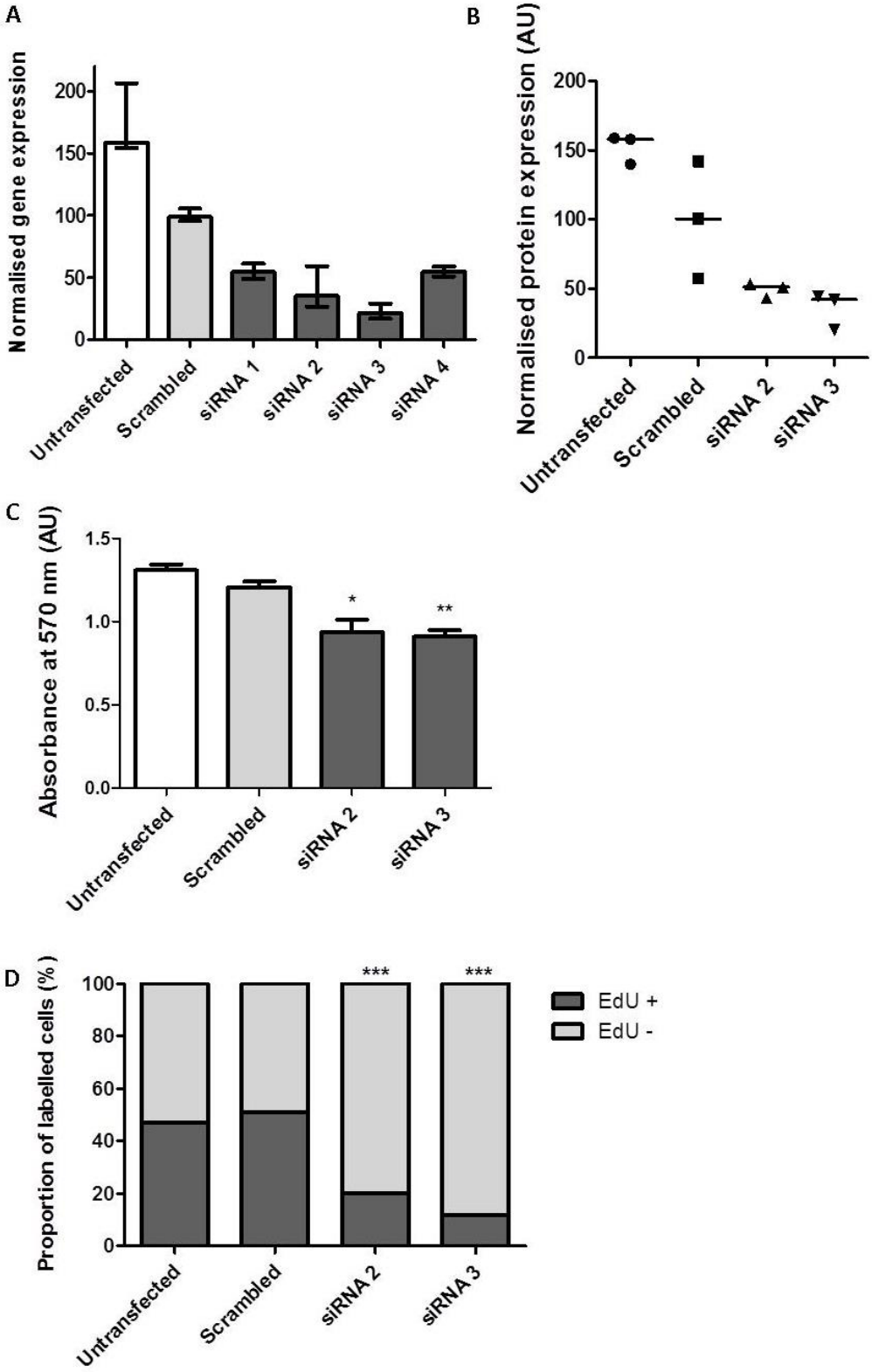

Figure 4.7 Proliferation of HPCs following knock-down of laminin alpha 5

A. qPCR for laminin alpha 5 expression relative to housekeeping gene PPIA, in cells treated with siRNA against laminin alpha 5 or a scrambled sequence. All values are normalised to the level of the scrambled sequence. Greatest knock-down is seen with sequences 2 and 3. n=3 independent samples per group. Kruskal-Wallis p 0.029. **B**. ELISA for laminin alpha 5 protein expression, normalised to total protein level, confirms knock-down with these sequences. n=3 independent samples per group. **C**. MTT performed 48 hours after transfection with siRNA or scrambled sequence shows a reduction in the number of viable cells following siRNA treatment. n=6 wells per group. Kruskal-Wallis test p 0.0036, post-test Dunnett's analysis for each siRNA vs scrambled *=$p<0.05$, **=$p<0.01$. **D**. Quantification of EdU incorporation confirms a lower proportion of proliferating cells following siRNA treatment. Cells were quantified in 5 low-powered fields per condition. Chi-squared $p < 0.001$. Data shown in **C** and **D** each represent the results from a single experiment but both were confirmed in independent replicates.

Differentiation of HPCs on laminins

In order to look for an effect of laminin isoforms on differentiation, I cultured Bmols for 72 hours in wells coated with the different recombinant laminins, and then harvested the cells for RNA extraction. Given the previous observations about the effect of serum in potentially masking a matrix effect, these experiments were done in 0.5% FCS. It can be seen from figure 4.8A-E that there were some morphological differences between cells grown on the different laminin isoforms. Whereas Bmols usually form clusters or islands of cells, Bmols cultured on laminin-511 appeared to remain separate with less cell-cell contact.

The progenitor cell markers EpCAM (figure 4.8F) and keratin-19 (figure 4.8G) were unaffected by the presence of exogenous laminins. In contrast, albumin transcription (figure 4.8H) was significantly reduced in the presence of all of the laminin isoforms, but most markedly in response to laminin-511. In view of the apparent reduction in cell-cell contact seen on phase contrast microscopy, I also looked at expression of E-cadherin (figure 4.8I). This was markedly reduced in the presence of both laminin-411 and -511.

Figure 4.8 Differentiation of Bmols on laminins

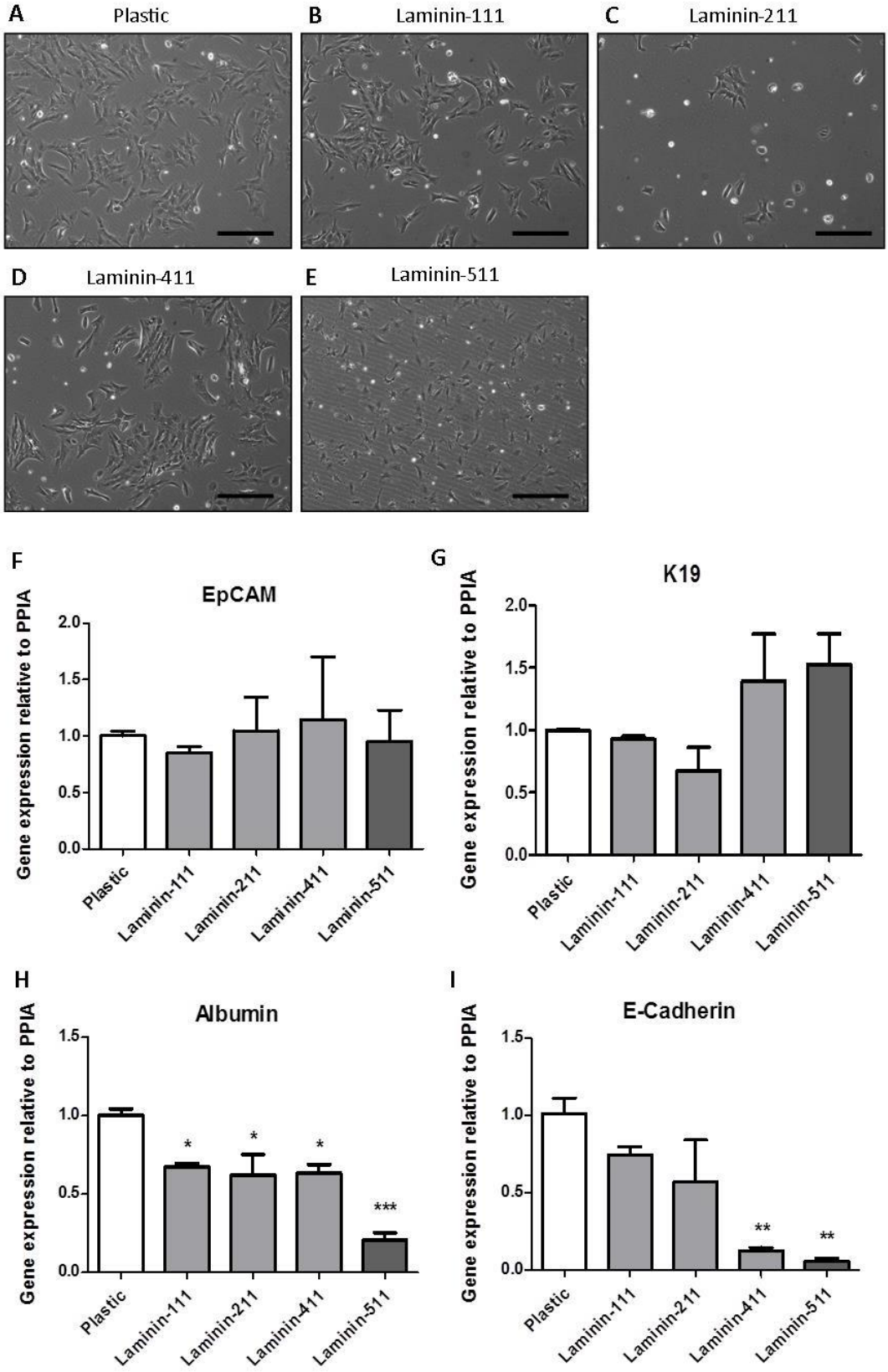

Figure 4.8 – Liver progenitor cells differentiation on matrix

A-E. Phase contrast microscopy of Bmol cells cultured on recombinant laminins for 72 hours shows a reduction in cell-cell contact in cells on laminin-511. Original magnification x100. Scale bars represent 100 μm. **F-I**. qPCR for differentiation markers in cells cultured on the different laminins. n=3 wells for each condition. There is no difference in EpCAM (**F**), p 0.97 or K19 (**G**), p 0.11. There is lower expression of albumin (**H**) by cells cultured on all of the laminins, but especially laminin-511, p 0.0003. Laminin -411 and -511 are also associated with a reduction in expression of e-cadherin (**I**), p 0.002.

Data are shown as mean, error bars represent standard error of mean. Analysed by One-way ANOVA with Dunnett's post-test comparison, for each column versus plastic, *p< 0.05, **p<0.01, *** p<0.001.

Differentiation of HPCs following knock-down of laminin alpha 5

Using the same siRNA knock-down described earlier, I inhibited endogenous laminin alpha 5 production and looked at changes in cell differentiation at 72 hours. Figure 4.9 shows the morphology of untransfected Bmols (A), compared with those treated with a scrambled sequence (B) and siRNA sequences directed against laminin alpha 5 (C,D). In both siRNA sequences, cells appear larger.

The progenitor cell marker EpCAM (figure 4.9E) was reduced by one of two siRNA sequences, relative to scrambled sequence. As this was limited to a single sequence, it is difficult to know whether this is of functional significance. A similar pattern is seen with K19 (figure 4.9F). However, albumin transcription was significantly increased by both siRNA sequences (figure 4.9G), suggesting differentiation towards a hepatocytic lineage. Despite the changes seen with exogenous laminins previously, transcription of e-cadherin (figure 4.9H) was not significantly altered by knock-down of laminin alpha 5.

Having shown that both exogenous and endogenous laminin alpha 5 inhibits differentiation towards a hepatocytic lineage, I wanted to see if induction of differentiation would result in a reduction in laminin synthesis. Oncostatin M has been shown to induce differentiation of rat liver progenitor cells towards a hepatocytic phenotype (Okaya et al., 2005). Bmols were cultured on tissue culture plastic in the presence or absence of oncostatin M for 5 days and then harvested for RNA extraction. Figure 4.9I shows a trend towards a reduction in laminin alpha 5 synthesis by the differentiated cells.

Figure 4.9 Effect of laminin alpha 5 knock-down on differentiation

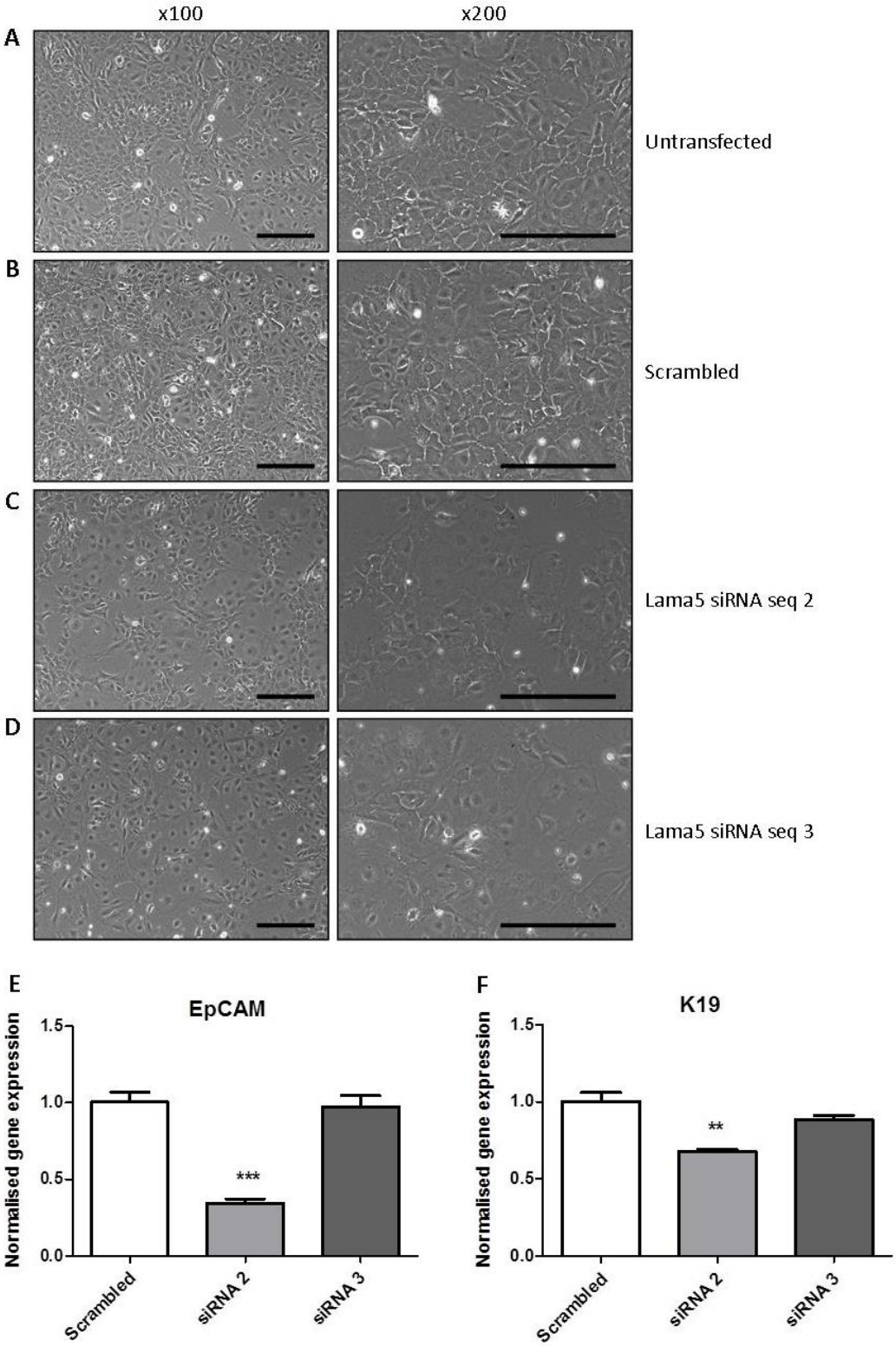

Figure 4.9 Effect of laminin alpha 5 knock-down on differentiation (continued)

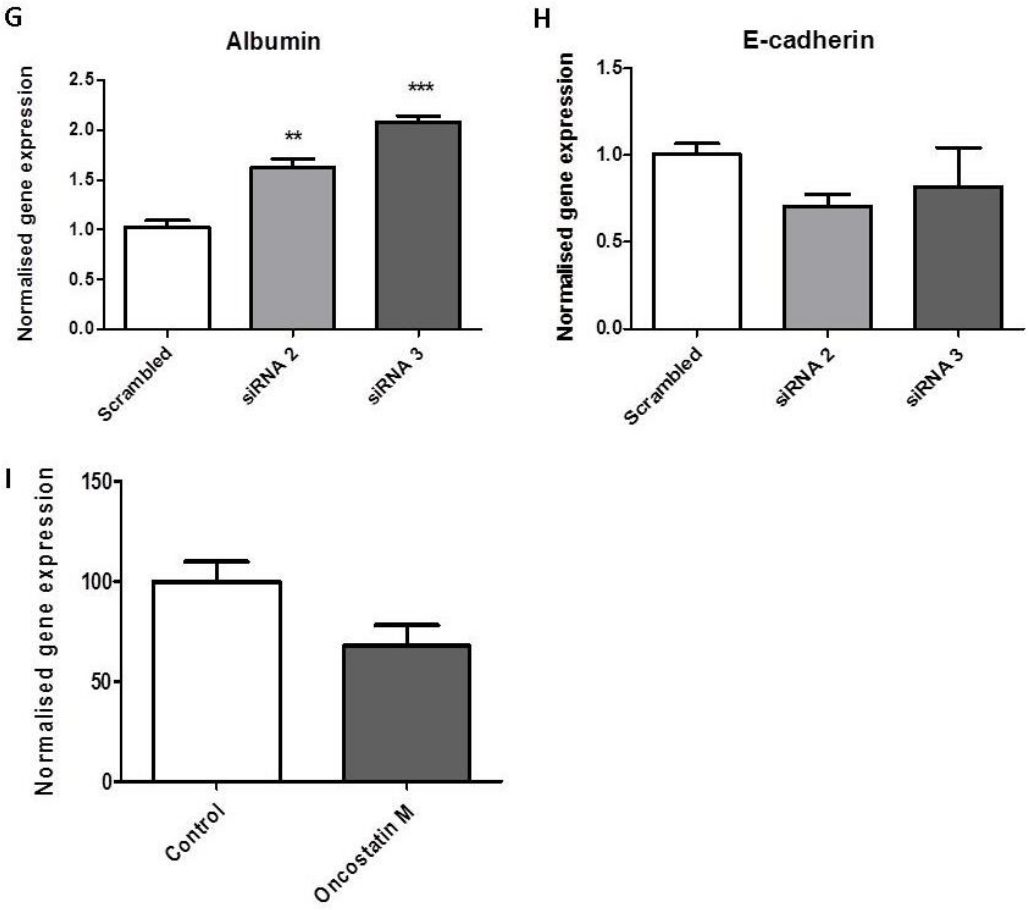

Figure 4.9 Differentiation of HPCs following knock-down of laminin alpha 5

A-D. Phase contrast microscopy of untransfected Bmols (**A**), Bmols treated with a scrambled sequence (**B**) and with targeted Lama5 siRNA sequences 2 (**C**) and 3 (**D**). Scale bars represent 100 μm. **E-H**. qPCR from cells 72 hours after treatment with siRNA. n=3 wells per group. Gene expression is normalised to the level of the housekeeping gene PPIA and analysed by one-way ANOVA, with Dunnett's post-test comparison for each sequence compared to scrambled. **E**. EpCAM expression is reduced with just one of two siRNA sequence, p 0.0003. **F**. Similarly, K19 expression is reduced by one sequence, p 0.0022. **G**. Albumin expression is reduced in response to both siRNA sequences, p 0.0029. **H**. E-cadherin is unaffected by laminin alpha 5 siRNA, p 0.37. **I**. Laminin alpha 5 transcription by Bmols in standard media (control) and in media containing oncostatin M (differentiated) shows a trend towards a reduction in laminin alpha 5 synthesis as cells differentiate (n=3 wells per group).

4.3 Discussion

In this chapter, I have confirmed that the Bmol cell line shares the characteristic markers of the adult hepatic progenitor cells that I described in the previous chapter. In particular, I have demonstrated that Bmols synthesise laminin alpha 5.

Using recombinant human laminins, I have demonstrated that Bmols adhere preferentially to laminin-511, as compared to laminin-111, -211, -411 or tissue culture plastic. This effect is partly but not completely blocked by antibodies against beta-1 integrin. Bmols also migrate more on laminin-511 than any of the other matrices.

When Bmols are cultured in 2% FCS, the presence of recombinant laminins did not affect cell proliferation as measured by either MTT assay or EdU incorporation. However, in low (0.5%) serum or serum-free conditions, laminin-511 was associated with higher cell viability. Similarly, knock-down of laminin alpha 5 using siRNA reduced cell numbers and proliferation.

Culturing Bmols on laminin-511 resulted in a reduction in albumin transcription, with no significant effect on progenitor cell markers. Conversely, siRNA knock-down of laminin alpha 5 increased albumin transcription. This suggests that endogenous laminin alpha 5 production by Bmols is helping to maintain the cells in a relatively undifferentiated state. As the cells were differentiated towards hepatocytes using oncostatin M, there was a trend to a reduction in laminin alpha 5 production.

The effects on adhesion and migration is perhaps not surprising as laminin-511 has been shown to be a potent adhesive and pro-migratory substrate for a number of tumour cell lines (Pouliot and Kusuma, 2013). It has even been suggested that laminin-511 plays a role in metastatic progression of breast cancer in a mouse model (Chia et al., 2007). However, I am not aware of any such effect on adhesion or migration being demonstrated for adult progenitor cells.

Although I did not use any matrix containing laminin alpha 3 (for reasons outlined earlier in the chapter), there is an intriguing suggestion from work on kidney epithelial cells that migration may be regulated by a haptotactic gradient formed by

both laminin-511 and -332 (Greciano et al., 2012). Given the consistent down-regulation of laminin alpha 3 chain seen in both models of HPC expansion in chapter 3, it is feasible that a similar polarity or gradient is important for HPCs. However, this requires further work to confirm such a mechanism.

The idea of laminin-511 acting in an autocrine fashion to regulate cell behaviour is not new, with a number of tumour cell lines that have been shown to synthesise, secrete and adhere to laminin-511 in culture (Kikkawa et al., 1998, Pouliot et al., 2000, Oikawa et al., 2011). Intriguingly, different cell lines adhere through different receptors. For example, the adhesion of JAR choriocarcinoma cells to laminin-511 is mediated via α6β1 integrin whereas that of PANC-1 pancreatic adenocarcinoma cells is via α3β1, even though both cell lines express both integrin receptors. α1β1 and α6β4 integrins have also been shown to mediate adhesion to laminin-511 (Kikkawa et al., 2008, Pouliot et al., 2001). Part of this variability may be explained by the expression of co-receptors which modulate the effect of integrin-binding. One such candidate is CD151, a member of the tetraspanin family of cell-surface receptors (Ke et al., 2011). This has been shown to modulate the binding of beta-1 integrin to laminin-511 in vitro (Yamada et al., 2008).

Although this work suggests a possible role for β1 integrin in mediating some of the interaction between HPCs and laminin-511, this only appears to account for a small part of the effect on adhesion. It is therefore likely that there are other receptors that are important in this. Potential candidates include β4 integrin, Lutheran/BCAM and syndecan. In particular, Lutheran is a highly specific laminin alpha 5 receptor and recent studies have shown an effective blocking antibody which could be used to explore this further.

The effect on differentiation suggests a role for laminin-511 in maintaining a naïve phenotype. This is consistent with work in embryonic stem cells and induced pluripotent stem cells that has shown that laminin-511 promotes long-term self-renewal and expression of the pluripotency markers OCT4, Nanog and SOX2 (Rodin et al., 2010).

A number of intracellular signalling pathways have been implicated in the effects of laminins on cellular behaviour. In particular, laminin-511 has been shown to affect the Wnt and Hedgehog pathways. Work looking at embryonic hair morphogenesis has shown that exogenous noggin or sonic hedgehog (Shh) are able to restore the changes in follicle development that are seen in laminin alpha 5-null mice (Gao et al., 2008). Laminin-511 appears to stimulate noggin, leading to LEF-1 expression and amplification of Shh signalling. In addition, studies of the small intestine of laminin alpha 5 knock-out mice identified changes in the Wnt and PI3K/Akt pathways (Ritie et al., 2012). Laminin alpha 5 appears to repress canonical Wnt signalling, and activate PI3K/Akt signalling. Although I have not assessed intracellular signalling pathways as part of this thesis, the same techniques described here could be applied to this.

One of the main concerns is interpreting this in vitro work is whether Bmols are truly representative of primary HPCs. In particular, a cell line that has undergone immortalisation may not behave in the same way as primary cells with regard to proliferation and differentiation. However, I chose not to use primary HPCs for these experiments for several reasons. At present, no specific cell surface markers have been identified that can accurately discriminate between progenitors and biliary epithelial cells. Progenitor cell isolation protocols therefore rely on a period of culture on matrix components to purify the cell populations, and this in itself may alter both cell surface receptor expression and cell behaviour. Furthermore, it is difficult to ensure reproducibility of cell purity between experiments using primary cell cultures. As many of the in vitro techniques require relatively large numbers of cells, this would require very large number of mice. Bmols, in contrast, have the advantages of ready availability in large numbers and reproducibility.

A further limitation is the use of a single cell type in culture experiments. I have already described the close association between HPCs and both hepatic stellate cells and macrophages. It is possible that cell-matrix interactions maybe modified in the presence of particular cell-cell signalling. Co-culture experiments may provide further information about how laminin alpha 5 influences the interactions between different cell types. However, even with co-cultures, it is not currently possible to

recreate the complexity of the HPC niche in culture. In the central nervous system, slice culture techniques have been used to maintain three-dimensional architecture whilst still allowing experimental manipulation of cells (Gahwiler et al., 1997). This technique has had limited success when applied to the liver but would be of great value if it could be developed further.

Chapter 5: Defining the effect of laminin alpha 5 chain on progenitor cell behaviour in vivo

5.1 Introduction

Having established a selective effect of laminin-511 on HPC behaviour in vitro, I then sought to confirm this effect in vivo by knocking down laminin alpha 5 synthesis. As the adhesion of HPCs to laminin-511 appeared to be at least partly mediated by beta-1 integrin, I also examined the effect of interfering with cell-matrix interactions by knocking down beta-1 integrin. As both of these genes are critical for embryonic development, their role in the regulation of adult liver regeneration cannot be assessed using conventional knock-out mice. However, as previously discussed, the use of Cre-lox technology allows targeted deletion of genes in a tissue- and time-dependent manner. This permits the knock-down of gene expression in the adult following normal embryonic development.

5.2 Results

Use of transgenic mice to study matrix effects in vivo

A tamoxifen-inducible Cre recombinase (Cre^{ERT}) was knocked into the endogenous keratin-19 (K19) locus. Recombined cells were irreversibly labelled by inducing expression of yellow fluorescent protein (YFP) using a loxP-STOP-loxP-YFP sequence in the ROSA26 locus, as illustrated in figure 5.1A. The K19-CreERT was initially described as an inducible marker of endodermally-derived epithelial cells, and labelled cells within the stomach, intestine, pancreas and liver (Means et al., 2008). Within the liver, K19 is expressed on biliary epithelial cells but is also a recognised marker of progenitor cells.

The K19-CreERT mouse was then crossed with one of two possible floxed alleles: laminin alpha 5 or beta-1 integrin. Mice were bred to homozygosity for the floxed gene alleles and for the YFP reporter allele. The Cre transgene was maintained as a

heterozygote. This generated 3 separate strains of mice for comparison (as illustrated in figure 5.1B):

K19-CreERT with a YFP reporter and no additional floxed alleles

K19-CreERT with a YFP reporter and a floxed laminin alpha 5 gene

K19-CreERT with a YFP reporter and a floxed beta-1 integrin gene

The effect of recombination was studied in each of these strains using adult (6 week old) mice. In order to compare the hepatic progenitor cell response of these three strains, I used the DDC model described in chapter 3 to stimulate biliary regeneration. However, it was not possible to use the Mdm2 model to simulate hepatocellular regeneration with these strains as there would be cross-reactivity between the two Cre-lox systems. I therefore used a second dietary model, the choline-deficient ethionine-supplemented (CDE) diet, to stimulate HPCs instead. Choline is an essential nutrient with roles in cell membrane integrity, transmembrane signalling and phosphatidylcholine synthesis. Choline deficiency promotes hepatic steatosis (Zeisel and Blusztajn, 1994). The three dietary conditions are shown in figure 5.1C.

8 mice (4 males and 4 females) of each genotype were exposed to each set of dietary conditions.

Figure 5.1 Experimental design for transgenic model

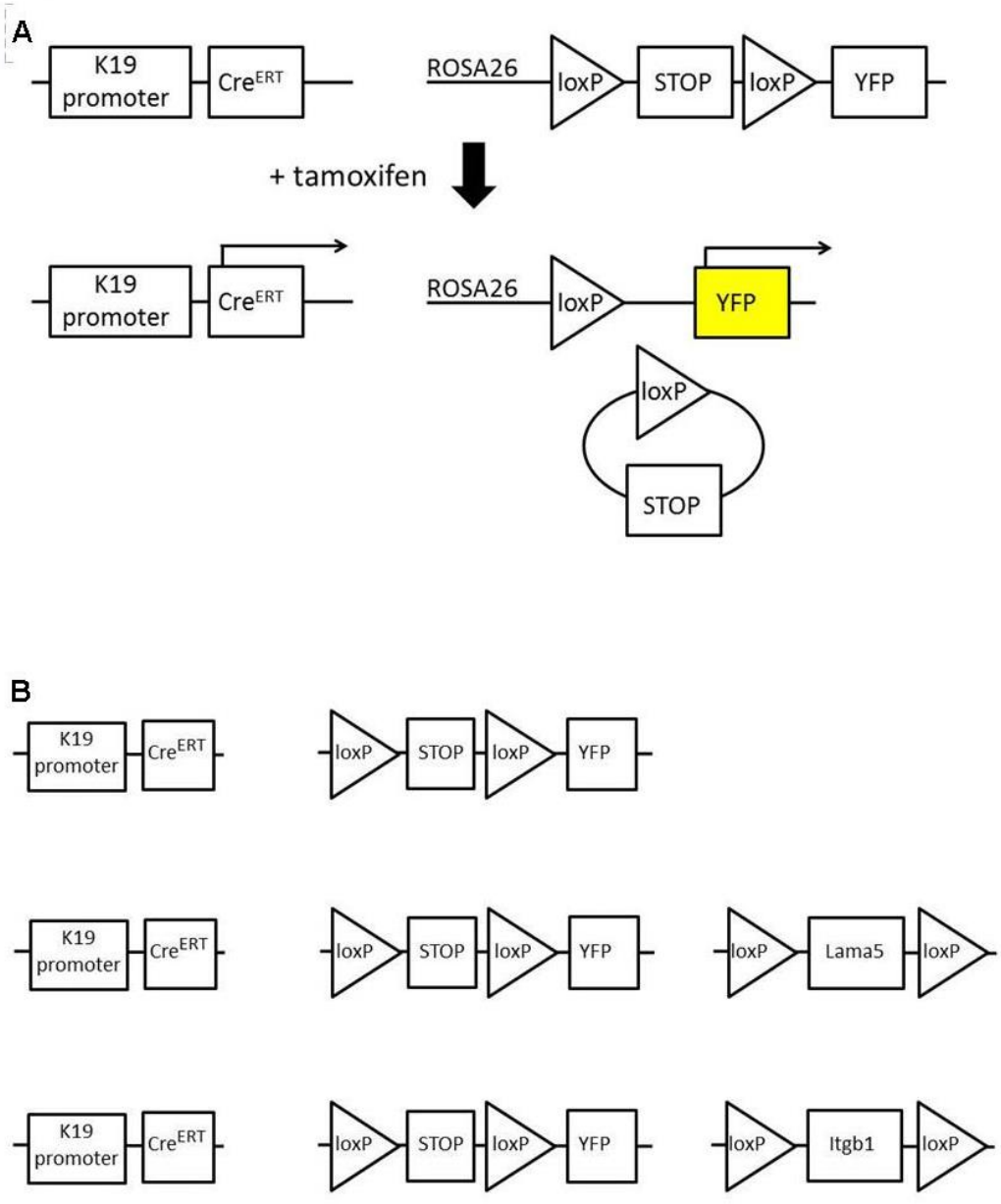

Figure 5.1 Experimental design for transgenic model (cont)

C

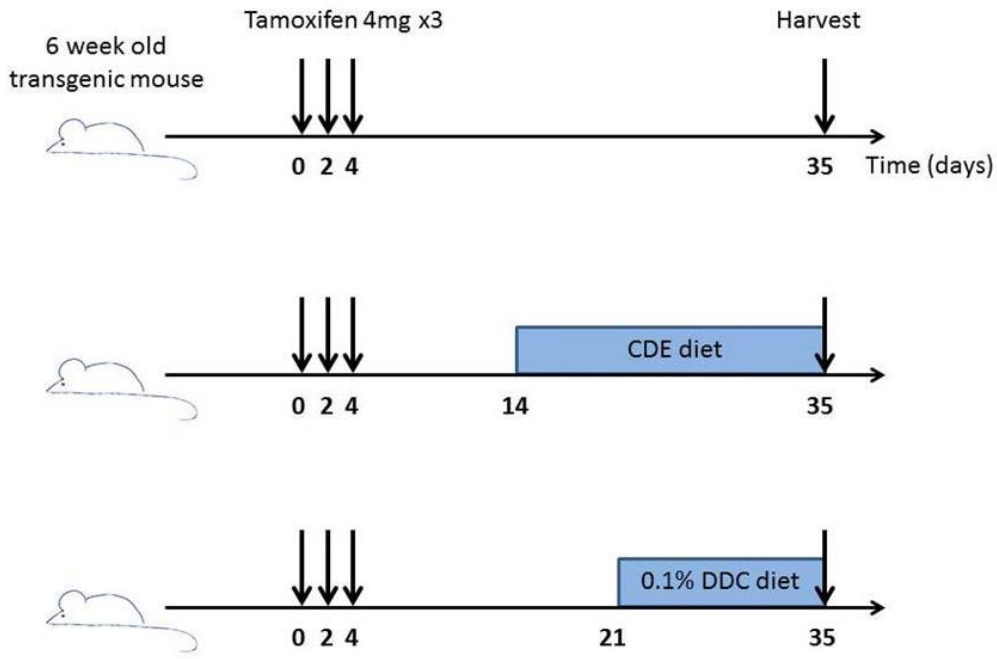

Figure 5.1 – Experimental design for transgenic model

A. Illustration of the genetic construct of the K19-CreERT and YFP reporter. Tamoxifen-induced recombination results in YFP activation in K19-expressing cells. **B.** This reporter can then be combined with other floxed alleles, to examine the effects of conditional loss of gene expression during regeneration. The illustration shows the three experimental combinations used in this chapter: YFP reporter alone, floxed laminin alpha 5 and floxed beta-1 integrin. **C**. 6 week old mice from all three genotypes were exposed to normal chow, CDE and DDC diets to examine the effects of altered cell-matrix signalling under normal and regenerative conditions.

K19-Cre labels bile ducts and progenitor cells

Although the YFP should be able to be visualised directly on frozen tissue sections using fluorescence microscopy, I fixed the tissue using formaldhyde in order to improve the preservation of morphological detail. The YFP was then detected using an antibody against green fluorescent protein (GFP), which could be visualised with either DAB or fluorescence. This method of visualisation had the additional benefit of allowing signal amplification.

In Cre-negative mice given tamoxifen (figure 5.2A) or Cre-positive mice in the absence of tamoxifen (figure 5.2B), there is no detectable YFP staining. However, Cre-positive mice given tamoxifen demonstrate YFP expression in a proportion of biliary epithelial cells (BECs), as shown in figure 5.2C. This is quantified in figure 5.2D, confirming the specificity of YFP labelling in this system.

In approximately half of the mice with the floxed laminin alpha 5 gene, much more widespread labelling of perisinusoidal cells was seen (figure 5.2E). This pattern was very unexpected and only present in some of the animals, with the remaining mice showing a predominantly biliary pattern. Subsequent discussions with the collaborator who supplied the mice with the floxed laminin alpha 5 gene revealed that although the original breeding pair had been genotyped as ‘Cre-negative’, they were from a colony that had contained a HoxB7-Cre-EGFP construct. Re-testing of my experimental animals confirmed that those with the widespread perisinusoidal YFP expression all had the HoxB7-Cre-EGFP, whereas the animals with the peribiliary YFP expression lacked this and had the expected K19-Cre. The HoxB7-Cre-EGFP mice were therefore excluded from any further analysis, resulting in a marked reduction in the experimental numbers within the floxed laminin alpha 5 groups (n=3-4, rather than the planned n=8).

The YFP co-localises with the progenitor cell markers panCK (figure 5.2F) and osteopontin (figure 5.2G). Finally, a very small number of YFP-positive small hepatocyte-like cells were seen close to the bile ducts in mice on the CDE diet (figure 5.2H), consistent with HPC differentiation.

Figure 5.2 K19-Cre labels bile ducts and progenitors

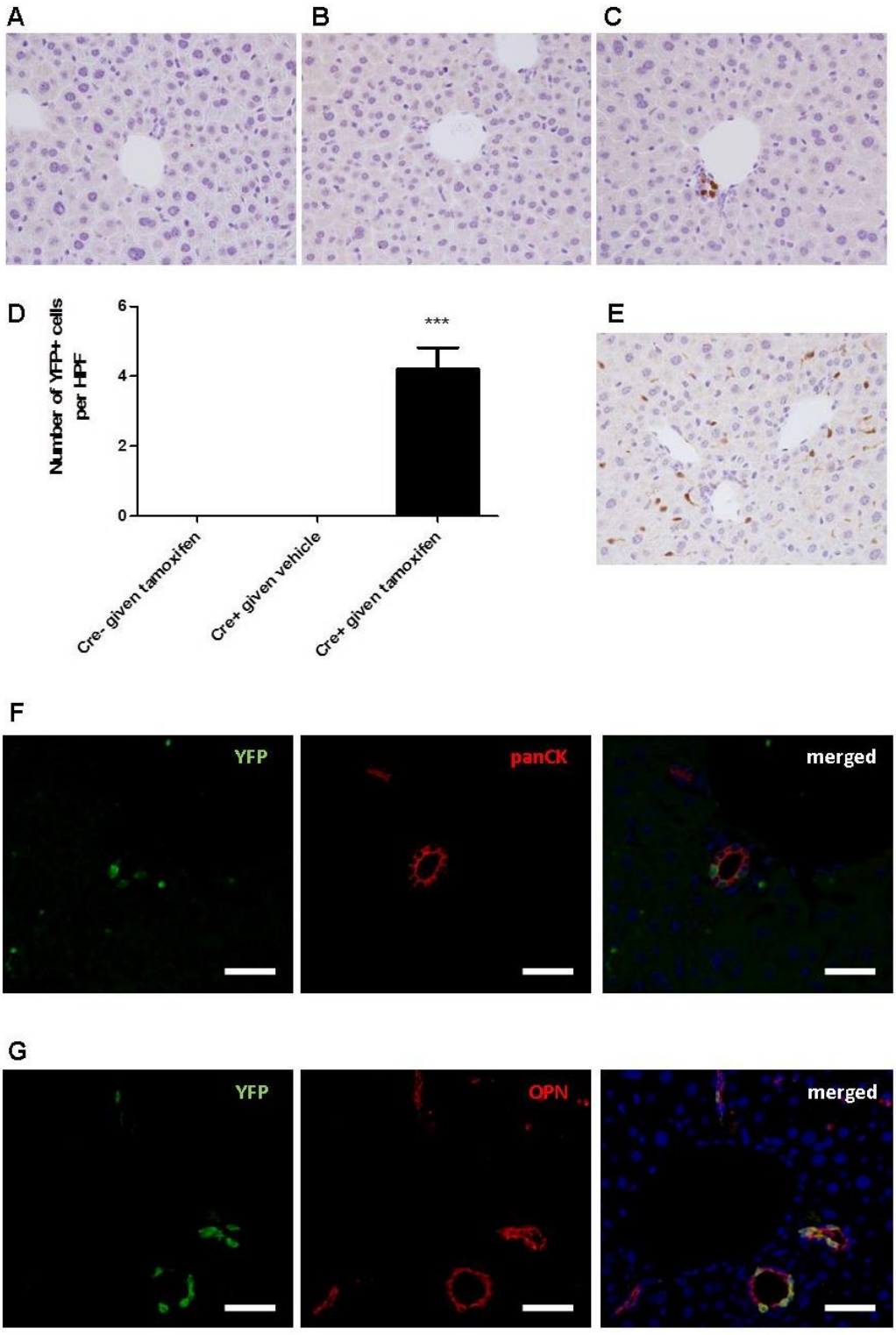

Figure 5.2 K19-Cre labels bile ducts and progenitors (cont)

H

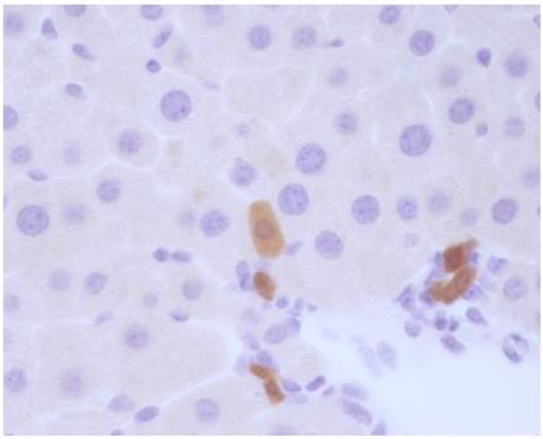

Figure 5.2 K19 labels bile ducts and progenitor cells

A-C. Immunostaining for YFP in the absence of Cre (**A**) or in the absence of tamoxifen (**B**) shows no labelled cells, whereas Cre-positive animals given tamoxifen (**C**) show YFP-positive cells in a predominantly biliary distribution. **D**. Quantification of YFP expression in the previously-listed situations confirms the specificity of the Cre (n=3-4 animals per group). One-way ANOVA $p<0.0001$ **E.** Marked perisinusoidal cell labelling in mice was found in a proportion of mice with the floxed laminin alpha 5 gene, subsequently shown to have accidental HoxB7-Cre-EGFP expression. These mice were excluded from further analysis. **F**. Dual immunofluorescence shows co-localisation of YFP (green) with panCK (red). Original magnification x400. **G.** Similarly, co-localisation of YFP (green) with osteopontin (red) confirms the labelling of HPCs. Original magnification x400. Scale bar represents 50 μm. **H.** YFP labelling of a small hepatocyte-like cell in close proximity to a bile duct in mice fed a CDE diet is consistent with the differentiation of HPCs into hepatocytes. Original magnification x600.

The effect of loss of laminin alpha 5 or beta-1 integrin genes in the uninjured liver

Recombination was induced in 6-week old mice of all 3 genotypes in the absence of any additional liver injury, as shown in figure 5.3A. There was no difference in the animals' weights following recombination between the 3 groups (figure 5.3B). There was a slight increase in serum bilirubin in both the floxed laminin alpha 5 and floxed beta-1 integrin mice (figure 5.3C), consistent with a mild impairment of biliary epithelial cell function. There was little evidence to support any hepatocellular injury as a result of recombination, with normal serum ALTs in all groups (figure 5.3D). The serum albumin was unexpectedly slightly (but statistically significantly) higher in both of the floxed groups. Although this could theoretically be explained by premature differentiation of progenitors towards a hepatocytic lineage, histology to examine the morphology and distribution of YFP labelled cells did not show any evidence of this (figure 5.3F-H).

Quantification of the number of YFP-positive cells showed a trend towards fewer YFP cells in the floxed laminin alpha 5 group (figure 5.3I). As the number of cells present will depend partly on the number and size of bile ducts present in the sections examined, the number of YFP-positive cells was calculated relative to the number of BECs present. Once this was taken into account, there was a significantly lower number of YFP-labelled cells in the floxed laminin alpha 5 group than either of the other two groups (figure 5.3J).

Figure 5.3 Effect of loss of laminin alpha 5 or beta 1 integrin in the uninjured liver

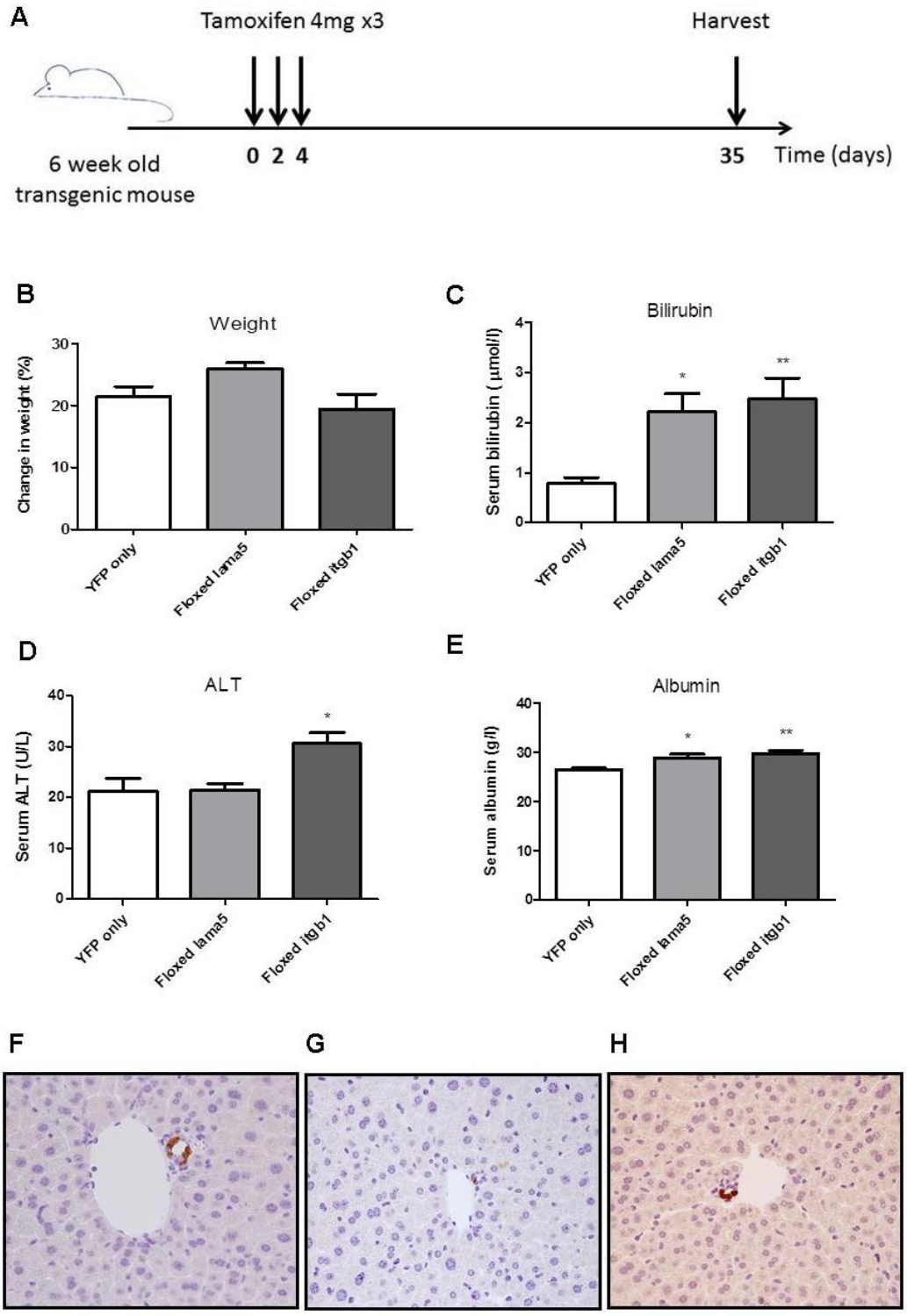

Figure 5.3 Effect of loss of laminin alpha 5 or beta 1 integrin in the uninjured liver (cont)

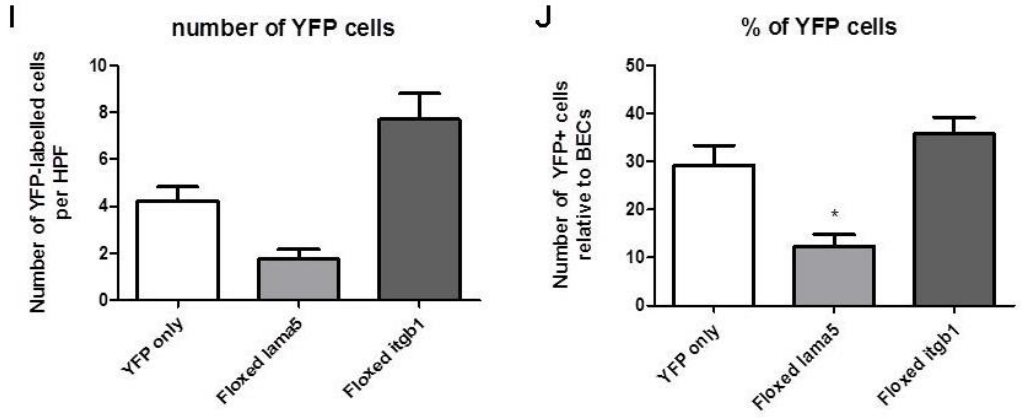

Figure 5.3 Effect of loss of laminin alpha 5 or beta-1 integrin in the uninjured liver

A. Illustration of experimental timeline for transgenic mice treated with tamoxifen and fed normal chow (n=4 animals in floxed laminin alpha 5 group, n=8 animals in YFP only and floxed beta 1 integrin group). **B**. Mouse weights from induction to harvest, expressed as a percentage change, do not show any effect of genotype. One-way ANOVA p 0.17. **C**. Serum bilirubin levels are mildly but statistically significantly raised in both of the floxed allele groups. One-way ANOVA p 0.0051. **D**. Serum ALT level is higher in the floxed beta 1 integrin group, although this remains within the normal range. One-way ANOVA p 0.013 **E**. Serum albumin levels were higher in both of the floxed allele groups. One-way ANOVA p 0.0026. **F-H.** Examples of YFP staining in the YFP only group (**F**), floxed laminin alpha 5 (**G**) and floxed beta-1 integrin (**H**) mice. **I.** Quantification of YFP staining, expressed as a total number of YFP-labelled cells per high-powered field, suggests a trend towards a reduction in YFP-labelled cells in the floxed laminin alpha 5 group, and an increase in the floxed beta 1 integrin group. **J**. When this is expressed relative to the number of biliary epithelial cells (BECs), the reduction in YFP-positive cells in the floxed laminin alpha 5 group becomes statistically significant.

For all of the above analyses, where a significant difference was found using ANOVA, Dunnett's post-test comparison was used to compare each floxed allele to the YFP only group, *p<0.05, **<0.01.

The effect of floxed alleles on the response to CDE diet

The CDE diet was used to model hepatocellular injury, using the same induction regimen as before. Mice were allowed to recover after the tamoxifen injections and then fed CDE diet for 3 weeks prior to harvest, as illustrated in figure 5.4A.

The genotype of the mice did not have any effect on the change in weight seen in response to the diet (figure 5.4B). Similarly, there was no difference in serum bilirubin at the end of the diet period (figure 5.4C).

A marked difference in serum ALT was observed, with significantly higher ALTs in the floxed beta-1 integrin group (mean 204 U/L) compared with either the floxed laminin group (54 U/L) or YFP only (41 U/L). This suggests a greater degree of hepatocellular injury in response to the diet. This was not reflected in any difference in the serum albumin (figure 5.4E).

Initial cell counts suggested a greater number of YFP-positive cells in the floxed beta-1 integrin group, with 7.04 cells per HPF compared to 4.84 in the YFP only group and 3.53 in the floxed laminin group (figure 5.4F). However, when the number of YFP-positive cells were corrected for the number of BECs per section, these differences were less marked. There did, however, appear to be a trend towards a lower number of recombined cells in the floxed laminin alpha 5 group (21.8% vs 31.5% and 34.2% in the other groups).

In CDE diet, the HPCs form cords extending away from the bile ducts and infiltrating the parenchyma. In order to distinguish HPCs from biliary epithelial cells, I counted the number of YFP-positive cells that were not in contact with a well-defined lumen. An example is shown in figure 5.4G. This is likely to still include a small number of BECs where just the edge of the duct has been caught in the section. However, this is likely to give a more accurate reflection of HPCs. Again, there was a non-significant reduction in the number of extraductular YFP-labelled cells in the floxed laminin alpha 5 group (figure 5.4H).

Figure 5.4 Effect of floxed alleles on response to CDE diet

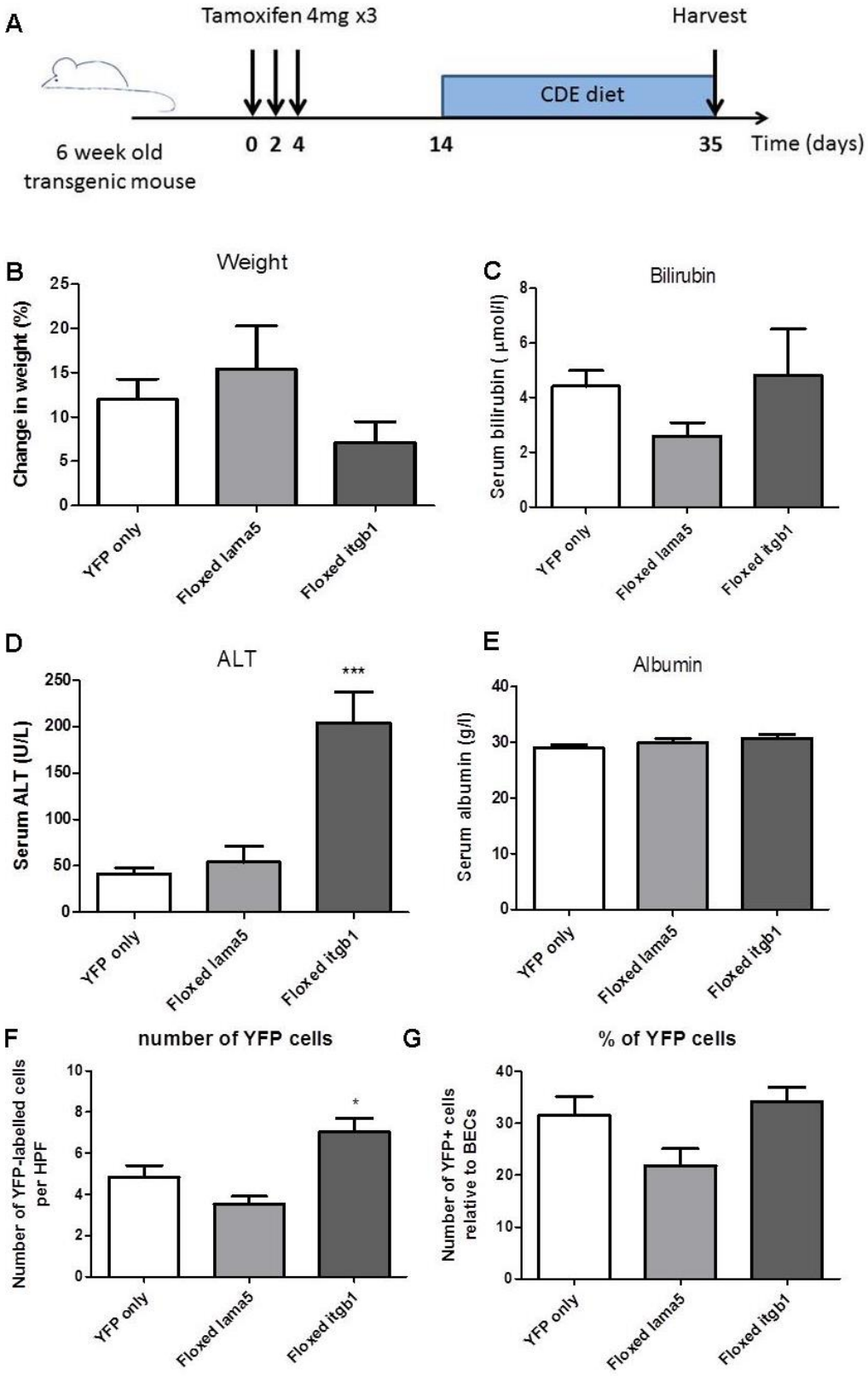

Figure 5.4 Effect of floxed alleles on response to CDE diet

H

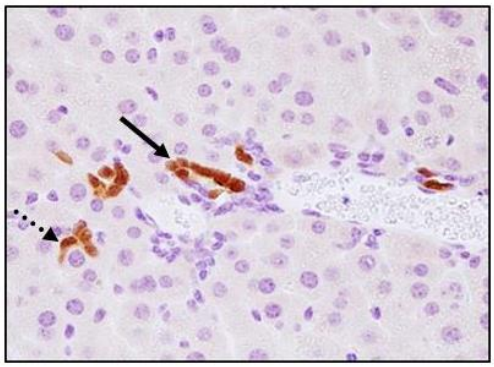

I

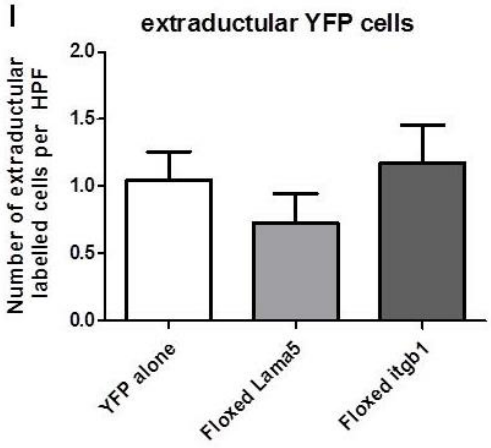

Figure 5.4 Effect of additional floxed alleles on response to CDE

A. Illustration of experimental timeline for transgenic mice given the CDE diet (n=4 animals in floxed laminin alpha 5 group, n=8 animals in YFP only and floxed beta 1 integrin groups). **B**. Mouse weights from induction to harvest, expressed as a percentage change, did not show any difference according to genotype. One-way ANOVA p 0.18. **C**. Serum bilirubin levels were not significantly different between groups. One-way ANOVA p 0.56. **D**. Serum ALT levels were markedly elevated in the floxed beta 1 integrin group. One-way ANOVA p 0.0007. **E**. Serum albumin levels were no different between groups. One-way ANOVA p 0.21. **F.** The absolute number of YFP-labelled cells per high powered field was greater in the floxed beta 1 integrin group; one-way ANOVA p 0.005. **G.** The number of YFP-labelled cells expressed relative to the number of biliary epithelial cells (BECs) did not show any significant differences, although there was a trend towards a lower number of labelled cells in the floxed laminin alpha 5 group. One-way ANOVA p 0.09. **H**. Example of YFP staining showing BECs clearly associated with a lumen (block arrow) and potential HPCs not associated with a lumen (dotted arrow). **I**. Quantification of the number of extraductular YFP cells shows a non-significantly lower number in the floxed laminin alpha 5 group.

Where significant differences were found on one-way ANOVA, Dunnett's test for multiple comparisons was used to compare each floxed allele against the YFP only group *$p<0.05$, ***$p<0.001$

The effect of floxed alleles on the response to DDC diet

Having demonstrated differences in the liver function tests and a possible (although non-significant) difference in the number of recombined cells in response to a predominantly hepatocellular injury with CDE diet, I then wanted to look at a model of biliary injury. For this, I used the DDC dietary model, as illustrated in figure 5.5A.

There was no difference in the weight change seen in response to the diet (figure 5.5B). However, there was a higher bilirubin level in the floxed laminin alpha 5 group, as shown in figure 5.5C. There was a mean bilirubin of 100.4 µmol/L in the floxed laminin alpha 5 group, compared with 40.4 µmol/L in the YFP only group and 23.0 µmol/L in the floxed beta-1 integrin group (one-way ANOVA p 0.033). This may suggest either greater damage or impaired regeneration.

There was also a significantly higher serum ALT in the floxed laminin alpha 5 group (figure 5.5D). The mean ALT in the laminin alpha 5 group was 711 U/L, compared with 323 U/L in the YFP only group and 449 U/L in the floxed beta-1 integrin group (one-way ANOVA p 0.033). This is suggestive of increased hepatocellular injury associated with loss of laminin alpha 5. There was no difference in serum albumin between the 3 genotypes (figure 5.5E).

Quantification of the number of YFP positive cells did not show any difference between groups (figure 5.5F). In the DDC diet, the HPCs form ductular structures around the portal tracts, rather than the extraductular cords described in CDE. This makes it more challenging to distinguish between the original mature bile duct cells and newly-formed HPCs. To try to address this, I looked at the number of bile ducts containing recombined cells, on the assumption that the mature bile duct cells would tend to be restricted to one bile duct per portal tract. This analysis showed significantly fewer ducts containing recombined cells in the floxed laminin alpha 5 group (figure 5.5 G). This would be consistent with a failure of recombined cells to migrate to form new ducts.

I also looked at the proliferation of recombined cells using dual YFP and Ki67 staining (figure 5.5 H-I). There is a trend towards lower rates of proliferation with both floxed alleles, although this fails to reach statistical significance.

Figure 5.5 Effect of floxed alleles on response to DDC diet

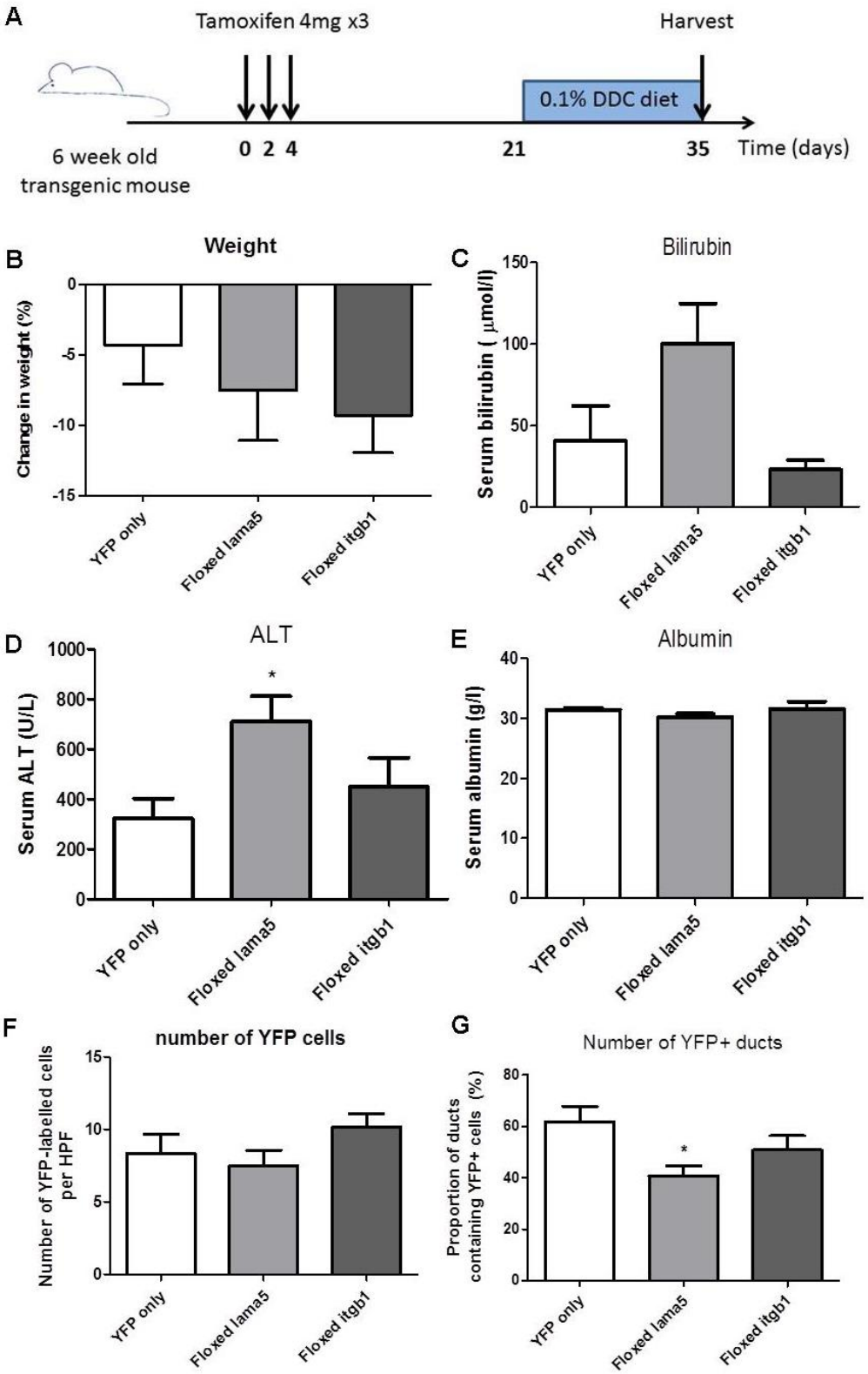

Figure 5.5 Effect of floxed alleles on response to DDC diet (cont)

H

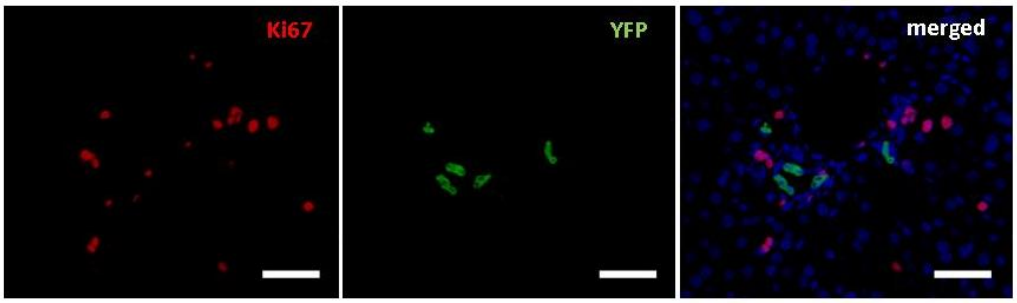

I

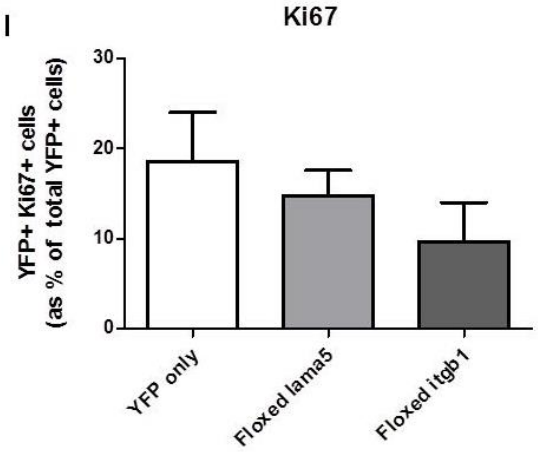

Figure 5.5 Effect of additional floxed alleles on response to DDC

A. Illustration of experimental timeline for transgenic mice given a DDC diet (n=3 aniamls in floxed laminin alpha 5 group, n=8 animals in YFP only and floxed beta 1 integrin groups). **B**. Mouse weights from induction to harvest, expressed as a percentage change, were not significantly different between genotypes. One-way ANOVA p 0.43. **C**. Serum bilirubin levels were highest in the floxed laminin alpha 5 group. One-way ANOVA p 0.033. **D**. Serum ALT levels were elevated in all groups, but were significantly higher in the floxed laminin alpha 5 group. One-way ANOVA p 0.033. **E**. Serum albumin levels were no different between groups. One-way ANOVA 0.36. **F**. Quantification of the number of YFP cells is not different between the groups. **G**. When looking at the number of ducts containing recombined cells, however, there is a lower number of ducts containing recombined cells in the floxed laminin alpha 5 group. **H**. Dual immunofluorescence with YFP (green) and Ki67 (red) to assess proliferation. Original magnification x400, scale bar represents 50 μm. **I.** There is a trend towards lower proliferation in both of the floxed allele groups, although this fails to reach statistical significance. n=3 animals per group for the dual immunofluorescence analysis.

Where significant differences were found on one-way ANOVA, Dunnett's test for multiple comparisons was used to compare each floxed allele against the YFP only group *$p<0.05$.

Effect on floxed alleles on fibrosis

As HPC expansion is generally associated with an increase in fibrosis, I looked at the the effect of the floxed alleles on fibrosis in the DDC diet. The image analysis for these experiments was performed by Alex Raven, using the tissue sections that I had generated. I performed the subsequent data analysis myself.

Both the floxed laminin alpha 5 and floxed beta 1 integrin groups showed significantly more fibrosis in response to the DDC diet than the YFP only group (figure 5.6A). This was supported by an increase in alpha smooth muscle actin (ASMA) staining in the same groups (figure 5.6B), suggesting an increase in the number of activated stellate cells.

Figure 5.6 Effect of floxed alleles on fibrosis

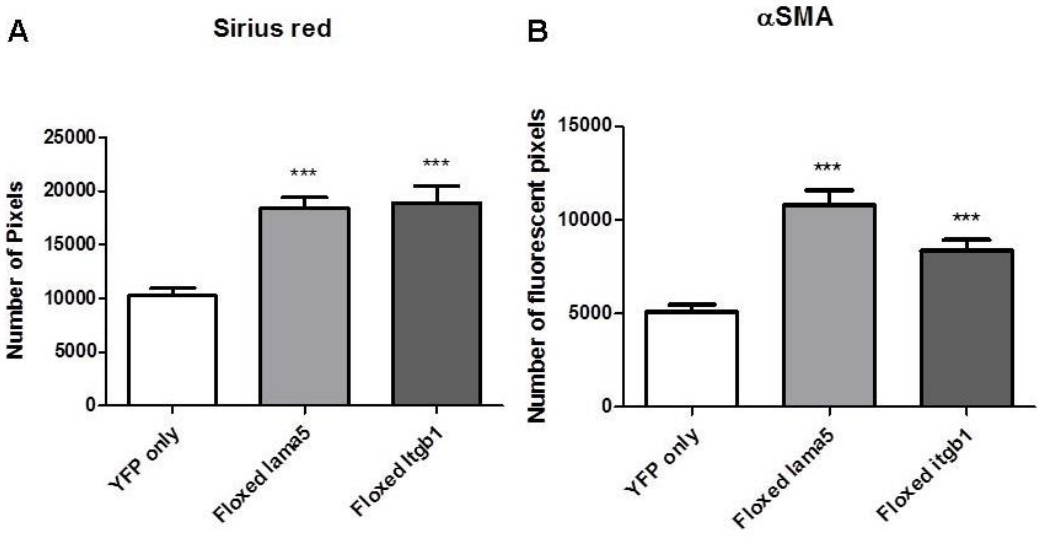

Figure 5.6 Effect of floxed alleles on fibrosis

Comparison of fibrosis markers in transgenic mice exposed to 2 weeks of DDC diet. **A**. Sirius red staining shows increased fibrosis in those mice with floxed laminin alpha 5 or floxed beta-1 integrin genes, compared to mice with the YFP reporter alone. One-way ANOVA $p<0.001$, Dunnett's post-test correction ***$p<0.001$. **B**. Alpha smooth muscle actin staining shows an increase in activated stellate cells in the two floxed gene groups.

Isolation of individual recombined cells using fluorescent reporter

As recombined cells express YFP, it should be possible to isolate them using fluorescence-activated cell sorting (FACS). However, several attempts to isolate cells using this method failed to detect any labelling of cells. Representative flow plots are shown in figure 5.7A. As recombination could be demonstrated on tissue sections using an antibody to amplify the signal, it was felt that the failure to detect fluorescent cells on FACS was likely to reflect a weak signal. However, attempts to amplify the signal using a fluorescent antibody against GFP were similarly unsuccessful (figure 5.7B). This could be explained by the fact that the permeabilisation stage required to allow the antibody into the cells may allow the YFP to diffuse out.

A number of new fluorescent proteins have been developed recently with improved brightness and photostability relative to YFP (Shaner et al., 2005). I therefore decided to use a different fluorescent reporter. tdTomato is an exceptionally bright red fluorescent protein developed through directed mutagenesis of the Discosoma-derived red fluorescent protein, DsRed (Shaner et al., 2004). As with the YFP reporter, tdTomato is available as a flox-stop-flox-tdTomato construct that will be expressed following Cre expression. The three transgenic mice strains were crossed with the tdTomato reporter in place of the YFP.

Further enhancements to the sorting protocol were the use of FSC gating to select singlet cells, and negative selection for CD45 (to exclude haematopoietic cells) and 7-AAD (to exclude dead cells). Using the brighter reporter and these additional criteria, I was able to identify a clear population of fluorescently labelled cells (figure 5.7C). The FACS experiments in this section were performed in collaboration with Wei-Yu Lu.

Recombined cells were isolated from mice from each of the three genotypes after exposure to 2 weeks of DDC diet, and were sent for a gene microarray. It was hoped that this would be used for a number of purposes. Firstly, to confirm the loss of specific laminin or integrin gene transcription in the floxed groups. Secondly, to identify any compensatory changes in other laminin or integrin subunits that may

occur secondary to the loss of the floxed alleles. Thirdly, to look for changes in intracellular signalling pathways that may be mediating the effects of cell-matrix interactions.

Unfortunately, due to the time taken to re-derive mice with the required genotypes, the results of the microarray are not available for inclusion in this thesis but will be hopefully be informative in helping to direct future work, as I will discuss in the next chapter.

Figure 5.7 Isolation of recombined cells

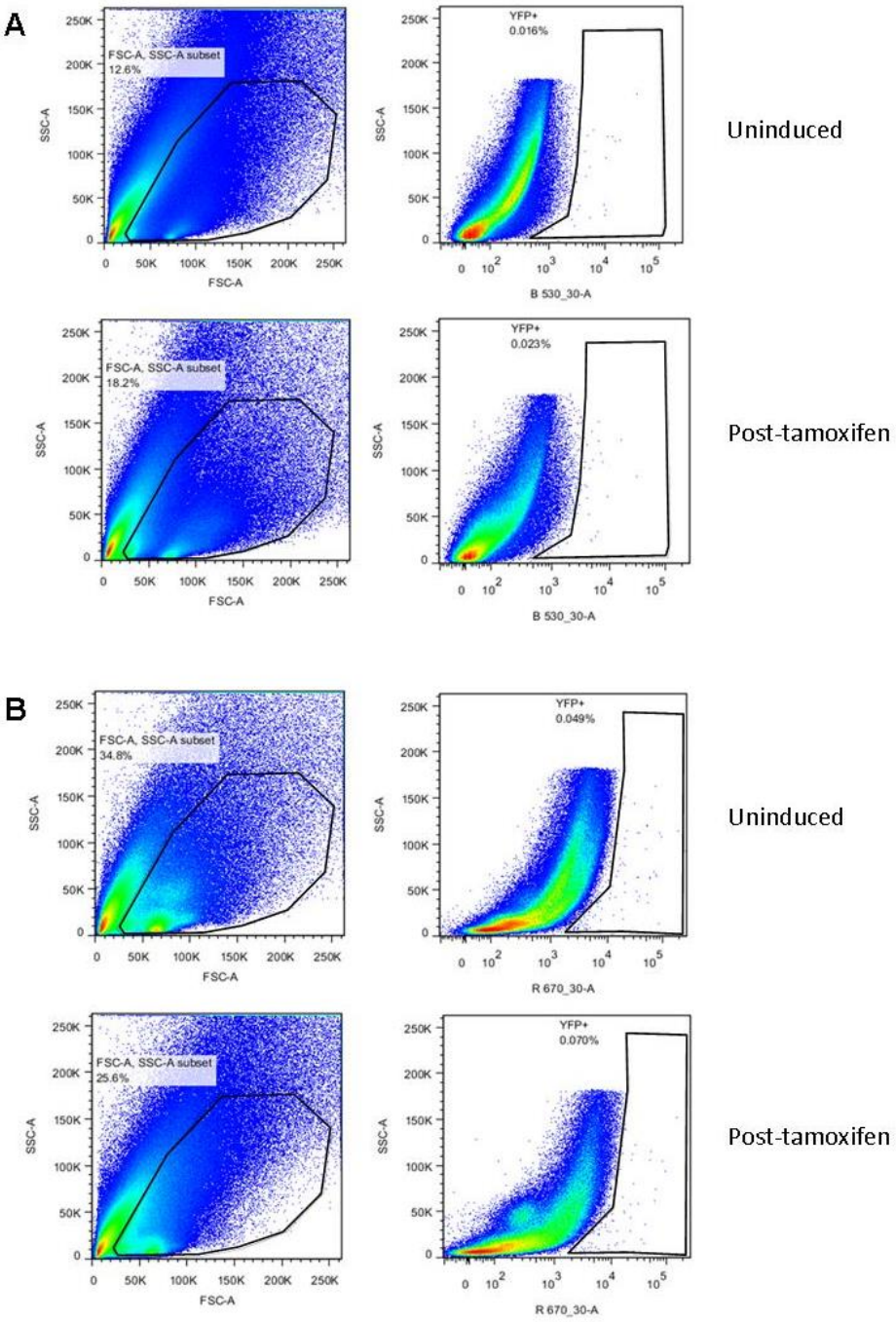

Figure 5.7 Isolation of recombined cells (cont)

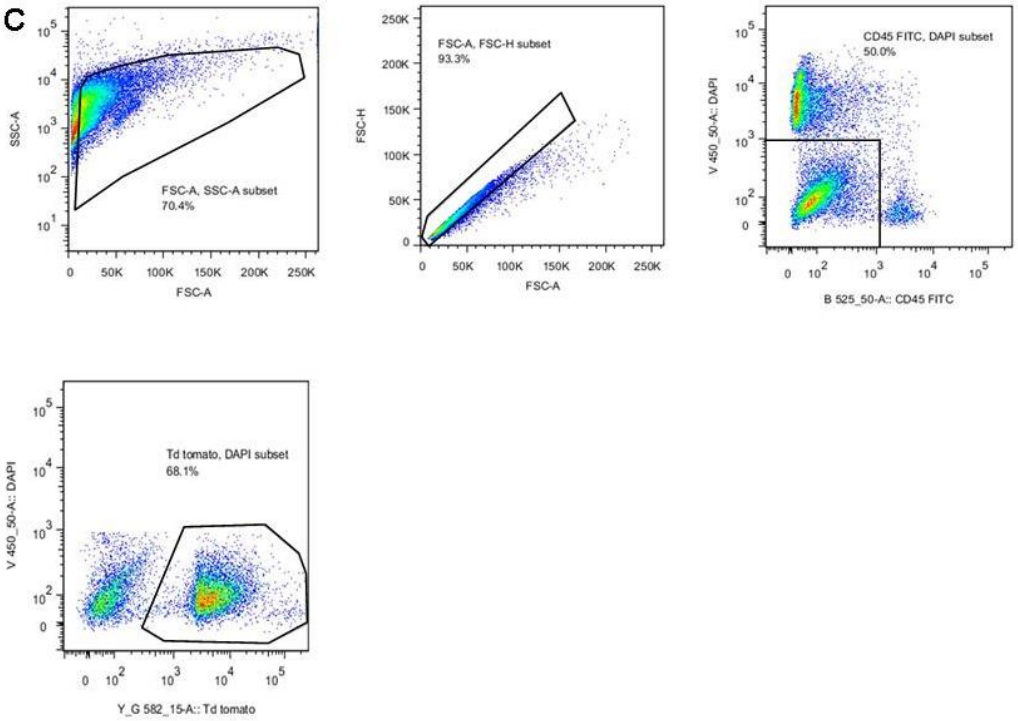

Figure 5.7 Isolation of individual recombined cells

A. Flow cytometry for non-parenchymal cells derived from K19Cre-YFP mice, comparing uninduced mice (top panels) with mice given 3 x 4mg tamoxifen to induce recombination (bottom panels). Cells were gated for using FSC/SSC (left-hand panels). There was no discrete identifiable population in the induced mice detectable using direct YFP detection (right hand panels). **B**. Matched flow plots for cells from the same experiment, treated with an anti-GFP antibody conjugated to APC. There was no discrete identifiable population in the induced mice using this approach either. **C**. Flow cytometry for non-parenchymal cells derived from K19Cre-tdTomato mice treated with 3 x 4mg tamoxifen. Cells were gated for using FSC/SSC, and singlets were selected using FSC-A/FSC-H. Cells that were double-negative for CD45 (to exclude haematopoietic cells) and 7-AAD (to exclude dead cells) were selected. In this case, a clear population of fluorescent cells are identifiable within the red wavelength.

5.3 Discussion

In this chapter, I have examined the effects of loss of either laminin alpha 5 or one of the subunits of its potential cell-surface receptors, beta 1 integrin. Each of these was knocked out in the adult mouse, targeting this effect to K19-expressing cells which will include biliary epithelial cells and HPCs. Unfortunately, these experiments were hindered by the need to exclude around half of the animals in the floxed laminin alpha 5 group, due to the presence of an additional unexpected Cre. This was only detected after completion of the experiments, leading to marked reduction in experimental numbers. This increases the risk of type II errors in the analysis, and has led me to comment on non-significant trends within this group. Although I am in the process of repeating the experiments with more mice from the floxed laminin alpha 5 group, the results of these were not ready in time to present in this thesis.

In the CDE diet, there was little effect of the floxed genes on mouse weight or liver function tests. The only significant abnormality was a markedly increased ALT in the floxed beta 1 integrin group, suggesting a greater degree of hepatocellular injury. This effect was not seen in the floxed laminin alpha 5 group, suggesting that this is mediated by loss of signalling from a different matrix component. As beta 1 integrin also forms part of both collagen and fibronectin receptors, it is possible that either of these matrix proteins may be implicated. There was a non-significant trend towards a reduction in the number of labelled cells in the floxed laminin alpha 5 group, suggesting a possible role of laminin alpha 5 in cell survival or proliferation.

In the DDC diet, there were more marked changes in the liver function tests. Mice in the floxed laminin alpha 5 group had higher serum bilirubin and ALT levels. Although DDC is described as a predominantly biliary injury due to accumulation of porphyrins, this can result in secondary hepatocellular damage. It is noteworthy that the ALTs were also elevated in the other genotypes on DDC diet, although the laminin alpha 5 group had significantly higher levels. There was also a significant increase in fibrosis with both of the floxed alleles.

One of the limitations of this work was the relatively low rate of recombination achieved with the K19-CreERT, making it difficult to measure effects on a whole

tissue level. Since this work was started, another group have published much more efficient recombination in HPCs using an inducible osteopontin-Cre (Espanol-Suner et al., 2012) with higher rates of lineage-traced hepatocytes. It is therefore possible that combining this osteopontin-Cre with the floxed alleles that I have used would provide more accurate results. In particular, it would be very interesting to be able to study the effects on differentiation, an event that was seen too infrequently in my model to be able to comment on reliably.

To get around the issue of low recombination rates, I have tried to assess individual recombined cells. This makes the assumption that cells that express Cre recombinase will be equally efficient in excising the reporter construct and the gene of interest. Although this is generally believed to be the case, this has not been demonstrated within this work. The awaited gene microarray of sorted cells will allow assessment of the efficiency of knock-down of both laminin alpha 5 and beta-1 integrin in the tdTomato-expressing cells.

Another limitation is the poor HPC response to the CDE diet. In both the YFP only group and floxed laminin alpha 5 group, the mean serum ALT was only minimally raised, suggesting only minor hepatocellular injury. Looking at the YFP only group, the number of labelled cells was only slightly higher following CDE than on a normal diet (4.8 vs 4.2), suggesting minimal expansion of HPCs with the diet. This is supported by the low number of recombined cells that occurred away from a bile duct lumen, even in the YFP only group. The very low rates of YFP-labelled hepatocytes seen in what was proposed to be a model of hepatocellular regeneration are likely to reflect this low rate of injury.

An alternative dietary model that might be used is the methionine- and choline-deficient (MCD) diet, with or without ethionine supplementation. In contrast to choline deficiency alone, additional methionine deficiency leads to more inflammation and fibrosis (Weltman et al., 1996). The MCD diet has the additional benefit of being a more clinically relevant model than CDE diet, as it mirrors some of the changes seen in human non-alcoholic steatohepatitis (Anstee and Goldin, 2006). It has been shown that methionine counteracts the effects of ethionine in a

choline-deficient diet (Sidransky and Verney, 1969). The combination of methionine- and choline-deficiency with ethionine supplementation (MCDE) produces significant HPC expansion (Jung et al., 2010, Huch et al., 2013).

A more robust HPC response was seen with the DDC diet. In this model, the effects on hepatocellular injury and fibrosis are intriguing. Although HPCs have been extensively studied with regard to their ability to form hepatocytes, it is only very recently that it has been suggested that they may play a role in modulating liver injury. A recent study showed that isoproterenol (a non-selective beta-adrenergic agonist) both stimulates HPC numbers and protects against acetaminophen-induced liver injury (Soeda et al., 2014). In vitro studies suggest that this effect may be mediated by increased expression of HPC-derived Wnt ligands on hepatocyte survival, and transplantation of HPCs also improved liver injury. It is possible that HPCs have a role in protecting against hepatocellular injury and that loss of laminin alpha 5 impairs this.

The increased fibrosis seen in the floxed laminin alpha 5 group may reflect the increased injury, or may due to altered signalling between HPCs and stellate cells, or a combination of both. In the case of the floxed beta 1 integrin group, the increase in fibrosis occurred in the absence of any change in ALT levels, suggesting that this effect is more likely to be a result of altered signalling to stellates.

In spite of the difficulties encountered during the transgenic experiments due to reduced experimental numbers, these results do suggest an altered regenerative response to injury with loss of either laminin alpha 5 or beta-1 integrin, and merit further investigation.

Chapter 6: Concluding remarks and future directions

The relationship between HPCs and extracellular laminins is well-recognised but incompletely understood. One factor that has often been overlooked is the heterogeneity within the laminin family. In this thesis, I have examined the changes in individual laminin alpha chains and shown a marked upregulation of laminin alpha 5 in two separate models of HPC expansion. This co-localises with the HPCs and appears to be produced predominantly by the progenitor cells themselves. Laminin alpha 5 is also shown in human liver disease associated with ductular reactions. The HPCs express the laminin-binding α6β1 integrin.

A series of in vitro experiments showed that laminin alpha 5-containing matrix promotes adhesion, spreading and migration of an HPC cell line. These effects are only partially blocked by antibodies targeting beta-1 integrin, a subunit common to a number of laminin-binding cell surface receptors. Disruption of endogenous laminin alpha 5 synthesis using siRNA causes a reduction in proliferation and resulted in differentiation towards a more hepatocyte-like phenotype. This suggests that laminin alpha 5 plays an important role in autocrine signalling amongst HPCs.

Lastly, loss of laminin alpha 5 in vivo modulates the response to HPC expansion, with an increase in hepatocellular injury and fibrosis in the DDC model. Loss of beta-1 integrin on the HPCs does not recapitulate all of these effects. This, along with the in vitro data, suggests that cell surface receptors other than integrins containing the beta-1 subunit are important in the interaction between HPCs and extracellular laminin alpha 5. This work opens up a number of exciting avenues for research.

I selected beta-1 integrin to study because of its occurrence in a number of the laminin-binding receptors but there are other integrins (α6β4) and non-integrin receptors (dystroglycan, syndecans and Lutheran blood group glycoprotein/BCAM) that may be mediating this interaction (Kikkawa et al., 2000, Tani et al., 1999,

Shimizu et al., 1999, El Nemer et al., 1998). Lutheran/BCAM is the most appealing of these, due to its high specificity for laminin alpha 5. It would be interesting to explore the expression of Lutheran/BCAM on HPCs during the models I have already used. If a correlation with HPC expansion is seen, there are Lutheran/BCAM knock-out and transgenic overexpressing mice that could be used to study the effects of altered signalling through this receptor (Moulson et al., 2001). Alternatively, it may be that co-signalling through other receptors, such as the tetraspanins, is important in modulating integrin signalling.

Throughout my thesis, I have focussed on the synthesis of matrix. However, it is important to remember that the extracellular matrix is dynamic and that degradation can play a role too. It is known that the laminin seen in association with HPC expansion is transient but there is little work on the regulation of laminin degradation in the liver. Much of the work on matrix remodelling in the liver has focussed on collagen turnover (Hemmann et al., 2007) but an improved understanding of the role of specific MMPs and TIMPs in regulating specific laminin isoforms may also identify further potential targets to enhance regeneration.

I have also focussed in my work on cell behaviour, rather than on the signalling pathways that lead to this. A further direction for study would be to identify the key intracellular regulators of the effects of laminin alpha 5. During embryonic development, laminin-511 is required for hair morphogenesis. It has been shown that laminin-511-null mice fail to express noggin (Gao et al., 2008). Noggin is an inhibitor of bone morphogenetic protein (BMP) which causes expression and activation of members of the Lef-1/TCF DNA-binding protein family, and subsequently activates Sonic hedgehog (Shh) signalling and down-regulates E-cadherin. Exogenous noggin or Shh were able to restore normal hair follicle development. In contrast, laminin-111 did not trigger noggin expression. Shh signalling has been shown to influence HPC behaviour and is a strong potential candidate for mediating the cell-matrix effect (Omenetti et al., 2011).

Work in embryonic intestinal tissue derived from Lama5 deficient mice has also identified marked changes in Wnt and PI3K/Akt signalling (Ritie et al., 2012). Cell

culture experiments suggest that laminin-511 inhibits Wnt signalling and stimulates the PI3K/Akt pathway. Cell polarity is important in both the regulation of stem cells and in the maintenance of epithelial functions, and laminins play a role in cell polarization (Li et al., 2003b).

It is not clear how the matrix-derived signals are integrated with the currently identified signalling pathways involved in HPC regulation (Santoni-Rugiu et al., 2005, Boulter et al., 2012). Further work is required to assess the interplay between laminin-511 and the influences of TWEAK, Wnt, Notch and Shh signalling. Co-culture experiments may be informative in assessing the interaction between cell-matrix and cell-cell signalling.

The effect of loss of laminin alpha 5 on both liver injury and fibrosis are also exciting findings. Although HPC expansion has recently been shown to be associated with a reduction in acute liver injury by Soeda et al (2014), my work provides further support to this novel concept.

By further understanding the role of the extracellular matrix in regulating HPC behaviour, we may hopefully be able to design more rational targeted therapies to influence both fibrosis and regeneration. As laminin-511 is widely distributed throughout adult epithelial and endothelial tissues, systemic therapies to alter expression levels are unlikely to be appropriate. However, a detailed understanding of the cell-matrix interaction may offer a more specific therapeutic target. Furthermore, any anti-fibrotic therapies should be assessed with regard to their effect on laminin isoform distribution to avoid any unwanted effect on HPCs.

A number of forms of cell therapy have been proposed for chronic liver disease, including bone marrow-derived cells, stem cells (ES and iPS-derived) and HPCs (Piscaglia et al., 2010, Lanthier et al., 2013). Extracellular matrix is likely to play an important role in the engraftment of any such exogenous cells. There is some evidence to suggest that laminin promotes the adhesion of bone marrow-derived stem cells in the liver following partial hepatectomy, although this work did not assess individual laminin isoforms (Carvalho et al., 2008). I would speculate that laminin

alpha 5-containing matrix is likely to be important in the engraftment of HPCs during cell therapy. My results also suggest that laminin-511 is likely to be beneficial for the ex vivo expansion of HPCs for any such cell therapy.

Macrophage cell therapy has been shown to result in increased expression of MMP-9 and MMP-13 within the liver, with an accompanying reduction in fibrosis and expansion of HPCs (Thomas et al., 2011). This demonstrates the potential for manipulation of matrix turnover, and an ability to influence laminin alpha 5 levels may have important implications for regeneration.

In conclusion, this work is the first description of the changes in laminin alpha chains during models of HPC expansion and identifies laminin alpha 5 as the predominant isoform. Laminin alpha 5 has significant autocrine effects on HPC behaviour in culture, and knock-down of laminin alpha 5 in K19-expressing HPCs produces an increase in liver injury and fibrosis in response to the DDC diet.

Chapter 7: References

AKHURST, B., CROAGER, E. J., FARLEY-ROCHE, C. A., ONG, J. K., DUMBLE, M. L., KNIGHT, B. & YEOH, G. C. 2001. A modified choline-deficient, ethionine-supplemented diet protocol effectively induces oval cells in mouse liver. *Hepatology,* 34**,** 519-22.

ANSTEE, Q. M. & GOLDIN, R. D. 2006. Mouse models in non-alcoholic fatty liver disease and steatohepatitis research. *Int J Exp Pathol,* 87**,** 1-16.

ARENSON, D. M., FRIEDMAN, S. L. & BISSELL, D. M. 1988. Formation of extracellular matrix in normal rat liver: lipocytes as a major source of proteoglycan. *Gastroenterology,* 95**,** 441-7.

AUMAILLEY, M., BRUCKNER-TUDERMAN, L., CARTER, W. G., DEUTZMANN, R., EDGAR, D., EKBLOM, P., ENGEL, J., ENGVALL, E., HOHENESTER, E., JONES, J. C., KLEINMAN, H. K., MARINKOVICH, M. P., MARTIN, G. R., MAYER, U., MENEGUZZI, G., MINER, J. H., MIYAZAKI, K., PATARROYO, M., PAULSSON, M., QUARANTA, V., SANES, J. R., SASAKI, T., SEKIGUCHI, K., SOROKIN, L. M., TALTS, J. F., TRYGGVASON, K., UITTO, J., VIRTANEN, I., VON DER MARK, K., WEWER, U. M., YAMADA, Y. & YURCHENCO, P. D. 2005. A simplified laminin nomenclature. *Matrix Biol,* 24**,** 326-32.

BARCZYK, M., CARRACEDO, S. & GULLBERG, D. 2010. Integrins. *Cell Tissue Res,* 339**,** 269-80.

BENNINGER, Y., COLOGNATO, H., THURNHERR, T., FRANKLIN, R. J., LEONE, D. P., ATANASOSKI, S., NAVE, K. A., FFRENCH-CONSTANT, C., SUTER, U. & RELVAS, J. B. 2006. Beta1-integrin signaling mediates premyelinating oligodendrocyte survival but is not required for CNS myelination and remyelination. *J Neurosci,* 26**,** 7665-73.

BENYON, R. C. & ARTHUR, M. J. 2001. Extracellular matrix degradation and the role of hepatic stellate cells. *Semin Liver Dis,* 21**,** 373-84.

BOULTER, L., GOVAERE, O., BIRD, T. G., RADULESCU, S., RAMACHANDRAN, P., PELLICORO, A., RIDGWAY, R. A., SEO, S. S., SPEE, B., VAN ROOIJEN, N., SANSOM, O. J., IREDALE, J. P., LOWELL, S., ROSKAMS, T. & FORBES, S. J. 2012. Macrophage-derived Wnt opposes Notch signaling to specify hepatic progenitor cell fate in chronic liver disease. *Nat Med,* 18**,** 572-9.

BOUVARD, D., BRAKEBUSCH, C., GUSTAFSSON, E., ASZODI, A., BENGTSSON, T., BERNA, A. & FASSLER, R. 2001. Functional consequences of integrin gene mutations in mice. *Circ Res,* 89**,** 211-23.

BRALET, M. P., BRANCHEREAU, S., BRECHOT, C. & FERRY, N. 1994. Cell lineage study in the liver using retroviral mediated gene transfer. Evidence against the streaming of hepatocytes in normal liver. *Am J Pathol,* 144**,** 896-905.

BRANDA, C. S. & DYMECKI, S. M. 2004. Talking about a revolution: The impact of site-specific recombinases on genetic analyses in mice. *Dev Cell,* 6**,** 7-28.

BRAUN, K. M., THOMPSON, A. W. & SANDGREN, E. P. 2003. Hepatic microenvironment affects oval cell localization in albumin-urokinase-type plasminogen activator transgenic mice. *Am J Pathol,* 162**,** 195-202.

CARVALHO, S., CORTEZ, E., STUMBO, A. C., THOLE, A., CAETANO, C., MARQUES, R., PELAJO-MACHADO, M., PORTO, L. C. & CARVALHO, L. 2008. Laminin expression during bone marrow mononuclear cell transplantation in hepatectomized rats. *Cell Biol Int,* 32**,** 1014-8.

CHEN, Y. H., CHANG, M. H., CHIEN, C. S., WU, S. H., YU, C. H. & CHEN, H. L. 2013. Contribution of mature hepatocytes to small hepatocyte-like progenitor cells in retrorsine-exposed rats with chimeric livers. *Hepatology,* 57**,** 1215-24.

CHIA, J., KUSUMA, N., ANDERSON, R., PARKER, B., BIDWELL, B., ZAMURS, L., NICE, E. & POULIOT, N. 2007. Evidence for a role of tumor-derived laminin-511 in the metastatic progression of breast cancer. *Am J Pathol,* 170**,** 2135-48.

CHIU, C. C., SHEU, J. C., CHEN, C. H., LEE, C. Z., CHIOU, L. L., CHOU, S. H., HUANG, G. T. & LEE, H. S. 2009. Global gene expression profiling reveals a key role of CD44 in hepatic oval-cell reaction after 2-AAF/CCl4 injury in rodents. *Histochem Cell Biol,* 132**,** 479-89.

CLOUSTON, A. D., JONSSON, J. R. & POWELL, E. E. 2009. Hepatic progenitor cell-mediated regeneration and fibrosis: chicken or egg? *Hepatology,* 49**,** 1424-6.

CLOUSTON, A. D., POWELL, E. E., WALSH, M. J., RICHARDSON, M. M., DEMETRIS, A. J. & JONSSON, J. R. 2005. Fibrosis correlates with a ductular reaction in hepatitis C: roles of impaired replication, progenitor cells and steatosis. *Hepatology,* 41**,** 809-18.

COLOGNATO, H. & YURCHENCO, P. D. 2000. Form and function: the laminin family of heterotrimers. *Dev Dyn,* 218**,** 213-34.

COUCHMAN, J. R. 2003. Syndecans: proteoglycan regulators of cell-surface microdomains? *Nat Rev Mol Cell Biol,* 4**,** 926-37.

DOHI, T. & BURKLY, L. C. 2012. The TWEAK/Fn14 pathway as an aggravating and perpetuating factor in inflammatory diseases: focus on inflammatory bowel diseases. *J Leukoc Biol,* 92**,** 265-79.

DOI, M., THYBOLL, J., KORTESMAA, J., JANSSON, K., IIVANAINEN, A., PARVARDEH, M., TIMPL, R., HEDIN, U., SWEDENBORG, J. & TRYGGVASON, K. 2002. Recombinant human laminin-10 (alpha5beta1gamma1). Production, purification, and migration-promoting activity on vascular endothelial cells. *J Biol Chem,* 277**,** 12741-8.

DOLLE, L., BEST, J., MEI, J., AL BATTAH, F., REYNAERT, H., VAN GRUNSVEN, L. A. & GEERTS, A. 2010. The quest for liver progenitor cells: a practical point of view. *J Hepatol,* 52**,** 117-29.

DOMOGATSKAYA, A., RODIN, S., BOUTAUD, A. & TRYGGVASON, K. 2008. Laminin-511 but not -332, -111, or -411 enables mouse embryonic stem cell self-renewal in vitro. *Stem Cells,* 26**,** 2800-9.

DORRELL, C., ERKER, L., SCHUG, J., KOPP, J. L., CANADAY, P. S., FOX, A. J., SMIRNOVA, O., DUNCAN, A. W., FINEGOLD, M. J., SANDER, M., KAESTNER, K. H. & GROMPE, M. 2011. Prospective isolation of a bipotential clonogenic liver progenitor cell in adult mice. *Genes Dev,* 25**,** 1193-203.

DUNCAN, A. W., DORRELL, C. & GROMPE, M. 2009. Stem cells and liver regeneration. *Gastroenterology,* 137**,** 466-81.

DURBEEJ, M. 2010. Laminins. *Cell Tissue Res,* 339**,** 259-68.
DURNEZ, A., VERSLYPE, C., NEVENS, F., FEVERY, J., AERTS, R., PIRENNE, J., LESAFFRE, E., LIBBRECHT, L., DESMET, V. & ROSKAMS, T. 2006. The clinicopathological and prognostic relevance of cytokeratin 7 and 19 expression in hepatocellular carcinoma. A possible progenitor cell origin. *Histopathology,* 49**,** 138-51.
EDGAR, R., DOMRACHEV, M. & LASH, A. E. 2002. Gene Expression Omnibus: NCBI gene expression and hybridization array data repository. *Nucleic Acids Res,* 30**,** 207-10.
EL NEMER, W., GANE, P., COLIN, Y., BONY, V., RAHUEL, C., GALACTEROS, F., CARTRON, J. P. & LE VAN KIM, C. 1998. The Lutheran blood group glycoproteins, the erythroid receptors for laminin, are adhesion molecules. *J Biol Chem,* 273**,** 16686-93.
ENDO, Y., ZHANG, M., YAMAJI, S. & CANG, Y. 2012. Genetic abolishment of hepatocyte proliferation activates hepatic stem cells. *PLoS One,* 7**,** e31846.
ESPANOL-SUNER, R., CARPENTIER, R., VAN HUL, N., LEGRY, V., ACHOURI, Y., CORDI, S., JACQUEMIN, P., LEMAIGRE, F. & LECLERCQ, I. A. 2012. Liver Progenitor Cells Yield Functional Hepatocytes in Response to Chronic Liver Injury in Mice. *Gastroenterology,* 143**,** 1564-1575.
EVARTS, R. P., NAGY, P., NAKATSUKASA, H., MARSDEN, E. & THORGEIRSSON, S. S. 1989. In vivo differentiation of rat liver oval cells into hepatocytes. *Cancer Res,* 49**,** 1541-7.
FALKOWSKI, O., AN, H. J., IANUS, I. A., CHIRIBOGA, L., YEE, H., WEST, A. B. & THEISE, N. D. 2003. Regeneration of hepatocyte 'buds' in cirrhosis from intrabiliary stem cells. *J Hepatol,* 39**,** 357-64.
FALLOWFIELD, J. A., MIZUNO, M., KENDALL, T. J., CONSTANDINOU, C. M., BENYON, R. C., DUFFIELD, J. S. & IREDALE, J. P. 2007. Scar-associated macrophages are a major source of hepatic matrix metalloproteinase-13 and facilitate the resolution of murine hepatic fibrosis. *J Immunol,* 178**,** 5288-95.
FASSLER, R. & MEYER, M. 1995. Consequences of lack of beta 1 integrin gene expression in mice. *Genes Dev,* 9**,** 1896-908.
FAUSTO, N. 2004. Liver regeneration and repair: hepatocytes, progenitor cells, and stem cells. *Hepatology,* 39**,** 1477-87.
FELLOUS, T. G., ISLAM, S., TADROUS, P. J., ELIA, G., KOCHER, H. M., BHATTACHARYA, S., MEARS, L., TURNBULL, D. M., TAYLOR, R. W., GREAVES, L. C., CHINNERY, P. F., TAYLOR, G., MCDONALD, S. A., WRIGHT, N. A. & ALISON, M. R. 2009. Locating the stem cell niche and tracing hepatocyte lineages in human liver. *Hepatology,* 49**,** 1655-63.
FLEISCHMAJER, R., KURODA, K., UTANI, A., DOUGLAS MACDONALD, E., PERLISH, J. S., ARIKAWA-HIRASAWA, E., SEKIGUCHI, K., SANZEN, N., TIMPL, R. & YAMADA, Y. 2000. Differential expression of laminin alpha chains during proliferative and differentiation stages in a model for skin morphogenesis. *Matrix Biol,* 19**,** 637-47.
FORBES, S., VIG, P., POULSOM, R., THOMAS, H. & ALISON, M. 2002. Hepatic stem cells. *J Pathol,* 197**,** 510-8.

FREISE, C., ERBEN, U., MUCHE, M., FARNDALE, R., ZEITZ, M., SOMASUNDARAM, R. & RUEHL, M. 2009. The alpha 2 chain of collagen type VI sequesters latent proforms of matrix-metalloproteinases and modulates their activation and activity. *Matrix Biol,* 28**,** 480-9.

FUCHS, E., TUMBAR, T. & GUASCH, G. 2004. Socializing with the neighbors: stem cells and their niche. *Cell,* 116**,** 769-78.

FUKUMOTO, S., MINER, J. H., IDA, H., FUKUMOTO, E., YUASA, K., MIYAZAKI, H., HOFFMAN, M. P. & YAMADA, Y. 2006. Laminin alpha5 is required for dental epithelium growth and polarity and the development of tooth bud and shape. *J Biol Chem,* 281**,** 5008-16.

FURUYAMA, K., KAWAGUCHI, Y., AKIYAMA, H., HORIGUCHI, M., KODAMA, S., KUHARA, T., HOSOKAWA, S., ELBAHRAWY, A., SOEDA, T., KOIZUMI, M., MASUI, T., KAWAGUCHI, M., TAKAORI, K., DOI, R., NISHI, E., KAKINOKI, R., DENG, J. M., BEHRINGER, R. R., NAKAMURA, T. & UEMOTO, S. 2011. Continuous cell supply from a Sox9-expressing progenitor zone in adult liver, exocrine pancreas and intestine. *Nat Genet,* 43**,** 34-41.

GADD, V. L., MELINO, M., ROY, S., HORSFALL, L., O'ROURKE, P., WILLIAMS, M. R., IRVINE, K. M., SWEET, M. J., JONSSON, J. R., CLOUSTON, A. D. & POWELL, E. E. 2013. Portal, but not lobular, macrophages express matrix metalloproteinase-9: association with the ductular reaction and fibrosis in chronic hepatitis C. *Liver Int,* 33**,** 569-79.

GAHWILER, B. H., CAPOGNA, M., DEBANNE, D., MCKINNEY, R. A. & THOMPSON, S. M. 1997. Organotypic slice cultures: a technique has come of age. *Trends Neurosci,* 20**,** 471-7.

GAO, J., DEROUEN, M. C., CHEN, C. H., NGUYEN, M., NGUYEN, N. T., IDO, H., HARADA, K., SEKIGUCHI, K., MORGAN, B. A., MINER, J. H., ORO, A. E. & MARINKOVICH, M. P. 2008. Laminin-511 is an epithelial message promoting dermal papilla development and function during early hair morphogenesis. *Genes Dev,* 22**,** 2111-24.

GIANCOTTI, F. G. & RUOSLAHTI, E. 1999. Integrin signaling. *Science,* 285**,** 1028-32.

GRECIANO, P. G., MOYANO, J. V., BUSCHMANN, M. M., TANG, J., LU, Y., RUDNICKI, J., MANNINEN, A. & MATLIN, K. S. 2012. Laminin 511 partners with laminin 332 to mediate directional migration of Madin-Darby canine kidney epithelial cells. *Mol Biol Cell,* 23**,** 121-36.

GRIER, J. D., YAN, W. & LOZANO, G. 2002. Conditional allele of mdm2 which encodes a p53 inhibitor. *Genesis,* 32**,** 145-7.

HAHN, E., WICK, G., PENCEV, D. & TIMPL, R. 1980. Distribution of basement membrane proteins in normal and fibrotic human liver: collagen type IV, laminin, and fibronectin. *Gut,* 21**,** 63-71.

HEMMANN, S., GRAF, J., RODERFELD, M. & ROEB, E. 2007. Expression of MMPs and TIMPs in liver fibrosis - a systematic review with special emphasis on anti-fibrotic strategies. *J Hepatol,* 46**,** 955-75.

HEWITT, R. E., POWE, D. G., MORRELL, K., BALLEY, E., LEACH, I. H., ELLIS, I. O. & TURNER, D. R. 1997. Laminin and collagen IV subunit

distribution in normal and neoplastic tissues of colorectum and breast. *Br J Cancer,* 75**,** 221-9.

HIGGINS, G. M. & ANDERSON, R. M. 1931. Experimental pathology of the liver I Restoration of the liver of the white rat following partial surgical removal. *Archives of Pathology,* 12**,** 186-202.

HUCH, M., DORRELL, C., BOJ, S. F., VAN ES, J. H., LI, V. S., VAN DE WETERING, M., SATO, T., HAMER, K., SASAKI, N., FINEGOLD, M. J., HAFT, A., VRIES, R. G., GROMPE, M. & CLEVERS, H. 2013. In vitro expansion of single Lgr5+ liver stem cells induced by Wnt-driven regeneration. *Nature,* 494**,** 247-50.

HUMPHRIES, J. D., BYRON, A. & HUMPHRIES, M. J. 2006. Integrin ligands at a glance. *J Cell Sci,* 119**,** 3901-3.

HUMPHRIES, M. J. 2009. Cell adhesion assays. *Methods Mol Biol,* 522**,** 203-10.

HYNES, R. O. 1992. Integrins: versatility, modulation, and signaling in cell adhesion. *Cell,* 69**,** 11-25.

HYNES, R. O. 2002. Integrins: bidirectional, allosteric signaling machines. *Cell,* 110**,** 673-87.

HYNES, R. O. 2009. The extracellular matrix: not just pretty fibrils. *Science,* 326**,** 1216-9.

IDO, H., ITO, S., TANIGUCHI, Y., HAYASHI, M., SATO-NISHIUCHI, R., SANZEN, N., HAYASHI, Y., FUTAKI, S. & SEKIGUCHI, K. 2008. Laminin isoforms containing the gamma3 chain are unable to bind to integrins due to the absence of the glutamic acid residue conserved in the C-terminal regions of the gamma1 and gamma2 chains. *J Biol Chem,* 283**,** 28149-57.

IRELAND, H., KEMP, R., HOUGHTON, C., HOWARD, L., CLARKE, A. R., SANSOM, O. J. & WINTON, D. J. 2004. Inducible Cre-mediated control of gene expression in the murine gastrointestinal tract: effect of loss of beta-catenin. *Gastroenterology,* 126**,** 1236-46.

JAKUBOWSKI, A., AMBROSE, C., PARR, M., LINCECUM, J. M., WANG, M. Z., ZHENG, T. S., BROWNING, B., MICHAELSON, J. S., BAETSCHER, M., WANG, B., BISSELL, D. M. & BURKLY, L. C. 2005. TWEAK induces liver progenitor cell proliferation. *J Clin Invest,* 115**,** 2330-40.

JELNES, P., SANTONI-RUGIU, E., RASMUSSEN, M., FRIIS, S. L., NIELSEN, J. H., TYGSTRUP, N. & BISGAARD, H. C. 2007. Remarkable heterogeneity displayed by oval cells in rat and mouse models of stem cell-mediated liver regeneration. *Hepatology,* 45**,** 1462-70.

JONES, R. G., LI, X., GRAY, P. D., KUANG, J., CLAYTON, F., SAMOWITZ, W. S., MADISON, B. B., GUMUCIO, D. L. & KUWADA, S. K. 2006. Conditional deletion of beta1 integrins in the intestinal epithelium causes a loss of Hedgehog expression, intestinal hyperplasia, and early postnatal lethality. *J Cell Biol,* 175**,** 505-14.

JUNG, Y., WITEK, R. P., SYN, W. K., CHOI, S. S., OMENETTI, A., PREMONT, R., GUY, C. D. & DIEHL, A. M. 2010. Signals from dying hepatocytes trigger growth of liver progenitors. *Gut,* 59**,** 655-65.

KALLIS, Y. N., ROBSON, A. J., FALLOWFIELD, J. A., THOMAS, H. C., ALISON, M. R., WRIGHT, N. A., GOLDIN, R. D., IREDALE, J. P. &

FORBES, S. J. 2011. Remodelling of extracellular matrix is a requirement for the hepatic progenitor cell response. *Gut,* 60**,** 525-33.

KAMIYA, A., KAKINUMA, S., YAMAZAKI, Y. & NAKAUCHI, H. 2009. Enrichment and clonal culture of progenitor cells during mouse postnatal liver development in mice. *Gastroenterology,* 137**,** 1114-26, 1126 e1-14.

KANTA, J. & CHLUMSKA, A. 1991. Regenerative ability of hepatocytes is inhibited in early stages of liver fibrosis. *Physiol Res,* 40**,** 453-8.

KATO, A., BAMBA, H., SHINOHARA, M., YAMAUCHI, A., OTA, S., KAWAMOTO, C. & YOSHIDA, Y. 2005. Relationship between expression of cyclin D1 and impaired liver regeneration observed in fibrotic or cirrhotic rats. *J Gastroenterol Hepatol,* 20**,** 1198-205.

KAWADA, N., KLEIN, H. & DECKER, K. 1992. Eicosanoid-mediated contractility of hepatic stellate cells. *Biochem J,* 285 (Pt 2)**,** 367-71.

KAZANIS, I., LATHIA, J. D., VADAKKAN, T. J., RABORN, E., WAN, R., MUGHAL, M. R., ECKLEY, D. M., SASAKI, T., PATTON, B., MATTSON, M. P., HIRSCHI, K. K., DICKINSON, M. E. & FFRENCH-CONSTANT, C. 2010. Quiescence and activation of stem and precursor cell populations in the subependymal zone of the mammalian brain are associated with distinct cellular and extracellular matrix signals. *J Neurosci,* 30**,** 9771-81.

KE, A. W., SHI, G. M., ZHOU, J., HUANG, X. Y., SHI, Y. H., DING, Z. B., WANG, X. Y., DEVBHANDARI, R. P. & FAN, J. 2011. CD151 amplifies signaling by integrin alpha6beta1 to PI3K and induces the epithelial-mesenchymal transition in HCC cells. *Gastroenterology,* 140**,** 1629-41 e15.

KIEL, M. J., HE, S., ASHKENAZI, R., GENTRY, S. N., TETA, M., KUSHNER, J. A., JACKSON, T. L. & MORRISON, S. J. 2007. Haematopoietic stem cells do not asymmetrically segregate chromosomes or retain BrdU. *Nature,* 449**,** 238-42.

KIKKAWA, Y., MOCHIZUKI, Y., MINER, J. H. & MITAKA, T. 2005. Transient expression of laminin alpha1 chain in regenerating murine liver: restricted localization of laminin chains and nidogen-1. *Exp Cell Res,* 305**,** 99-109.

KIKKAWA, Y., SANZEN, N., FUJIWARA, H., SONNENBERG, A. & SEKIGUCHI, K. 2000. Integrin binding specificity of laminin-10/11: laminin-10/11 are recognized by alpha 3 beta 1, alpha 6 beta 1 and alpha 6 beta 4 integrins. *J Cell Sci,* 113 (Pt 5)**,** 869-76.

KIKKAWA, Y., SANZEN, N. & SEKIGUCHI, K. 1998. Isolation and characterization of laminin-10/11 secreted by human lung carcinoma cells. laminin-10/11 mediates cell adhesion through integrin alpha3 beta1. *J Biol Chem,* 273**,** 15854-9.

KIKKAWA, Y., SUDO, R., KON, J., MIZUGUCHI, T., NOMIZU, M., HIRATA, K. & MITAKA, T. 2008. Laminin alpha 5 mediates ectopic adhesion of hepatocellular carcinoma through integrins and/or Lutheran/basal cell adhesion molecule. *Exp Cell Res,* 314**,** 2579-90.

KNIGHT, B., AKHURST, B., MATTHEWS, V. B., RUDDELL, R. G., RAMM, G. A., ABRAHAM, L. J., OLYNYK, J. K. & YEOH, G. C. 2007a. Attenuated liver progenitor (oval) cell and fibrogenic responses to the choline deficient,

ethionine supplemented diet in the BALB/c inbred strain of mice. *J Hepatol,* 46**,** 134-41.

KNIGHT, B., LIM, R., YEOH, G. C. & OLYNYK, J. K. 2007b. Interferon-gamma exacerbates liver damage, the hepatic progenitor cell response and fibrosis in a mouse model of chronic liver injury. *J Hepatol,* 47**,** 826-33.

KNITTEL, T., MEHDE, M., KOBOLD, D., SAILE, B., DINTER, C. & RAMADORI, G. 1999. Expression patterns of matrix metalloproteinases and their inhibitors in parenchymal and non-parenchymal cells of rat liver: regulation by TNF-alpha and TGF-beta1. *J Hepatol,* 30**,** 48-60.

KON, J., OOE, H., OSHIMA, H., KIKKAWA, Y. & MITAKA, T. 2006. Expression of CD44 in rat hepatic progenitor cells. *J Hepatol,* 45**,** 90-8.

KORDES, C. & HAUSSINGER, D. 2013. Hepatic stem cell niches. *J Clin Invest,* 123**,** 1874-80.

KURAMITSU, K., SVERDLOV, D. Y., LIU, S. B., CSIZMADIA, E., BURKLY, L., SCHUPPAN, D., HANTO, D. W., OTTERBEIN, L. E. & POPOV, Y. 2013. Failure of fibrotic liver regeneration in mice is linked to a severe fibrogenic response driven by hepatic progenitor cell activation. *Am J Pathol,* 183**,** 182-94.

KUWAHARA, R., KOFMAN, A. V., LANDIS, C. S., SWENSON, E. S., BARENDSWAARD, E. & THEISE, N. D. 2008. The hepatic stem cell niche: identification by label-retaining cell assay. *Hepatology,* 47**,** 1994-2002.

LAISHES, B. A. & ROLFE, P. B. 1981. Search for endogenous liver colony-forming units in F344 rats given a two-thirds hepatectomy during short-term feeding of 2-acetylaminofluorene. *Cancer Res,* 41**,** 1731-41.

LANTHIER, N., RUBBIA-BRANDT, L. & SPAHR, L. 2013. Liver progenitor cells and therapeutic potential of stem cells in human chronic liver diseases. *Acta Gastroenterol Belg,* 76**,** 3-9.

LEE, V. M., CAMERON, R. G. & ARCHER, M. C. 1998. Zonal location of compensatory hepatocyte proliferation following chemically induced hepatotoxicity in rats and humans. *Toxicol Pathol,* 26**,** 621-7.

LEFEBVRE, O., SOROKIN, L., KEDINGER, M. & SIMON-ASSMANN, P. 1999. Developmental expression and cellular origin of the laminin alpha2, alpha4, and alpha5 chains in the intestine. *Dev Biol,* 210**,** 135-50.

LEI, L., LIU, D., HUANG, Y., JOVIN, I., SHAI, S. Y., KYRIAKIDES, T., ROSS, R. S. & GIORDANO, F. J. 2008. Endothelial expression of beta1 integrin is required for embryonic vascular patterning and postnatal vascular remodeling. *Mol Cell Biol,* 28**,** 794-802.

LEMAIGRE, F. P. 2009. Mechanisms of liver development: concepts for understanding liver disorders and design of novel therapies. *Gastroenterology,* 137**,** 62-79.

LEMIRE, J. M., SHIOJIRI, N. & FAUSTO, N. 1991. Oval cell proliferation and the origin of small hepatocytes in liver injury induced by D-galactosamine. *Am J Pathol,* 139**,** 535-52.

LEON, D. A. & MCCAMBRIDGE, J. 2006. Liver cirrhosis mortality rates in Britain from 1950 to 2002: an analysis of routine data. *Lancet,* 367**,** 52-6.

LI, J., TZU, J., CHEN, Y., ZHANG, Y. P., NGUYEN, N. T., GAO, J., BRADLEY, M., KEENE, D. R., ORO, A. E., MINER, J. H. & MARINKOVICH, M. P. 2003a. Laminin-10 is crucial for hair morphogenesis. *EMBO J,* 22**,** 2400-10.

LI, S., EDGAR, D., FASSLER, R., WADSWORTH, W. & YURCHENCO, P. D. 2003b. The role of laminin in embryonic cell polarization and tissue organization. *Dev Cell,* 4**,** 613-24.

LORENZINI, S., BIRD, T. G., BOULTER, L., BELLAMY, C., SAMUEL, K., AUCOTT, R., CLAYTON, E., ANDREONE, P., BERNARDI, M., GOLDING, M., ALISON, M. R., IREDALE, J. P. & FORBES, S. J. 2010. Characterisation of a stereotypical cellular and extracellular adult liver progenitor cell niche in rodents and diseased human liver. *Gut,* 59**,** 645-54.

LOWES, K. N., BRENNAN, B. A., YEOH, G. C. & OLYNYK, J. K. 1999. Oval cell numbers in human chronic liver diseases are directly related to disease severity. *Am J Pathol,* 154**,** 537-41.

MAHER, J. J., BISSELL, D. M., FRIEDMAN, S. L. & ROLL, F. J. 1988. Collagen measured in primary cultures of normal rat hepatocytes derives from lipocytes within the monolayer. *J Clin Invest,* 82**,** 450-9.

MAHONEY, Z. X., STAPPENBECK, T. S. & MINER, J. H. 2008. Laminin alpha 5 influences the architecture of the mouse small intestine mucosa. *J Cell Sci,* 121**,** 2493-502.

MALATO, Y., NAQVI, S., SCHURMANN, N., NG, R., WANG, B., ZAPE, J., KAY, M. A., GRIMM, D. & WILLENBRING, H. 2011. Fate tracing of mature hepatocytes in mouse liver homeostasis and regeneration. *J Clin Invest,* 121**,** 4850-60.

MARSHALL, A., RUSHBROOK, S., DAVIES, S. E., MORRIS, L. S., SCOTT, I. S., VOWLER, S. L., COLEMAN, N. & ALEXANDER, G. 2005. Relation between hepatocyte G1 arrest, impaired hepatic regeneration, and fibrosis in chronic hepatitis C virus infection. *Gastroenterology,* 128**,** 33-42.

MARTHIENS, V., KAZANIS, I., MOSS, L., LONG, K. & FFRENCH-CONSTANT, C. 2010. Adhesion molecules in the stem cell niche--more than just staying in shape? *J Cell Sci,* 123**,** 1613-22.

MARTINEZ-HERNANDEZ, A. & AMENTA, P. S. 1993. The hepatic extracellular matrix. I. Components and distribution in normal liver. *Virchows Arch A Pathol Anat Histopathol,* 423**,** 1-11.

MEANS, A. L., XU, Y., ZHAO, A., RAY, K. C. & GU, G. 2008. A CK19(CreERT) knockin mouse line allows for conditional DNA recombination in epithelial cells in multiple endodermal organs. *Genesis,* 46**,** 318-23.

MEDERACKE, I., HSU, C. C., TROEGER, J. S., HUEBENER, P., MU, X., DAPITO, D. H., PRADERE, J. P. & SCHWABE, R. F. 2013. Fate tracing reveals hepatic stellate cells as dominant contributors to liver fibrosis independent of its aetiology. *Nat Commun,* 4**,** 2823.

MICHALOPOULOS, G. K. 2007. Liver regeneration. *J Cell Physiol,* 213**,** 286-300.

MINER, J. H., CUNNINGHAM, J. & SANES, J. R. 1998. Roles for laminin in embryogenesis: exencephaly, syndactyly, and placentopathy in mice lacking the laminin alpha5 chain. *J Cell Biol,* 143**,** 1713-23.

MINER, J. H. & LI, C. 2000. Defective glomerulogenesis in the absence of laminin alpha5 demonstrates a developmental role for the kidney glomerular basement membrane. *Dev Biol,* 217**,** 278-89.

MINER, J. H., LI, C., MUDD, J. L., GO, G. & SUTHERLAND, A. E. 2004. Compositional and structural requirements for laminin and basement membranes during mouse embryo implantation and gastrulation. *Development,* 131**,** 2247-56.

MINER, J. H., PATTON, B. L., LENTZ, S. I., GILBERT, D. J., SNIDER, W. D., JENKINS, N. A., COPELAND, N. G. & SANES, J. R. 1997. The laminin alpha chains: expression, developmental transitions, and chromosomal locations of alpha1-5, identification of heterotrimeric laminins 8-11, and cloning of a novel alpha3 isoform. *J Cell Biol,* 137**,** 685-701.

MINER, J. H. & YURCHENCO, P. D. 2004. Laminin functions in tissue morphogenesis. *Annu Rev Cell Dev Biol,* 20**,** 255-84.

MITAKA, T., SATO, F., MIZUGUCHI, T., YOKONO, T. & MOCHIZUKI, Y. 1999. Reconstruction of hepatic organoid by rat small hepatocytes and hepatic nonparenchymal cells. *Hepatology,* 29**,** 111-25.

MIYAGOE, Y., HANAOKA, K., NONAKA, I., HAYASAKA, M., NABESHIMA, Y., ARAHATA, K. & TAKEDA, S. 1997. Laminin alpha2 chain-null mutant mice by targeted disruption of the Lama2 gene: a new model of merosin (laminin 2)-deficient congenital muscular dystrophy. *FEBS Lett,* 415**,** 33-9.

MIYAOKA, Y., EBATO, K., KATO, H., ARAKAWA, S., SHIMIZU, S. & MIYAJIMA, A. 2012. Hypertrophy and unconventional cell division of hepatocytes underlie liver regeneration. *Curr Biol,* 22**,** 1166-75.

MOULSON, C. L., LI, C. & MINER, J. H. 2001. Localization of Lutheran, a novel laminin receptor, in normal, knockout, and transgenic mice suggests an interaction with laminin alpha5 in vivo. *Dev Dyn,* 222**,** 101-14.

MURATA, K., AKASHIO, K. & OCHIAI, Y. 1984. Changes in acidic glycosaminoglycan components at different stages of human liver cirrhosis. *Hepatogastroenterology,* 31**,** 261-5.

NAGATO, M., HEIKE, T., KATO, T., YAMANAKA, Y., YOSHIMOTO, M., SHIMAZAKI, T., OKANO, H. & NAKAHATA, T. 2005. Prospective characterization of neural stem cells by flow cytometry analysis using a combination of surface markers. *J Neurosci Res,* 80**,** 456-66.

NEJJARI, M., COUVELARD, A., MOSNIER, J. F., MOREAU, A., FELDMANN, G., DEGOTT, C., MARCELLIN, P. & SCOAZEC, J. Y. 2001. Integrin up-regulation in chronic liver disease: relationship with inflammation and fibrosis in chronic hepatitis C. *J Pathol,* 195**,** 473-81.

NGUYEN, N. M., KELLEY, D. G., SCHLUETER, J. A., MEYER, M. J., SENIOR, R. M. & MINER, J. H. 2005. Epithelial laminin alpha5 is necessary for distal epithelial cell maturation, VEGF production, and alveolization in the developing murine lung. *Dev Biol,* 282**,** 111-25.

NGUYEN, N. M. & SENIOR, R. M. 2006. Laminin isoforms and lung development: all isoforms are not equal. *Dev Biol,* 294**,** 271-9.

NITOU, M., SUGIYAMA, Y., ISHIKAWA, K. & SHIOJIRI, N. 2002. Purification of fetal mouse hepatoblasts by magnetic beads coated with monoclonal anti-e-cadherin antibodies and their in vitro culture. *Exp Cell Res,* 279**,** 330-43.

NOVOYATLEVA, T., SCHYMURA, Y., JANSSEN, W., STROBL, F., SWIERCZ, J. M., PATRA, C., POSERN, G., WIETELMANN, A., ZHENG, T. S., SCHERMULY, R. T. & ENGEL, F. B. 2013. Deletion of Fn14 receptor protects from right heart fibrosis and dysfunction. *Basic Res Cardiol,* 108**,** 325.

O'REILLY, A. M., LEE, H. H. & SIMON, M. A. 2008. Integrins control the positioning and proliferation of follicle stem cells in the Drosophila ovary. *J Cell Biol,* 182**,** 801-15.

OIKAWA, Y., HANSSON, J., SASAKI, T., ROUSSELLE, P., DOMOGATSKAYA, A., RODIN, S., TRYGGVASON, K. & PATARROYO, M. 2011. Melanoma cells produce multiple laminin isoforms and strongly migrate on alpha5 laminin(s) via several integrin receptors. *Exp Cell Res,* 317**,** 1119-33.

OKABE, M., TSUKAHARA, Y., TANAKA, M., SUZUKI, K., SAITO, S., KAMIYA, Y., TSUJIMURA, T., NAKAMURA, K. & MIYAJIMA, A. 2009. Potential hepatic stem cells reside in EpCAM+ cells of normal and injured mouse liver. *Development,* 136**,** 1951-60.

OKAYA, A., KITANAKA, J., KITANAKA, N., SATAKE, M., KIM, Y., TERADA, K., SUGIYAMA, T., TAKEMURA, M., FUJIMOTO, J., TERADA, N., MIYAJIMA, A. & TSUJIMURA, T. 2005. Oncostatin M inhibits proliferation of rat oval cells, OC15-5, inducing differentiation into hepatocytes. *Am J Pathol,* 166**,** 709-19.

OMENETTI, A., CHOI, S., MICHELOTTI, G. & DIEHL, A. M. 2011. Hedgehog signaling in the liver. *J Hepatol,* 54**,** 366-73.

PAKU, S., NAGY, P., KOPPER, L. & THORGEIRSSON, S. S. 2004. 2-acetylaminofluorene dose-dependent differentiation of rat oval cells into hepatocytes: confocal and electron microscopic studies. *Hepatology,* 39**,** 1353-61.

PAKU, S., SCHNUR, J., NAGY, P. & THORGEIRSSON, S. S. 2001. Origin and structural evolution of the early proliferating oval cells in rat liver. *Am J Pathol,* 158**,** 1313-23.

PALMER, E. L., RUEGG, C., FERRANDO, R., PYTELA, R. & SHEPPARD, D. 1993. Sequence and tissue distribution of the integrin alpha 9 subunit, a novel partner of beta 1 that is widely distributed in epithelia and muscle. *J Cell Biol,* 123**,** 1289-97.

PATTON, B. L., CUNNINGHAM, J. M., THYBOLL, J., KORTESMAA, J., WESTERBLAD, H., EDSTROM, L., TRYGGVASON, K. & SANES, J. R. 2001. Properly formed but improperly localized synaptic specializations in the absence of laminin alpha4. *Nat Neurosci,* 4**,** 597-604.

PAULSSON, M. 1992. The role of laminin in attachment, growth, and differentiation of cultured cells: a brief review. *Cytotechnology,* 9**,** 99-106.

PHAM VAN, T., COUCHIE, D., MARTIN-GARCIA, N., LAPERCHE, Y., ZAFRANI, E. S. & MAVIER, P. 2008. Expression of matrix metalloproteinase-2 and -9 and of tissue inhibitor of matrix metalloproteinase-1 in liver regeneration from oval cells in rat. *Matrix Biol,* 27**,** 674-81.

PISCAGLIA, A. C., CAMPANALE, M., GASBARRINI, A. & GASBARRINI, G. 2010. Stem cell-based therapies for liver diseases: state of the art and new perspectives. *Stem Cells Int,* 2010**,** 259461.

POULIOT, N., CONNOLLY, L. M., MORITZ, R. L., SIMPSON, R. J. & BURGESS, A. W. 2000. Colon cancer cells adhesion and spreading on autocrine laminin-10 is mediated by multiple integrin receptors and modulated by EGF receptor stimulation. *Exp Cell Res,* 261**,** 360-71.

POULIOT, N. & KUSUMA, N. 2013. Laminin-511: a multi-functional adhesion protein regulating cell migration, tumor invasion and metastasis. *Cell Adh Migr,* 7**,** 142-9.

POULIOT, N., NICE, E. C. & BURGESS, A. W. 2001. Laminin-10 mediates basal and EGF-stimulated motility of human colon carcinoma cells via alpha(3)beta(1) and alpha(6)beta(4) integrins. *Exp Cell Res,* 266**,** 1-10.

PREISEGGER, K. H., FACTOR, V. M., FUCHSBICHLER, A., STUMPTNER, C., DENK, H. & THORGEIRSSON, S. S. 1999. Atypical ductular proliferation and its inhibition by transforming growth factor beta1 in the 3,5-diethoxycarbonyl-1,4-dihydrocollidine mouse model for chronic alcoholic liver disease. *Lab Invest,* 79**,** 103-9.

QIU, Q., HERNANDEZ, J. C., DEAN, A. M., RAO, P. H. & DARLINGTON, G. J. 2011. CD24-positive cells from normal adult mouse liver are hepatocyte progenitor cells. *Stem Cells Dev,* 20**,** 2177-88.

QUONDAMATTEO, F., KEMPKENSTEFFEN, C., MIOSGE, N., SONNENBERG, A. & HERKEN, R. 2004. Ultrastructural localization of integrin subunits alpha3 and alpha6 in capillarized sinusoids of the human cirrhotic liver. *Histol Histopathol,* 19**,** 799-806.

RAGHAVAN, S., BAUER, C., MUNDSCHAU, G., LI, Q. & FUCHS, E. 2000. Conditional ablation of beta1 integrin in skin. Severe defects in epidermal proliferation, basement membrane formation, and hair follicle invagination. *J Cell Biol,* 150**,** 1149-60.

RATIB, S., WEST, J., CROOKS, C. J. & FLEMING, K. M. 2014. Diagnosis of liver cirrhosis in England, a cohort study, 1998-2009: a comparison with cancer. *Am J Gastroenterol,* 109**,** 190-8.

REBUSTINI, I. T., PATEL, V. N., STEWART, J. S., LAYVEY, A., GEORGES-LABOUESSE, E., MINER, J. H. & HOFFMAN, M. P. 2007. Laminin alpha5 is necessary for submandibular gland epithelial morphogenesis and influences FGFR expression through beta1 integrin signaling. *Dev Biol,* 308**,** 15-29.

RITIE, L., SPENLE, C., LACROUTE, J., BOLCATO-BELLEMIN, A. L., LEFEBVRE, O., BOLE-FEYSOT, C., JOST, B., KLEIN, A., ARNOLD, C., KEDINGER, M., BAGNARD, D., OREND, G. & SIMON-ASSMANN, P. 2012. Abnormal Wnt and PI3Kinase signaling in the malformed intestine of lama5 deficient mice. *PLoS One,* 7**,** e37710.

RODIN, S., DOMOGATSKAYA, A., STROM, S., HANSSON, E. M., CHIEN, K. R., INZUNZA, J., HOVATTA, O. & TRYGGVASON, K. 2010. Long-term self-renewal of human pluripotent stem cells on human recombinant laminin-511. *Nat Biotechnol,* 28**,** 611-5.

ROSENBERG, D., ILIC, Z., YIN, L. & SELL, S. 2000. Proliferation of hepatic lineage cells of normal C57BL and interleukin-6 knockout mice after cocaine-induced periportal injury. *Hepatology,* 31**,** 948-55.

ROSKAMS, T., YANG, S. Q., KOTEISH, A., DURNEZ, A., DEVOS, R., HUANG, X., ACHTEN, R., VERSLYPE, C. & DIEHL, A. M. 2003. Oxidative stress and oval cell accumulation in mice and humans with alcoholic and nonalcoholic fatty liver disease. *Am J Pathol,* 163**,** 1301-11.

ROUNTREE, C. B., BARSKY, L., GE, S., ZHU, J., SENADHEERA, S. & CROOKS, G. M. 2007. A CD133-expressing murine liver oval cell population with bilineage potential. *Stem Cells,* 25**,** 2419-29.

RYAN, M. C., LEE, K., MIYASHITA, Y. & CARTER, W. G. 1999. Targeted disruption of the LAMA3 gene in mice reveals abnormalities in survival and late stage differentiation of epithelial cells. *J Cell Biol,* 145**,** 1309-23.

SANTONI-RUGIU, E., JELNES, P., THORGEIRSSON, S. S. & BISGAARD, H. C. 2005. Progenitor cells in liver regeneration: molecular responses controlling their activation and expansion. *APMIS,* 113**,** 876-902.

SCHEELE, S., NYSTROM, A., DURBEEJ, M., TALTS, J. F., EKBLOM, M. & EKBLOM, P. 2007. Laminin isoforms in development and disease. *J Mol Med,* 85**,** 825-36.

SCHLOTZER-SCHREHARDT, U., DIETRICH, T., SAITO, K., SOROKIN, L., SASAKI, T., PAULSSON, M. & KRUSE, F. E. 2007. Characterization of extracellular matrix components in the limbal epithelial stem cell compartment. *Exp Eye Res,* 85**,** 845-60.

SCHRADER, J., GORDON-WALKER, T. T., AUCOTT, R. L., VAN DEEMTER, M., QUAAS, A., WALSH, S., BENTEN, D., FORBES, S. J., WELLS, R. G. & IREDALE, J. P. 2011. Matrix stiffness modulates proliferation, chemotherapeutic response, and dormancy in hepatocellular carcinoma cells. *Hepatology,* 53**,** 1192-205.

SCHUPPAN, D., SCHMID, M., SOMASUNDARAM, R., ACKERMANN, R., RUEHL, M., NAKAMURA, T. & RIECKEN, E. O. 1998. Collagens in the liver extracellular matrix bind hepatocyte growth factor. *Gastroenterology,* 114**,** 139-52.

SCOAZEC, J. Y. 1996. Adhesion molecules in normal human liver. *Hepatogastroenterology,* 43**,** 1103-5.

SELL, S. 1978. Distribution of alpha-fetoprotein- and albumin-containing cells in the livers of Fischer rats fed four cycles of N-2-fluorenylacetamide. *Cancer Res,* 38**,** 3107-13.

SELL, S. 1998. Comparison of liver progenitor cells in human atypical ductular reactions with those seen in experimental models of liver injury. *Hepatology,* 27**,** 317-31.

SHANER, N. C., CAMPBELL, R. E., STEINBACH, P. A., GIEPMANS, B. N., PALMER, A. E. & TSIEN, R. Y. 2004. Improved monomeric red, orange and yellow fluorescent proteins derived from Discosoma sp. red fluorescent protein. *Nat Biotechnol,* 22**,** 1567-72.

SHANER, N. C., STEINBACH, P. A. & TSIEN, R. Y. 2005. A guide to choosing fluorescent proteins. *Nat Methods,* 2**,** 905-9.

SHARON, N. 1986. IUPAC-IUB Joint Commission on Biochemical Nomenclature (JCBN). Nomenclature of glycoproteins, glycopeptides and peptidoglycans. Recommendations 1985. *Eur J Biochem,* 159**,** 1-6.

SHEN, Q., WANG, Y., KOKOVAY, E., LIN, G., CHUANG, S. M., GODERIE, S. K., ROYSAM, B. & TEMPLE, S. 2008. Adult SVZ stem cells lie in a vascular niche: a quantitative analysis of niche cell-cell interactions. *Cell Stem Cell,* 3**,** 289-300.

SHIMIZU, H., HOSOKAWA, H., NINOMIYA, H., MINER, J. H. & MASAKI, T. 1999. Adhesion of cultured bovine aortic endothelial cells to laminin-1 mediated by dystroglycan. *J Biol Chem,* 274**,** 11995-2000.

SHINOZUKA, H., LOMBARDI, B., SELL, S. & IAMMARINO, R. M. 1978. Early histological and functional alterations of ethionine liver carcinogenesis in rats fed a choline-deficient diet. *Cancer Res,* 38**,** 1092-8.

SIDRANSKY, H. & VERNEY, E. 1969. Influence of ethionine on choline-deficiency fatty liver. *J Nutr,* 97**,** 419-30.

SOEDA, J., MOURALIDARANE, A., RAY, S., NOVELLI, M., THOMAS, S., ROSKAMS, T., DIEHL, A. M. & OBEN, J. A. 2014. The beta-adrenoceptor agonist Isoproterenol rescues acetaminophen-injured livers through increasing progenitor numbers via Wnt. *Hepatology*.

SRINIVAS, S., WATANABE, T., LIN, C. S., WILLIAM, C. M., TANABE, Y., JESSELL, T. M. & COSTANTINI, F. 2001. Cre reporter strains produced by targeted insertion of EYFP and ECFP into the ROSA26 locus. *BMC Dev Biol,* 1**,** 4.

STREULI, C. H. & AKHTAR, N. 2009. Signal co-operation between integrins and other receptor systems. *Biochem J,* 418**,** 491-506.

SUZUKI, A., SEKIYA, S., ONISHI, M., OSHIMA, N., KIYONARI, H., NAKAUCHI, H. & TANIGUCHI, H. 2008. Flow cytometric isolation and clonal identification of self-renewing bipotent hepatic progenitor cells in adult mouse liver. *Hepatology,* 48**,** 1964-78.

SUZUKI, A., ZHENG, Y., KONDO, R., KUSAKABE, M., TAKADA, Y., FUKAO, K., NAKAUCHI, H. & TANIGUCHI, H. 2000. Flow-cytometric separation and enrichment of hepatic progenitor cells in the developing mouse liver. *Hepatology,* 32**,** 1230-9.

SWIDERSKA-SYN, M., SYN, W. K., XIE, G., KRUGER, L., MACHADO, M. V., KARACA, G., MICHELOTTI, G. A., CHOI, S. S., PREMONT, R. T. & DIEHL, A. M. 2013. Myofibroblastic cells function as progenitors to regenerate murine livers after partial hepatectomy. *Gut*.

TAJBAKHSH, S. 2009. Stem cell: what's in a name?

TANI, T., LEHTO, V. P. & VIRTANEN, I. 1999. Expression of laminins 1 and 10 in carcinoma cells and comparison of their roles in cell adhesion. *Exp Cell Res,* 248**,** 115-21.

TANIGUCHI, Y., IDO, H., SANZEN, N., HAYASHI, M., SATO-NISHIUCHI, R., FUTAKI, S. & SEKIGUCHI, K. 2009. The C-terminal region of laminin beta chains modulates the integrin binding affinities of laminins. *J Biol Chem,* 284**,** 7820-31.

TANIMIZU, N., KIKKAWA, Y., MITAKA, T. & MIYAJIMA, A. 2012. alpha1- and alpha5-Containing laminins regulate the development of bile ducts via beta1-integrin signals. *J Biol Chem*.

TANIMIZU, N., NISHIKAWA, M., SAITO, H., TSUJIMURA, T. & MIYAJIMA, A. 2003. Isolation of hepatoblasts based on the expression of Dlk/Pref-1. *J Cell Sci,* 116**,** 1775-86.

TANIMIZU, N., SAITO, H., MOSTOV, K. & MIYAJIMA, A. 2004. Long-term culture of hepatic progenitors derived from mouse Dlk+ hepatoblasts. *J Cell Sci,* 117**,** 6425-34.

TATE, M. C., GARCIA, A. J., KESELOWSKY, B. G., SCHUMM, M. A., ARCHER, D. R. & LAPLACA, M. C. 2004. Specific beta1 integrins mediate adhesion, migration, and differentiation of neural progenitors derived from the embryonic striatum. *Mol Cell Neurosci,* 27**,** 22-31.

THEISE, N. D., SAXENA, R., PORTMANN, B. C., THUNG, S. N., YEE, H., CHIRIBOGA, L., KUMAR, A. & CRAWFORD, J. M. 1999. The canals of Hering and hepatic stem cells in humans. *Hepatology,* 30**,** 1425-33.

THOMAS, J. A., POPE, C., WOJTACHA, D., ROBSON, A. J., GORDON-WALKER, T. T., HARTLAND, S., RAMACHANDRAN, P., VAN DEEMTER, M., HUME, D. A., IREDALE, J. P. & FORBES, S. J. 2011. Macrophage therapy for murine liver fibrosis recruits host effector cells improving fibrosis, regeneration, and function. *Hepatology,* 53**,** 2003-15.

THYBOLL, J., KORTESMAA, J., CAO, R., SOININEN, R., WANG, L., IIVANAINEN, A., SOROKIN, L., RISLING, M., CAO, Y. & TRYGGVASON, K. 2002. Deletion of the laminin alpha4 chain leads to impaired microvessel maturation. *Mol Cell Biol,* 22**,** 1194-202.

TIRNITZ-PARKER, J. E., TONKIN, J. N., KNIGHT, B., OLYNYK, J. K. & YEOH, G. C. 2007. Isolation, culture and immortalisation of hepatic oval cells from adult mice fed a choline-deficient, ethionine-supplemented diet. *Int J Biochem Cell Biol,* 39**,** 2226-39.

TRYGGVASON, K. 1993. The laminin family. *Curr Opin Cell Biol,* 5**,** 877-82.

TSANG, K. Y., CHEUNG, M. C., CHAN, D. & CHEAH, K. S. 2010. The developmental roles of the extracellular matrix: beyond structure to regulation. *Cell Tissue Res,* 339**,** 93-110.

TURCK, N., GROSS, I., GENDRY, P., STUTZMANN, J., FREUND, J. N., KEDINGER, M., SIMON-ASSMANN, P. & LAUNAY, J. F. 2005. Laminin isoforms: biological roles and effects on the intracellular distribution of nuclear proteins in intestinal epithelial cells. *Exp Cell Res,* 303**,** 494-503.

TURNER, R., LOZOYA, O., WANG, Y., CARDINALE, V., GAUDIO, E., ALPINI, G., MENDEL, G., WAUTHIER, E., BARBIER, C., ALVARO, D. & REID, L. M. 2011. Human hepatic stem cell and maturational liver lineage biology. *Hepatology,* 53**,** 1035-45.

VACHON, P. H. & BEAULIEU, J. F. 1995. Extracellular heterotrimeric laminin promotes differentiation in human enterocytes. *Am J Physiol,* 268**,** G857-67.

VAN HUL, N. K., ABARCA-QUINONES, J., SEMPOUX, C., HORSMANS, Y. & LECLERCQ, I. A. 2009. Relation between liver progenitor cell expansion and extracellular matrix deposition in a CDE-induced murine model of chronic liver injury. *Hepatology,* 49**,** 1625-35.

VIG, P., RUSSO, F. P., EDWARDS, R. J., TADROUS, P. J., WRIGHT, N. A., THOMAS, H. C., ALISON, M. R. & FORBES, S. J. 2006. The sources of parenchymal regeneration after chronic hepatocellular liver injury in mice. *Hepatology,* 43**,** 316-24.

VOLPES, R., VAN DEN OORD, J. J. & DESMET, V. J. 1991. Distribution of the VLA family of integrins in normal and pathological human liver tissue. *Gastroenterology,* 101**,** 200-6.

VOOG, J. & JONES, D. L. 2010. Stem cells and the niche: a dynamic duo. *Cell Stem Cell,* 6**,** 103-15.

WALLQUIST, W., PLANTMAN, S., THAMS, S., THYBOLL, J., KORTESMAA, J., LANNERGREN, J., DOMOGATSKAYA, A., OGREN, S. O., RISLING, M., HAMMARBERG, H., TRYGGVASON, K. & CULLHEIM, S. 2005. Impeded interaction between Schwann cells and axons in the absence of laminin alpha4. *J Neurosci,* 25**,** 3692-700.

WANG, J., HOSHIJIMA, M., LAM, J., ZHOU, Z., JOKIEL, A., DALTON, N. D., HULTENBY, K., RUIZ-LOZANO, P., ROSS, J., JR., TRYGGVASON, K. & CHIEN, K. R. 2006. Cardiomyopathy associated with microcirculation dysfunction in laminin alpha4 chain-deficient mice. *J Biol Chem,* 281**,** 213-20.

WANG, X., FOSTER, M., AL-DHALIMY, M., LAGASSE, E., FINEGOLD, M. & GROMPE, M. 2003. The origin and liver repopulating capacity of murine oval cells. *Proc Natl Acad Sci U S A,* 100 Suppl 1**,** 11881-8.

WATANABE, T., NAKAGAWA, K., OHATA, S., KITAGAWA, D., NISHITAI, G., SEO, J., TANEMURA, S., SHIMIZU, N., KISHIMOTO, H., WADA, T., AOKI, J., ARAI, H., IWATSUBO, T., MOCHITA, M., SATAKE, M., ITO, Y., MATSUYAMA, T., MAK, T. W., PENNINGER, J. M., NISHINA, H. & KATADA, T. 2002. SEK1/MKK4-mediated SAPK/JNK signaling participates in embryonic hepatoblast proliferation via a pathway different from NF-kappaB-induced anti-apoptosis. *Dev Biol,* 250**,** 332-47.

WELTMAN, M. D., FARRELL, G. C. & LIDDLE, C. 1996. Increased hepatocyte CYP2E1 expression in a rat nutritional model of hepatic steatosis with inflammation. *Gastroenterology,* 111**,** 1645-53.

WILLIAMS, M. J., CLOUSTON, A. D. & FORBES, S. J. 2014. Links between hepatic fibrosis, ductular reaction, and progenitor cell expansion. *Gastroenterology,* 146**,** 349-56.

WOOD, M. J., GADD, V. L., POWELL, L. W., RAMM, G. A. & CLOUSTON, A. D. 2013. The ductular reaction in hereditary haemochromatosis: The link between hepatocyte senescence and fibrosis progression. *Hepatology*.

YAMADA, M., SUMIDA, Y., FUJIBAYASHI, A., FUKAGUCHI, K., SANZEN, N., NISHIUCHI, R. & SEKIGUCHI, K. 2008. The tetraspanin CD151 regulates cell morphology and intracellular signaling on laminin-511. *FEBS J,* 275**,** 3335-51.

YANG, L., JUNG, Y., OMENETTI, A., WITEK, R. P., CHOI, S., VANDONGEN, H. M., HUANG, J., ALPINI, G. D. & DIEHL, A. M. 2008. Fate-mapping evidence that hepatic stellate cells are epithelial progenitors in adult mouse livers. *Stem Cells,* 26**,** 2104-13.

YANGER, K., ZONG, Y., MAGGS, L. R., SHAPIRA, S. N., MADDIPATI, R., AIELLO, N. M., THUNG, S. N., WELLS, R. G., GREENBAUM, L. E. & STANGER, B. Z. 2013. Robust cellular reprogramming occurs spontaneously during liver regeneration. *Genes Dev,* 27**,** 719-24.

YIMLAMAI, D., CHRISTODOULOU, C., GALLI, G. G., YANGER, K., PEPE-MOONEY, B., GURUNG, B., SHRESTHA, K., CAHAN, P., STANGER, B. Z. & CAMARGO, F. D. 2014. Hippo pathway activity influences liver cell fate. *Cell,* 157**,** 1324-38.

YIN, L., LYNCH, D. & SELL, S. 1999. Participation of different cell types in the restitutive response of the rat liver to periportal injury induced by allyl alcohol. *J Hepatol,* 31**,** 497-507.

YOON, S. M., GERASIMIDOU, D., KUWAHARA, R., HYTIROGLOU, P., YOO, J. E., PARK, Y. N. & THEISE, N. D. 2011. Epithelial cell adhesion molecule (EpCAM) marks hepatocytes newly derived from stem/progenitor cells in humans. *Hepatology,* 53**,** 964-73.

YOVCHEV, M. I., GROZDANOV, P. N., ZHOU, H., RACHERLA, H., GUHA, C. & DABEVA, M. D. 2008. Identification of adult hepatic progenitor cells capable of repopulating injured rat liver. *Hepatology,* 47**,** 636-47.

YURCHENCO, P. D., AMENTA, P. S. & PATTON, B. L. 2004. Basement membrane assembly, stability and activities observed through a developmental lens. *Matrix Biol,* 22**,** 521-38.

ZAJICEK, G., OREN, R. & WEINREB, M., JR. 1985. The streaming liver. *Liver,* 5**,** 293-300.

ZEISEL, S. H. & BLUSZTAJN, J. K. 1994. Choline and human nutrition. *Annu Rev Nutr,* 14**,** 269-96.

ZHANG, W., CHEN, X. P., ZHANG, W. G., ZHANG, F., XIANG, S., DONG, H. H. & ZHANG, L. 2009. Hepatic non-parenchymal cells and extracellular matrix participate in oval cell-mediated liver regeneration. *World J Gastroenterol,* 15**,** 552-60.

ZHOU, H., ROGLER, L. E., TEPERMAN, L., MORGAN, G. & ROGLER, C. E. 2007. Identification of hepatocytic and bile ductular cell lineages and candidate stem cells in bipolar ductular reactions in cirrhotic human liver. *Hepatology,* 45**,** 716-24.

ZHU, C., COOMBE, D. R., ZHENG, M. H., YEOH, G. C. & LI, L. 2012. Liver progenitor cell interactions with the extracellular matrix. *J Tissue Eng Regen Med*.